

POLITECNICO DI TORINO

Collegio di Ingegneria Energetica

**Corso di Laurea Magistrale
in Ingegneria Energetica e Nucleare**

Tesi di Laurea Magistrale

**Dynamic Simulation of a PEMFC Gen-set for
Non-Stationary Application**



Relatore

prof. Massimo Santarelli

Candidato

Hector Francisco Elias Gutierrez

Aprile 2018

ABSTRACT

Nowadays the need of reduction of the impact of our activities on the environment has created the necessity to improve and extend new technologies as a solution for the environmental problem. One of these solutions is the PEM fuel cell that relies on the hydrogen as energetic carrier. In fact, the need to move from fossil fuels to renewable energy sources has been pushed more on the last decades creating new systems and more innovative solutions. Of course, this period of changes and improvements has to be thought in a long term, and for that reason each solution and each new technology has to be reliable and efficient in such a way they result to be convenient respect to the traditional solutions. This point is one of the key aspects we want to discuss in our thesis regarding of course the PEM fuel cell and its application as a generator set, better known as gen-set.

In the first chapter we will describe the main characteristics of the generator set, making a comparison with the alternative solution. We will also analyse all the positive aspects of the solution in order to understand better the purpose of this study. In the following chapter, instead, we will describe more in detail the PEM fuel cell and all phenomena occurring into the device. To achieve this goal is necessary making descriptions of all the equations and models used in order to give a better understand of the totality of the system under analysis. In the third chapter we will finally describe the system configuration created in Aspen Plus, pointing out all the assumptions made and making a comparison between the solutions obtained by the varying of size. In the following chapter the results from the load following are shown together with some consideration regarding the optimal size. After that, a complete analysis of the main components is done, giving a resume of the operative parameters of each of them. In this chapter a description of the final scheme of the gen-set is also given. In the last chapter, the conclusion together with some considerations will be reported, giving us an overview of all the study. The annex that follows will, instead, contain the codes used for the calculations using other software such as Matlab and Fortran.

RIASSUNTO

Oggigiorno, la sempre più stringente necessità di controllare e ridurre l'impatto sull'ambiente sta portando la nostra civiltà a dover diffondere e migliorare tecnologie sempre più innovative. Infatti, con problemi legati all'emissione sempre più crescenti, risulta pressoché necessario lavorare su alternative efficienti ed allo stesso tempo affidabili che sfruttino a pieno le energie rinnovabili. Tuttavia, affidabilità ed efficienza risultano spesso un grosso scoglio per le nuove tecnologie se paragonate a quelle tradizionali.

Tra le molte alternative che stanno prendendo piede, le celle a combustibile risultano tra le più promettenti, in quanto convertono direttamente l'energia chimica in energia elettrica senza dover passare per una conversione termica, evitando così le conseguenti perdite che inutilmente si sarebbero generate a causa delle irreversibilità.

Nella presente tesi, ci soffermeremo principalmente sulla applicazione della cella combustibile PEM come gen-set. Infatti, nel primo capitolo parleremo proprio del gruppo elettrogeno e delle sue caratteristiche, facendo alla fine un confronto con la soluzione alternativa data dalla cella a combustibile, così da mettere in evidenza i vantaggi e le caratteristiche che portano tale soluzione ad essere particolarmente interessante. Nel secondo capitolo, invece, entreremo molto più in dettaglio nella descrizione della PEM fuel cell, descrivendo i fenomeni che avvengono al suo interno e mostrando i modelli e le equazioni utilizzate per la sua rappresentazione. Successivamente, nel terzo capitolo, ci soffermeremo meglio sui vari blocchi necessari a descrivere nella sua interezza il modello generato in Aspen Plus per la simulazione. In tale capitolo, ovviamente, verranno messe in risalto le scelte effettuate e le assunzioni fatte nella creazione del modello oltre ad una presentazione delle particolari differenze che si hanno al variare della taglia. Nel quarto capitolo, invece, verranno affrontate le problematiche riguardanti l'inseguimento delle potenze richieste dall'utenza da parte del generatore a cella a combustibile, a cui poi seguiranno alcune considerazioni riguardanti la scelta della taglia ottimale. Successivamente uno studio sul dimensionamento dei principali componenti del PEMFC gen-set verrà affrontato, concludendosi con la descrizione dello schema finale del gruppo elettrogeno risultante. Infine, nell'ultimo capitolo, una conclusione con alcune considerazioni su tutto il lavoro svolto verrà fornita. Per quanto riguarda l'appendice che segue, esso conterrà i codici Matlab e Fortran utilizzati durante lo svolgimento dell'elaborato per i calcoli e le simulazioni.

CONTENTS

Abstract	I
Riassunto	II
List of figures	VI
List of tables	VIII
Chapter 1 Gen-set and PEMFC Gen-set	1
1.1 Diesel Generator set.....	1
1.1.1 Components.....	1
1.1.2 Rating and size	4
1.2 PEMFC Gen-set.....	6
1.2.1 Components.....	7
Chapter 2 Proton Exchange Membrane FC	10
2.1 PEMFC description	10
2.1.1 Electrolyte	11
2.2 Fuel cell potential	12
2.3 Electrochemical model	12
2.3.1 Activation overvoltage	13
2.3.2 Ohmic overvoltage	15
2.3.3 Diffusion overvoltage.....	16
2.3.4 Internal current density.....	17
2.4 Water management.....	17
2.5 Water crossover	19
2.5.1 Electro-osmotic drag	20
2.5.2 Back diffusion	21
2.6 Thermal management	21
2.7 PEMFC characteristics	22
Chapter 3 Load profile and Aspen modelling.....	25
3.1 User load profile	25

3.1.1	Gen-set sizing	27
3.2	System configuration	28
3.3	Fuel cell modelling	30
3.4	Humidification modelling.....	34
3.5	Calculator blocks	36
3.5.1	C-ICURR.....	36
3.5.2	C-WREC	38
3.5.3	C-HUMC	39
3.5.4	C-FU.....	39
3.5.5	C-PEMFC.....	40
3.5.6	C-COOL	40
3.6	Simulation sequence	41
3.7	Stack Temperature	43
3.7.1	Temperature during the start-up.....	43
Chapter 4	Load following and Final configuration.....	46
4.1	Load following	46
4.2	Gen-set size analysis.....	53
4.2.1	Battery bank sizing.....	53
4.3	Gen-set cost analysis	56
4.4	Main components sizing.....	59
4.4.1	Storage tank sizing	59
4.4.2	Blower sizing.....	61
4.4.3	Pump sizing	63
4.5	Scheme and final configuration.....	64
Chapter 5	Concluding remarks	67
5.1	Conclusions and consideration	67
Reference.....		i
Appendix		iii

Ringraziamenti XXX

LIST OF FIGURES

Figure 1.1: Gen-set for construction site application	1
Figure 1.2: Electric starter motor	2
Figure 1.3: Flywheel and driveshaft.....	2
Figure 1.4: Electric governor	3
Figure 1.5: Automatic voltage regulator	3
Figure 1.6: Large scale Gen-set.....	5
Figure 1.7: PEMFC generator [5]	6
Figure 1.8: Commercial PEMFC gen-set	7
Figure 1.9: Fuel cell stack	8
Figure 1.10: DC/DC converter	8
Figure 2.1: PEM fuel cell	10
Figure 2.2: Nafion molecule.....	11
Figure 2.3: Polarization curve	13
Figure 2.4: Vapour pressure plot.....	18
Figure 2.5: Polarization curve at varying temperature of operation	18
Figure 2.6: Water crossover phenomena.....	19
Figure 2.7: PEMFC polarization curve at 70°C	22
Figure 2.8: PEMFC power characteristic	23
Figure 2.9: Cell efficiency.....	24
Figure 3.1: Electrical consumption profile.....	26
Figure 3.2: Comparison between the gen-set sizes chosen and the user load.....	27
Figure 3.3: System configuration	28
Figure 3.4: Aspen modelling of the FC	31
Figure 3.5: Aspen modelling of the heat equation	32
Figure 3.6: Aspen modelling of the BOP configuration	33
Figure 3.7: Membrane humidifier	34
Figure 3.8: RH profile at the anode exit for the size of 10 kW at varying of current	35
Figure 3.9: Variation of the RH profiles at the anode exit with size.....	35
Figure 3.10: Fuel utilization profile at varying current.....	37
Figure 3.11: Air utilization profile at varying current.....	37
Figure 3.12: Aspen modelling of the cathode's humidifier	39
Figure 3.13: Aspen modelling of the cooling circuit	41
Figure 3.14: Temperature profile during start-up at varying of the starting current.....	44

Figure 3.15: Temperature profile during start-up at varying of the size	45
Figure 4.1: Load following profile of a 6 kW gen-set	47
Figure 4.2: Load following profile of a 8 kW gen-set	48
Figure 4.3: Load following profile of a 10 kW gen-set	48
Figure 4.4: Current profile of a 6 kW gen-set	49
Figure 4.5: Current profile of a 8 kW gen-set	50
Figure 4.6: Current profile of a 10 kW gen-set	50
Figure 4.7: Stack efficiency profile of a 6 kW gen-set	51
Figure 4.8: Stack efficiency profile of a 8 kW gen-set	52
Figure 4.9: Stack efficiency profile of a 10 kW gen-set	52
Figure 4.10: Possibilities of connection among batteries	55
Figure 4.11: Cost trend of the PEMFC system with size	57
Figure 4.12: Cost trend of the battery bank with size	57
Figure 4.13: Life cycle profile at varying of the DOD [16]	58
Figure 4.14: Cost trend of both solution during time	60
Figure 4.15: Scheme of the final configuration of the gen-set	66

LIST OF TABLES

Table 1.1: Power consumption of common electrical tools [4]	5
Table 2.1: Input for the η_{act} calculation	15
Table 2.2: Input for the η_{ohm} calculation	16
Table 2.3: Input for the η_{diff} calculation	17
Table 2.4: Nafion 117 input data [6] [7]	21
Table 3.1: Electrical tools chosen for the load profile [4].....	25
Table 3.2: Data of the relative humidity exiting the anode	38
Table 3.3: FC stack data	43
Table 4.1: Load following results summary.....	49
Table 4.2: Average efficiency at varying of the size.....	51
Table 4.3: Adjusted capacity factors	54
Table 4.4: Results of the battery bank capacity at varying of the size	54
Table 4.5: Data for the calculation of the battery configuration	55
Table 4.6: Battery configuration at varying of the size.....	55
Table 4.7: Gen-set economic data	56
Table 4.8: Battery economic data.....	56
Table 4.9: Resume of the main initial costs	56
Table 4.10: Hydrogen operative cost and consumption.....	58
Table 4.11: Economic results at varying of the size	59
Table 4.12: Configuration tank results	60
Table 4.13: Data for the calculation of the storage size	61
Table 4.14: Stack pressure drops [6].....	62
Table 4.15: Perma Pure FC-400 data	62
Table 4.16: Recirculation blower sizing parameters	63
Table 4.17: Air circulation blower sizing parameters	63
Table 4.18: Cooling circuit pressure drops	63
Table 4.19: Pump sizing parameters	64
Table 4.20: Resume table of the final configuration.....	65

Chapter 1

GEN-SET AND PEMFC GEN-SET

1.1 Diesel Generator set

A Diesel generator set, better known as gen-set, is a device that has the primary purpose to convert energy contained in the fuel into electrical energy. This machinery is normally used in places without connection to the electrical grid, and for that reason, it is interesting as a stand-alone power supply, other than as emergency power supply. For the purpose of our study, we will focus on the first category, especially for events and construction sites applications which are the targets of our study.



Figure 1.1: Gen-set for construction site application

1.1.1 Components

In order to better understand the working operation of this machine we need first to describe and identify the main components. They are taken from [1], [2] and can be quickly summarized as following:

- **Diesel engine:**
An internal combustion engine that use the heat of compression to ignite the fuel.
- **Starter motor:**
An electric motor (DC motor) used to crank-up the internal combustion engine.

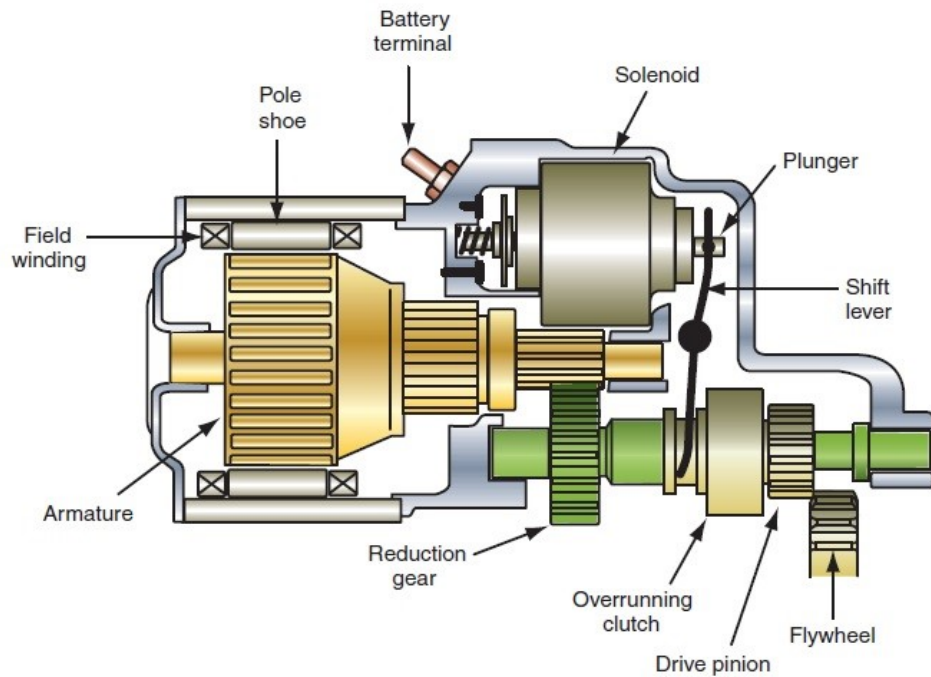


Figure 1.2: Electric starter motor

It uses the current from the starting battery to push the drive pinion on the flywheel in order to start up the driveshaft and consequently the engine.

➤ **Flywheel:**

A rotating mechanical device that is used to store rotational energy.

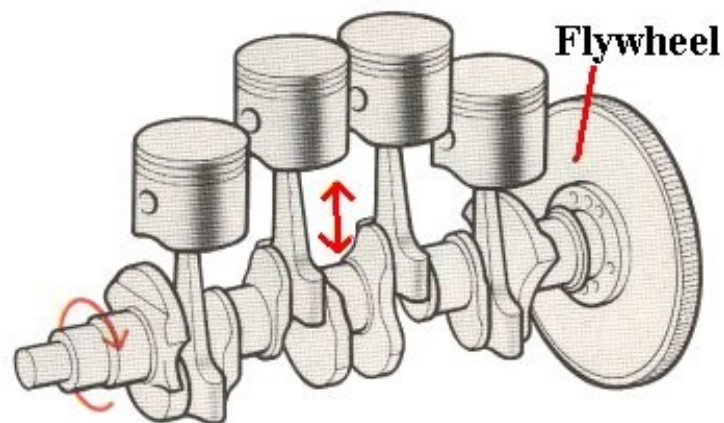


Figure 1.3: Flywheel and driveshaft

Since the energy source is not continuous, this component is quite necessary. In fact, it has a significant moment of inertia so it permits to resist to quickly changes in rotational speed.

➤ **Governor:**

It is the speed limiter, so the device used to measure and regulate the speed of the engine.



Figure 1.4: Electric governor

It is a necessary component in order to maintain under values of acceptability the frequency during a variation of load.

➤ **Muffler:**

It is the device used to decrease the amount of noise emitted by the exhausts of the internal combustion engine.

➤ **Alternator:**

An electromechanical device that converts mechanical energy to electrical energy in the form of alternating current (AC).

➤ **Voltage regulator:**

It is called automatic voltage regulator (AVR), and is an electronic device, that has to maintain the generator output terminal voltage at set value under varying of load.



Figure 1.5: Automatic voltage regulator

➤ **Battery:**

A type of rechargeable battery that supplies electric energy to power the starter motor. Its efficiency is an important parameter for the reliability of the gen-set. The most spread type of battery used for gen-set applications is the lead battery.

➤ **Control panel:**

A complex piece of electronics with a microprocessor that manipulates inputs from sensors in order to let the machine to manage itself. The panel can be set up on the body of the generator itself, which is usually the case with small generators. For larger generator instead, the control panel is completely separated from the generator.

➤ **Cooling system:**

Internal combustion engine are often cooled by passing a water based coolant through the engine block, where it is heated. Then, through a radiator, it loses that heat to the atmosphere, returning back to the engine and starting again the loop.

1.1.2 Rating and size

Engine-generators are available in a wide range of power ratings, which are defined in the ISO 8528-1 [3] that is the standard regulation for diesel generators.

In this document, these units are classified as: continuous, prime or stand-by. Continuous rating is used where the generator is expected to be operating 24 hours a day, 365 days a year, at a constant load. Prime rating, instead, allows some fluctuations in the load supplied, while stand-by rating is used for back-up supply applications where running time is up to 200 hours per year.

The generator rating should be calculated to meet the maximum demand of electrical loads. To do so, a parameter called “load factor” has to be considered. It represents a ratio of the average load demand to the rated generator power. Generator ratings can be specified as either in kW or kVA. In the first case, a load factor equal to 0.8 is assumed.

Now, considering the variety of applications that these generators have, we understand that is not easy classifying them in terms of size due to the wide range available. However, in order to have a better idea of the targets of our applications, we can roughly subdivide them in three main categories:

- Small engine-generator
- Mid-size engine-generator
- Large scale engine-generator

The first category includes handy and portable units that can supply from several watts to a several thousand of watts. Generators with power supply capacities from 5 kW to 100 kW, are considered in the mid-size range and they are mostly used for homes, small shops and offices. They can be also used as power supplies on construction sites, and, for this reason, we will focus more on this range of power during our study. The third category, instead, comprises higher size

from 100 kW to over 3 MW, that are necessary in hospitals, industrial power plants, business and data centres, in order to meet their higher power requirements. In fact, these units are particularly useful in providing back-up power solutions for companies, which have serious economic and human costs associated with an unplanned shutdown, such as a black-out. In the case of power plants, the gen-set can be also used as a power utility during peak periods. Diesel generators are also being broadly used in ships, for the sake of providing auxiliary power, but also propulsion.



Figure 1.6: Large scale Gen-set

At this point, to determine the right size of the gen-set, we need to know that there are available lots of software that accomplish this job, and, for this reason, we will not enter into detail on this aspect. In fact, since it is not the purpose of our thesis, we will only focus on some interesting points that need to be considered during the process. Of course, to size properly the engine-generator we need to know the power requirements of the items that has to be powered by the generator, but not only the running wattage. In fact, also the starting wattage of the devices you intend to power is crucial for an accurate calculation of the power requirements.

Table 1.1: Power consumption of common electrical tools [4]

Item	Starting Wattage (W)	Running Wattage (W)
Circular Saw	2400	1200
Drill	1800	720
Edger	2400	960
Electric Chainsaw	2400	1200
Electric Lawn Mower	4320	1440
Electric Pressure Washer	3600	1200
Electric String Trimmer	1500	600
Jig Saw	1800	720
Miter Saw	2100	840
Orbital Sander	1800	600
Paint Sprayer	1080	360
Planer	2400	960
Router	1500	600

Water Pump	3000	1000
Wet/Dry Vacuum	2500	888
Winch	5400	1800
Furnace Fan, gas/fuel oil furnace		
1/8 horsepower (hp)	500	300
1/6 horsepower (hp)	750	500
1/4 horsepower (hp)	1000	600
2/5 horsepower (hp)	1400	700
3/5 horsepower (hp)	2350	875
Central Air Conditioner		
10,000 BTU	2200	1500
20,000 BTU	3300	2500
24,000 BTU	4950	3800
32,000 BTU	6500	5000
40,000 BTU	6700	6000
1/4' Drill	300	300
Jigsaw	300	300
Electric Weed Trimmer	500	500
Belt Sander	1000	1000
Disc Sander	1200	1200
Chain Saw	1200	1200
Worm Drive Saw	3100	1560
12' Concrete Cutter	3600	1800
7 1/4' Circular Saw	3000	1500
Disc Grinder	4000	2000
Air Compressor (Average)	4000	2000

Of course, the values indicated on the table above are simply examples of possible values for the tools considered, but, anyway, they are reported in order to demonstrate how starting and running wattages differ from each other, but also to have an idea on the specific consumption needs.

1.2 PEMFC Gen-set

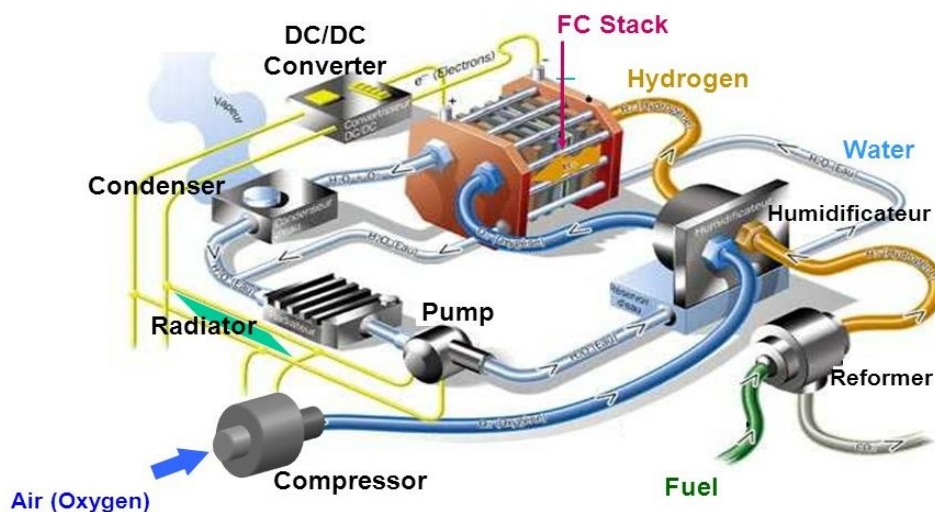


Figure 1.7: PEMFC generator [5]

In comparison to the traditional solution, the PEMFC gen-set uses hydrogen to produce electricity, and for this reason it is quite interesting as a clean technology. In fact, the device is emission free, and this is due to the fact that the diesel engine and the alternator are substituted by the PEM fuel cell. This means that there is no combustion in the process, obtaining a renewable source of electricity, that is achieved through electrochemical reactions. Indeed, we have a direct conversion of the chemical energy contained in the fuel into electricity (DC electrical current), resulting in a less complex system with very few moving parts.



Figure 1.8: Commercial PEMFC gen-set

This results to be a very good aspect, especially in terms of reliability due to the less potential failure, but also in terms of operational costs due to the reduction of its maintenance (especially in the case where the gen-set is used as a back-up power supply). Another important aspect, that has to be underlined, is the less impact of the machine in terms of noise. This is due to the lack of the combustion chamber and moving parts, resulting to be a winning solution for many locations where the level of noise and vibrations are a constraint.

1.2.1 Components

From the system configuration of the device, we understand that the machine is quite different from the traditional solution, in fact, the process throughout which the electricity is obtained is completely different. For this reason seems to be quite important to summarize the main components of the device that are the following:

➤ **Fuel cell stack:**

Core of the system in which the electrochemical reactions occur.

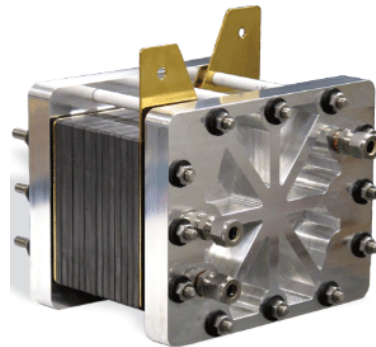


Figure 1.9: Fuel cell stack

➤ **Humidifier:**

It is a device used to humidify the reactants entering the stack, in order to control the water content in the electrolyte.

➤ **Pump:**

Component needed to move the coolant in the cooling circuit.

➤ **Radiator:**

A heat exchanger that is used to transfer out the heat from the coolant.

➤ **Compressor:**

It is a device used to compress the air entering the stack. It permits to control the amount of reactant during variation of load.

➤ **Condenser:**

Component needed to separate the water exiting the stack.

➤ **DC/DC converter:**

An electronic circuit that converts a source of direct current from one voltage level to another one.



Figure 1.10: DC/DC converter

Since the importance and the role of these components will be further described in following chapters, we will not enter too much into the detail of their description now. The only thing we

want to point out is the fact that in our system configuration the hydrogen is taken from a compressed bottle. This aspect, due to the kind of application, is quite important since the bottle has to be self-sufficient for the period of running of the machine, so needs to be well designed. Although, since the purpose of our study is the response of the PEMFC generator to an electrical load, we will not enter too much into detail on the dynamic of the bottle, but we suppose only to have hydrogen entering the stack at the conditions required. This simplification was also necessary due to the limits of programs used for the generation of the model as we will see later on.

Chapter 2

PROTON EXCHANGE MEMBRANE FC

2.1 PEMFC description

Before starting to study if the PEMFC would work appropriately as a Gen-set, we need to describe in detail how the fuel cell system works. As we know, the fuel cell does not exploit the combustion reaction, but is an electrochemical device made by two electrodes in which the two different electrochemical reactions occur. These electrodes, called respectively anode and cathode, are porous media in which is inserted the electrolyte that in a PEMFC is a solid polymer that has the capability to let the protons move from one side to the other. These cells run at quite low temperature (50°C - 80°C), so the problem of slow reactions rate is addressed by using sophisticated catalyst such as Au, Pt and Ag that are inserted in small percentages.

Concerning the reactions, as we said, there are two electrochemical reactions occurring at the anode and cathode side respectively that are:

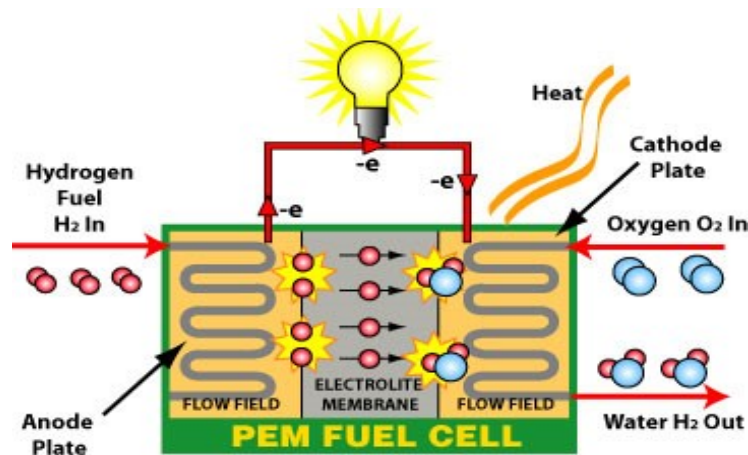
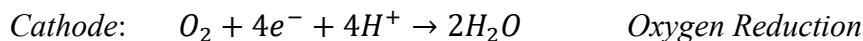


Figure 2.1: PEM fuel cell

The assemble of the two electrodes and electrolyte is called MEA (membrane electrode assembly), and these ones are connected in series, using bipolar plates, in order to form the fuel cell stack. The MEA could have a width of approximately $2.3 \cdot 10^{-4}$ m, so the PEM fuel cell is quite compact. This means that the PEMFC is quite interesting for portable applications, other than mobility and transportation, due to its fast start-up and load following.

2.1.1 Electrolyte

The most used electrolyte for PEM fuel cell is the so called Nafion that is a polymeric material obtained from the polytetrafluorethylene (known as Teflon) through sulphonation.

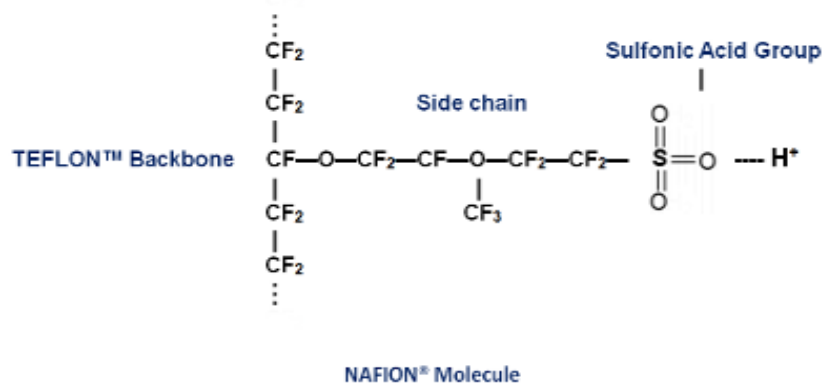


Figure 2.2: Nafion molecule

This is done in order to obtain a group SO_3^- that has the purpose to create a mutual attraction between the ion H^+ and itself. In fact, this bond is very weak permitting a very high mobility of the H^+ ions through the structure of the polymer. But, it is important to say that the hopping mechanism is effective only if the electrolyte is well hydrated, in fact when the Nafion is dried we obtain a very low ion conductivity.

The reason why we use the Nafion as a electrolyte is due to the fact that it creates a good operation conditions since the Teflon backbone is hydrophobic while the sulfonic acid group is hydrophilic, permitting us to obtain an hydrated region that is favourable for the hopping mechanism. For what concerns the ions conducted, in reality, we don't have only H^+ , but also hydrated ions such as H_3O^+ , H_5O_2^+ and H_7O_3^+ . So, in the end, we can resume that the fuel cell has the necessity to maintain hydrated the membrane, maintaining a low temperature in order to control the water content in the electrolyte but at the same time the drying effect of air.

2.2 Fuel cell potential

From thermodynamics we know that the maximum electrical energy available from a cell at a constant temperature T and pressure P is equal to the change in Gibbs free energy:

$$W_{el} = \Delta G^0(T, P) = -z_F \cdot F \cdot OCV(T, P)$$

Where z_F is the number of electrons produced per mole of fuel, and F is the Faraday's constant. For what concerns the OCV (open circuit voltage) instead, it represents the ideal potential of the cell that is the difference in terms of electrical potential between the two terminals of the device when disconnected from any circuit.

Considering a PEM fuel cell, we have that the number of electrons released during the process for 1 mole of hydrogen is 2, so the previous equation becomes:

$$OCV(T, P) = -\frac{\Delta G^0(T, P)}{2 \cdot F}$$

Of course, this potential is valid for standard temperature and pressure, but considering that the PEMFC usually works at higher temperature, we need to write it in this form:

$$OCV(T, P_0) = \frac{\Delta G(T, P_0)}{2 \cdot F} + \frac{R \cdot T}{2 \cdot F} \cdot \ln \frac{\prod_R \left(\frac{P_i}{P_0}\right)^{\nu}}{\prod_P \left(\frac{P_i}{P_0}\right)^{\nu}}$$

In this way, we reduce the open circuit voltage to a certain extent depending on the temperature T of operation. Anyways, the difference is so small that could be considered negligible, so we decide to not considering this aspect in order to simplify the model.

2.3 Electrochemical model

As we understand, the open circuit voltage, seen previously, is an ideal value that in a real operation we cannot obtain. In fact, the lower value respect to the ideal one is due to the irreversible losses in the cell reaction that are proportional to the current drawn by the electric circuit during the operation. This phenomenon is known as polarization, and the link between the voltage and current is described by the so called “polarization curve”.

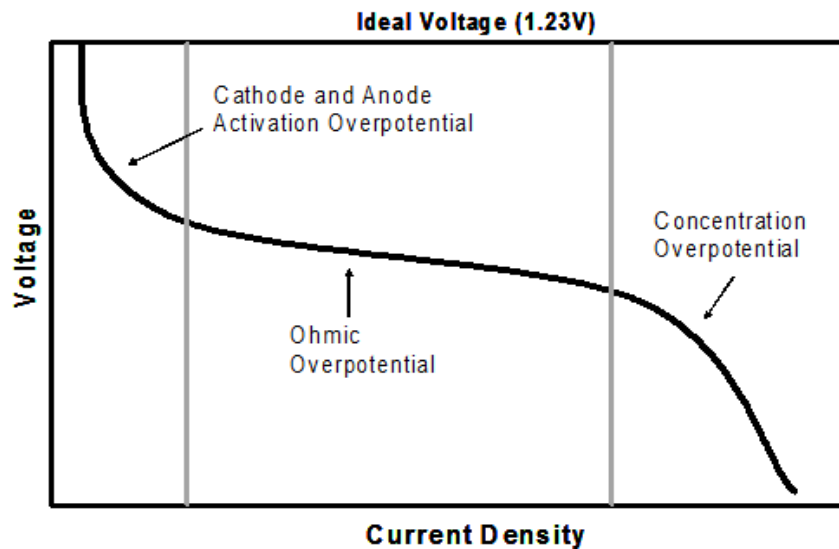


Figure 2.3: Polarization curve

As we can see from the curve, we can distinguish three different zones in which the voltage of the cell V_C and the current I have a different behaviour. In fact, cell's voltage decreases significantly at low currents, after that, the voltage decreases more linearly until higher currents are reached, where another significant drop of voltage is shown. These behaviours are due to different effects that are the following:

- Charge transfer: process related to the kinetic behaviour of electrochemical reactions (this phenomenon is predominant at low currents).
- Charge conduction: process related to the conduction of ions in the electrolyte layer. It is related to the ohmic drop of voltage.
- Mass transport: process related to the molecular diffusion into porous electrodes (this phenomenon is predominant at high currents).

At this point we can distinguish three types of overvoltage according to each of these phenomena that are: activation overvoltage η_{act} , ohmic overvoltage η_{ohm} and concentration overvoltage η_{diff} . In the end, the cell voltage of a fuel cell can be defined by the following expression:

$$V_C = OCV(T, P_0) - \eta_{act} - \eta_{ohm} - \eta_{diff}$$

So, we understand that in order to simulate properly the voltage of the cell, we need to determine an expression for each of these terms which is the purpose of the following paragraphs.

2.3.1 Activation overvoltage

The activation overvoltage can be thought as the drop of voltage “spent” in order to activate an electrochemical reaction, so it represents the voltage required to overcome the activation energy

of the cell reactions. Since the overvoltage considered is the sum of the cathode and anode overpotential, we need to determine each of these two terms that are different, since they depends on the electrochemical reactions occurring at their respective electrode. In fact, the reactions at the anode are very fast in comparison to the cathode ones. For this reason, the anode overpotential is usually neglected.

A way to compute this term is using the so called Butler-Volmer equation:

$$i = i_0 \cdot \left[\exp\left(\frac{\alpha_a \cdot F}{R \cdot T} \cdot \eta_{act}\right) - \exp\left(\frac{\alpha_c \cdot F}{R \cdot T} \cdot \eta_{act}\right) \right]$$

Where i_0 is the exchange current density, which is the reference current density of the electrode, and α is the transfer coefficient, which is a constant that represents the fraction of electrical energy exploited to change the rate of an electrochemical reaction. The last can be expressed as:

$$\alpha_a = \beta \cdot \eta_{RDS}$$

$$\alpha_c = (1 - \beta) \cdot \eta_{RDS}$$

Where β is the symmetric factor while η_{RDS} is the number of electrons transferred in the “rate determining step” (RDS) that is the slowest step of a reaction. In the case of the anode, this value is equal to 4, while it is equal to 1 in the case of the cathode. Instead, for what concerns the symmetric factor, we have assumed a value of 0.5.

In the case we assume equal transfer coefficients in both electrodes, the Butler-Volmer equation is simplified since the two exponential can be cast in the form of a hyperbolic sine function, so the previous expression becomes:

$$i = 2 \cdot i_0 \cdot \sinh\left(\frac{\alpha \cdot F}{R \cdot T} \cdot \eta_{act}\right)$$

At this point, considering the activation overvoltage for both electrodes, we obtain the following expression that represents the activation overpotential of the cell:

$$\eta_{act} = \eta_{act,an} + \eta_{act,cath} = \frac{R \cdot T}{\alpha_{an} \cdot F} \cdot \sinh^{-1}\left(\frac{i}{2 \cdot i_{0,an}}\right) + \frac{R \cdot T}{\alpha_{cath} \cdot F} \cdot \sinh^{-1}\left(\frac{i}{2 \cdot i_{0,cath}}\right)$$

In the table below, we resume all the values used in our simulation for the calculation of the activation overvoltage:

Table 2.1: Input for the η_{act} calculation

Anode data	Value	Cathode data	Value
β [-]	0.5	β [-]	0.5
η_{RDS} [-]	4	η_{RDS} [-]	1
α_{an} [-]	2	α_{cath} [-]	0.5
$i_{0,an}$ [A/cm ²]	0.1	$i_{0,cath}$ [A/cm ²]	0.0002

2.3.2 Ohmic overvoltage

Regarding the ohmic overvoltage, we can say that is related to the conduction of ions in the electrolyte layer and electrons in the electrodes and external circuit. Of course, both of these aspects generate a drop of voltage due to the electrical resistance of the electrodes and due to the resistance against the flow of ions in the electrolyte. For simplification purpose, we consider only the resistance due to the electrolyte since it is the most relevant term. For the sake of defining it, we need to consider the thickness and the average water content of the membrane, in fact, this is a key aspect for the evaluation since the ionic conductivity depends on the level of hydration of the electrolyte. As we know, it depends also on the temperature of the stack and this dependence can be expressed in the following way:

$$\sigma(T_{cell}) = \exp \left[1268 \cdot \left(\frac{1}{303} - \frac{1}{273 + T_{cell}} \right) \right] \cdot \sigma_{30}$$

$$\sigma_{30} = 0.005139 \cdot \lambda - 0.00326$$

Where λ is the water content of the membrane that is a function of the temperature and level of humidification of the reactant streams entering the stack. At this point, the ohmic overvoltage can be determined by the following equation:

$$\eta_{ohm} = \rho \cdot t_m \cdot i = ASR \cdot i$$

Where ASR is the area specific resistance that depends on the resistivity (inverse of the ionic conductivity) of the Nafion and on the thickness of the electrolyte layer.

Table 2.2: Input for the η_{ohm} calculation

Data	Value
T_{cell} [°C]	70
λ [-]	8.5
t_m [cm]	0.0183

2.3.3 Diffusion overvoltage

The diffusion overvoltage is a drop of voltage related to the molecular diffusion through a porous electrode. This means that it becomes more important at high currents when the rate of reaction is higher. In fact, in this condition the mechanism of diffusion of molecules in the porous electrode becomes too slow to replace with enough speed the molecules that react over the catalyst, causing a progressive reduction of the concentration in the active layer and consequently a reduction of the partial pressure and voltage. This can be easily seen from the Nernst's equation, expressed in terms of concentrations, written below:

$$OCV(T, P_0) = \frac{\Delta G(T, P_0)}{2 \cdot F} + \frac{R \cdot T}{2 \cdot F} \cdot \ln \frac{\prod_R C_R^v}{\prod_P C_P^v}$$

To obtain explicitly a relation between the diffusion overvoltage and the current, we have to describe the variation of concentration that happens in the electrode due to the Nernstian effect. To do this, we can consider to apply the Fick's law, expressed by the following equation:

$$J = -D \cdot \nabla C$$

It describes the phenomenon of diffusion and tell us that the diffusion flux goes from a region of high concentration to a region of low concentration. Looking at this equation, we can easily understand that the concentration gradient increases until we reach the condition in which the concentration at the active surface falls to zero. This is the condition in which there is no reaction where we have the maximum current density, called "limiting current density".

At the end, the diffusion overpotential can be mathematically correlated to the limiting current density obtaining the following expression:

$$\eta_{diff} = \eta_{diff,an} + \eta_{diff,cath} = \frac{R \cdot T}{2 \cdot F} \cdot \ln \left(1 - \frac{i}{i_{l,an}} \right) + \frac{R \cdot T}{4 \cdot F} \cdot \ln \left(1 - \frac{i}{i_{l,cath}} \right)$$

Of course, is clearly obvious that in the moment we reach the lowest value among the two limiting current densities, the reaction cannot proceed since there is a lack of one of the

reactants. So, we understand that this value is the ideal maximum value we can achieve in our simulation even if, in reality, there are other considerations to make that will reduce it further more.

Table 2.3: Input for the η_{diff} calculation

Anode data	Value	Cathode data	Value
$i_{l,an}$ [A/cm ²]	1.5	$i_{l,cath}$ [A/cm ²]	0.75

2.3.4 Internal current density

At this point, to complete the model, we need to consider the losses due to the crossover effects, in fact the conduction of the electrons and fuel in the Nafion generates a drop in voltage of the cell. To solve this problem we need to add a fictitious current to the current density, which is called “internal current density”. This term is quite interesting since it takes also in consideration the experimental fact that, at open circuit, the voltage of the cell is lower than the reversible one. In our simulation we have assumed, for this term, a value of 0.002 A/cm².

2.4 Water management

As we said, talking about the electrolyte, the water management is a key aspect of a PEM fuel cell, and, for that reason, has to be properly considered in the model. To do so, firstly, we have considered the effect of temperature, since, at temperature higher than 50°C, this aspect is not negligible due to the drying effect of the air. In fact, in this condition the water produced during the operation by the electrochemical reactions could not be sufficient to maintain a correct humidification of the cell. So is quite necessary to add a humidification section to the stack.

In our model, a humidifier that recovers the water exiting with the stream at the cathode side is considered. This means that the correct level of hydration of the cell is achieved through internal humidification that occurs to the streams before entering the stack. In the current model, we consider to humidify only the air stream, since we suppose that the anode side would be hydrated by the phenomenon of water crossover that we will explain later on.

Regarding the humidification section, we model it fixing the value of the relative humidity (RH), that is defined as the ratio of the partial pressure of vapour, to the partial pressure of the saturated mixture at the same temperature:

$$RH = \frac{P_v(T)}{P_{sat}(T)}$$

To compute the partial pressure of the saturated mixture we used the Buck equation since it is the most accurate model in the range of temperature between 0 and 100 °C. In fact, the vapour pressure has a non-linear dependence on the temperature, as we can see from the following formula:

$$P_{sat} = 0.61121 \cdot \exp\left(\left(18.678 - \frac{T}{234.5}\right) \cdot \left(\frac{T}{257.14 + T}\right)\right)$$

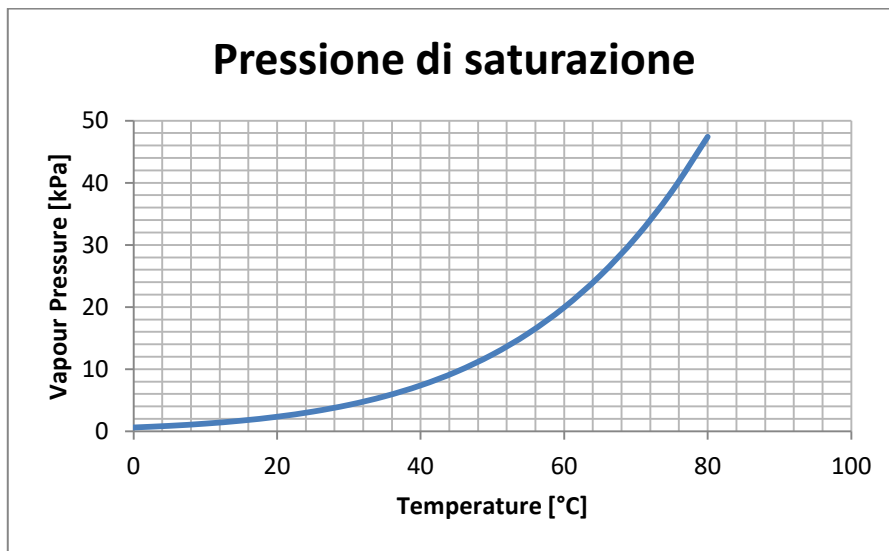


Figure 2.4: Vapour pressure plot

So, we understand that this aspect is something to keep in mind when we select the optimal temperature of operation.

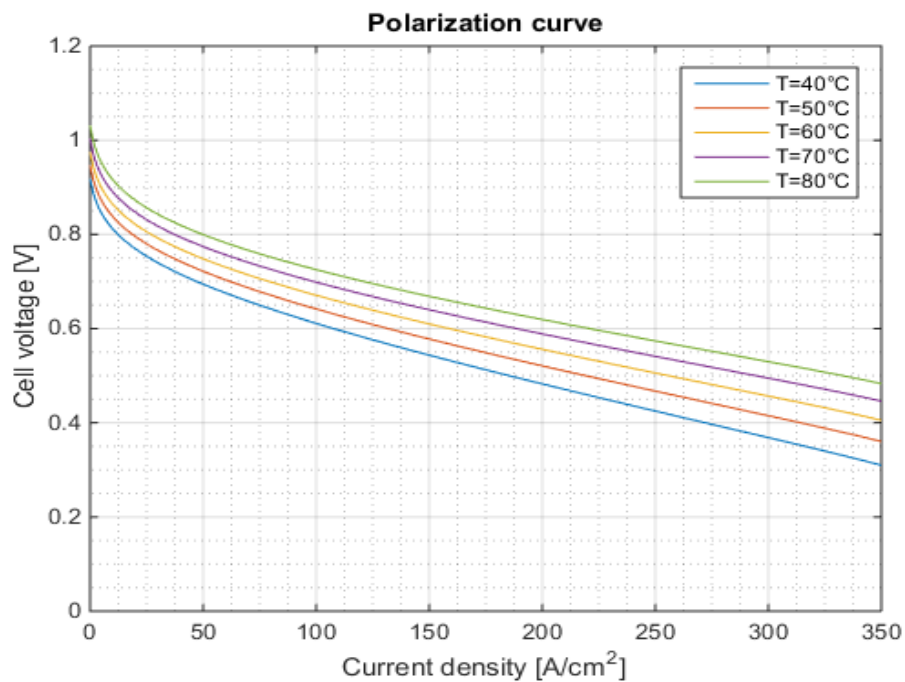


Figure 2.5: Polarization curve at varying temperature of operation

In fact, as we can see from the plot at higher temperature, we have better performance reducing both the activation and ohmic overpotential, but we also increase problems with the humidification section. Lastly, after considering all these aspects, we decide to select a value of temperature around 70°C, which is a quite standard temperature of operation for a PEMFC. In this way, we make an improvement of the cell working conditions, avoiding at the same time problems with the sizing of the humidification section.

For what concerns the partial pressure of vapour in the stream entering the stack, it can be evaluated based on the molar fraction of water containing in it. In fact, we have this:

$$P_v = x_v \cdot P_{stream}$$

So, at the end, the water quantity requested by the humidification section is obtained as:

$$x_v = RH \cdot \frac{P_{sat}}{P_{stream}} \rightarrow m_{H_2O} = x_v \cdot m_{stream}$$

This represents the amount of water transferred from the cathode exhaust to the inlet stream entering the stack. Of course, we need to check that the amount of water produced by the cell is enough to fulfil the request of the humidification section.

2.5 Water crossover

At this point, in order to complete the description of all the phenomena occurring inside the cell, we need to add other two phenomena, called respectively “osmotic drag” and “back diffusion”.

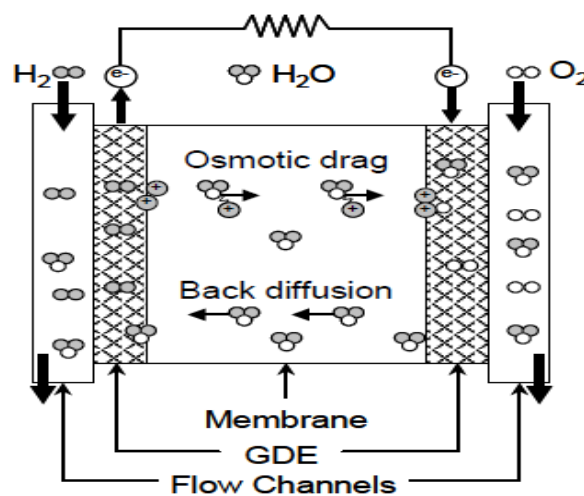


Figure 2.6: Water crossover phenomena

These two, as we can see from the picture, are water transport phenomena that occur across the MEA. In fact, the first consists in the transportation of water molecules dragged along with

protons, while the second one is a movement of water caused by the difference in water concentration at the two electrodes. Moreover, in order to describe in detail these two aspects, we need to understand that both of them depend on the water content in the electrolyte, so we need to enter much in depth in the description of this important parameter.

The water content λ represents the amount of water uptake per sulfonic acid groups, and, as we said before, it highly influences the ionic conductivity of the membrane. It is assumed that the water content at the interface is determined by the activity of the water vapour present between the electrode and the membrane. The following expressions are used:

$$\lambda = 0.043 + 17.18 \cdot a_w - 39.85 \cdot a_w^2 + 36 \cdot a_w^3 \quad 0 \leq a_w \leq 1$$

$$\lambda = 14 + 1.4 \cdot (a_w - 1) \quad 1 < a_w \leq 3$$

In the former study we also assumed a linear water content profile across the membrane thickness [6], so the water content of the entire membrane is evaluated as:

$$\lambda = \frac{\lambda_a + \lambda_c}{2}$$

Normally this parameter varies between a range depending on the working condition considered, but if the electrolyte is well hydrated this parameter assumes the value of 14, as we can easily see from the relationships written above. The water activity, instead, is defined as the ratio of the partial vapour pressure to the saturated pressure:

$$a_w = \frac{P_w}{P_{sat}}$$

2.5.1 Electro-osmotic drag

Regarding the electro-osmotic drag, we can say that, in order to describe this phenomenon, we need to determine how many molecules of water are transported with each molecule of ion H^+ . So, we need to determine the so called electro-osmotic drag n_{drag} that is the number of dragged molecules that varies from 0.5-5 water molecules per hydrogen ion. It is obtained from the following relationship:

$$n_{drag} = 2.5 \cdot \frac{\lambda_m}{22}$$

At this point, the water molar flow rate due to the electro-osmotic drag can be obtained as:

$$G_{H_2O,drag} = 2 \cdot n_{drag} \cdot \frac{i \cdot A}{z_F \cdot F}$$

2.5.2 Back diffusion

For what concerns, instead, the back diffusion phenomenon, we can say that it depends on the diffusion coefficient that is expressed by the following relationship:

$$D_w = D_\lambda \cdot \exp \left[2416 \left(\frac{1}{303} - \frac{1}{T_c} \right) \right]$$

As we can see, the diffusion coefficient is a function of temperature and water content of the membrane, where the last one dependency is casted on the term D_λ that can be expressed as:

$$D_\lambda = 10^{-6} \cdot (2.563 - 0.33 \cdot \lambda_m + 0.0264 \cdot \lambda_m^2 - 0.000671 \cdot \lambda_m^3)$$

At this point, the water molar flow rate due to the back diffusion can be obtained as:

$$G_{H_2O,diff} = \frac{\rho_m}{M_m} \cdot D_w \cdot \left(\frac{\lambda_c - \lambda_a}{t_m} \right) \cdot A$$

Table 2.4: Nafion 117 input data [6] [7]

Parameter	Value
t_m [cm]	0,0183
ρ_m [g/cm ³]	1,98
M_m [g/mol]	1100

2.6 Thermal management

During the operation of the cell, there is also generation of heat because of the irreversibility. This, of course, has to be removed in order to control the temperature in the stack for the reasons explained above. To do so, the best solution is to cool down the system with a cooling fluid (air, demineralized water or water + glycol), that depends on the use of this heat and on the environmental conditions. In our model, we suppose to maintain constant the temperature of the stack, controlling the coolant flow rate, that, in our case, is simply demineralized water, since we would give some use to the heat recovered. From the theory, since we are working with a galvanic cell, we know that the heat produced by the stack is equal to:

$$\phi_{th,stack} = \left(-\frac{\Delta h}{z_F \cdot F} - V_c \right) \cdot n_c \cdot I$$

At this point, the mass flow rate of the coolant can be easily obtained as follows:

$$G_{H_2O} = \frac{\phi_{th,stack}}{c_{p,H_2O} \cdot (T_{H_2O,out} - T_{H_2O,in})}$$

We assume to maintain the temperature of the coolant exiting the stack equal to 60°C in order to get a pinch point of 10°C. For what concerns, instead, the temperature of the coolant entering the stack, we assume it equal to 50°C, in order to avoid thermal gradients in the stack.

2.7 PEMFC characteristics

Considering all the aspects described in this chapter, the characteristics of the single PEM fuel cell modelled (see appendix A.1) present a quite standard behaviour along all the range of possible operation.

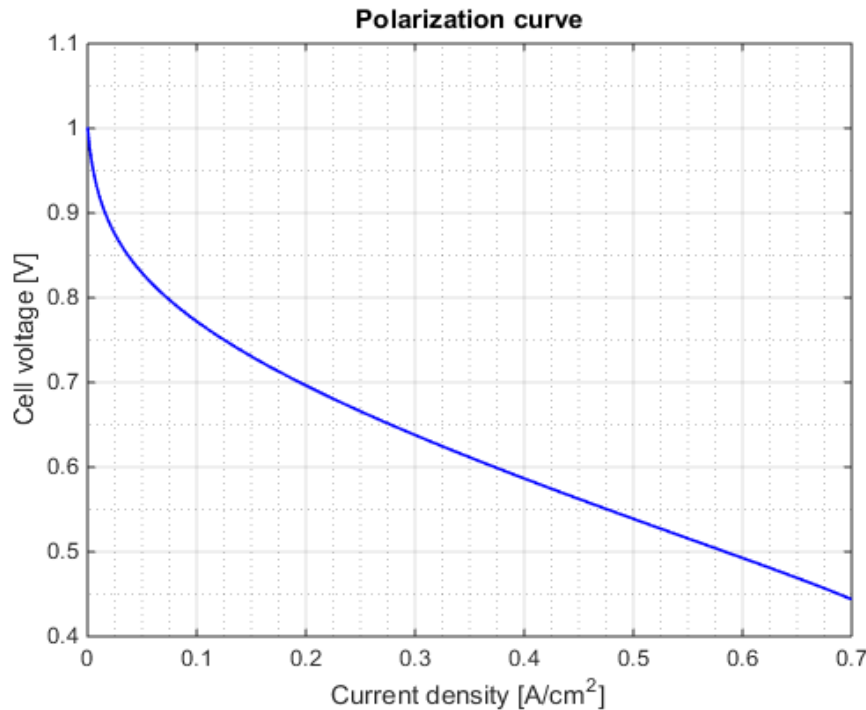


Figure 2.7: PEMFC polarization curve at 70°C

Looking at the former plot, is relevant pointing out that the curve cannot proceed over the value of current density of 0.75 due to how the diffusion overvoltage is modelled. In fact, after this point the model considered is not reliable and the values obtained are meaningless. So, the high effects of this overpotential term are not shown as in figure 2.3. Anyway, this range of operative condition is not even taken into account during real operation, and, for that reason, is not considered in the modelling of the cell.

Regarding the cell power, we can notice the fact that its value is quite low to cover the user consumption. For this reason, we need to consider a higher amount of cells depending on the size of the generator set needed.

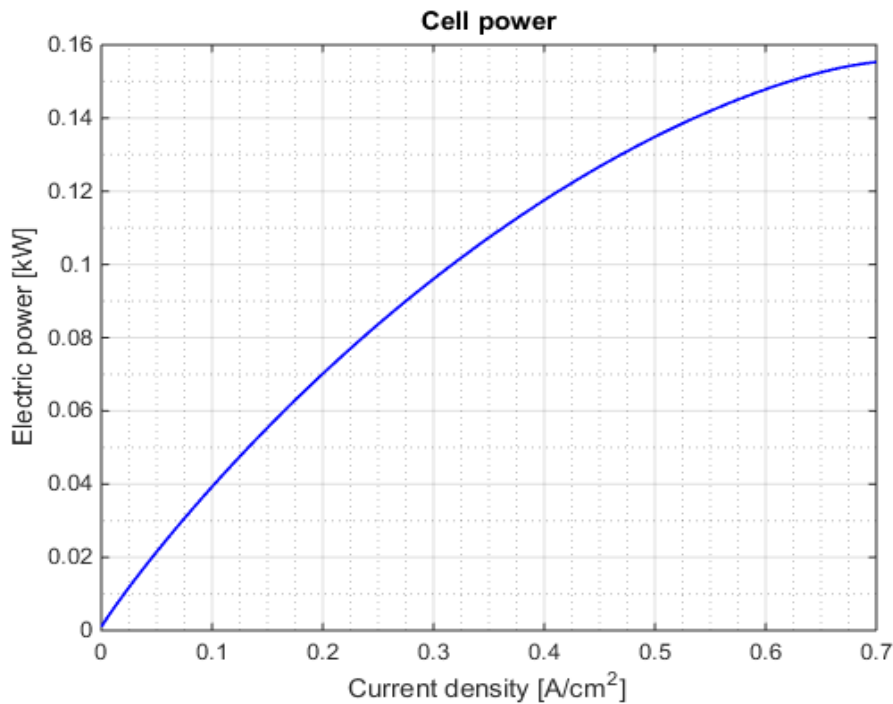


Figure 2.8: PEMFC power characteristic

For what concerns the cell efficiency, we need to make some considerations to better underline how these values are obtained. In fact, since we are not able to measure the real consumption of fuel of the cell we need to assume a specific value for those. We consider that the amount of hydrogen consumed is equal to the one obtained by the Faraday's law:

$$\dot{n}_{H_2} = \frac{I}{z \cdot F} \cdot PM_{H_2}$$

This aspect is quite important since during operation the amount of hydrogen supplied to the cell varies depending on the conditions reached, as we will see later on. Said that the efficiency of the cell is computed as following:

$$\eta = \frac{P_c}{LHV_{H_2} \cdot G_{H_2}}$$

As we noticed, this efficiency is related only to the cell, as expected, and of course it will differ from the efficiency of the system of the gen-set since the power produced by the cell will be depurated by all the power requested by the auxiliary components needed for the correct operation of the device.

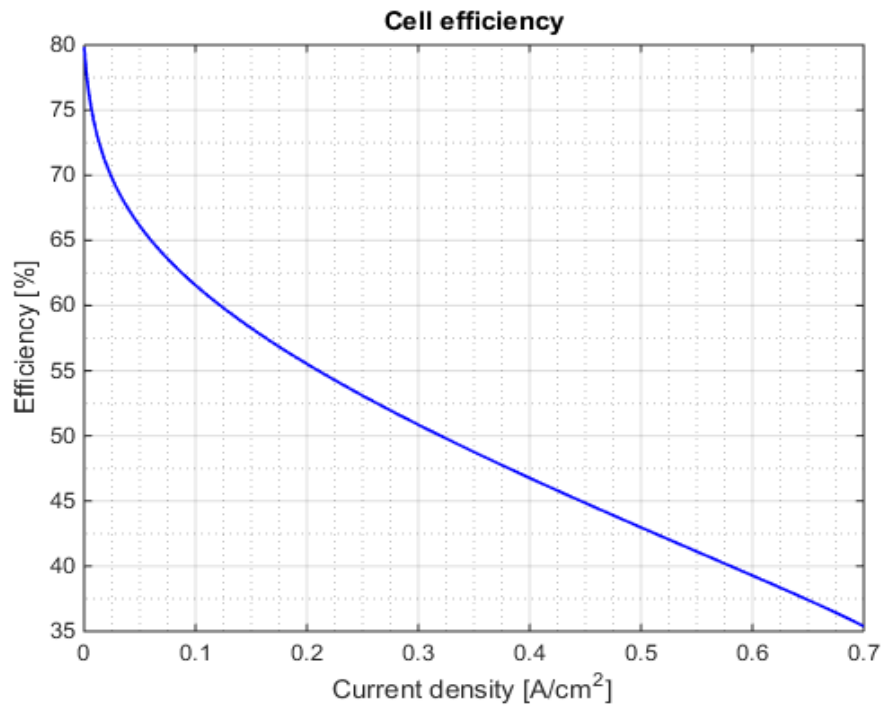


Figure 2.9: Cell efficiency

Chapter 3

LOAD PROFILE AND ASPEN MODELLING

3.1 User load profile

As we have discussed before, the purpose of our study is to make an analysis of the response of the device under load variations during the period of operation. To do so, seems necessary to have a profile of the consumptions of the users for a given machine under operation. In fact, in order to verify if the PEMFC gen-set can follow the variation of load as the traditional solution, a load profile is needed, but due to the difficulties encountered during the searching, we decide to recreate such load using the data of consumption of the common tools reported on the table 1.1. To do so, we select some of the tools reported, using the corresponding values as consumption during the interval of period we suppose to use it.

Table 3.1: Electrical tools chosen for the load profile [4]

Tool	Starting wattage [W]	Running wattage [W]
Circular saw	2400	1200
Drill	1800	720
Planer	2400	960
Miter saw	2100	840
Chainsaw	2400	1200
Winch	5400	1800
Disc grinder	4000	2000
Water pump	3000	1000
Concrete cutter	3600	1800
Jig saw	1800	720
Disc sander	1200	1200

In order to put the right value of consumption in the right time step, we need to underline the difference between the starting and running wattage. In fact, these values differ a lot from each other, so it is quite important to make some considerations. Considering a discretized time step

of 10s for the creation of the load profile, we suppose to use the starting wattage only for the time step in which the tool is connected, while, in the remaining time, the consumption is supposed to be equal to the running wattage. This was supposed to be in this way due to the rapidity of lighting of the electrical devices connected to a source of electricity. In fact, we have that the time of start-up of electrical engines (period in which peak currents occur) is quite low and depends on the size of the engine as we have seen in [8]. In our case, since we are considering electrical tools with low power, we can easily confirm the hypothesis made and at the same time being conservative. Said that, considering the connection and disconnection of these tools to the device, the load profile is easily obtained.

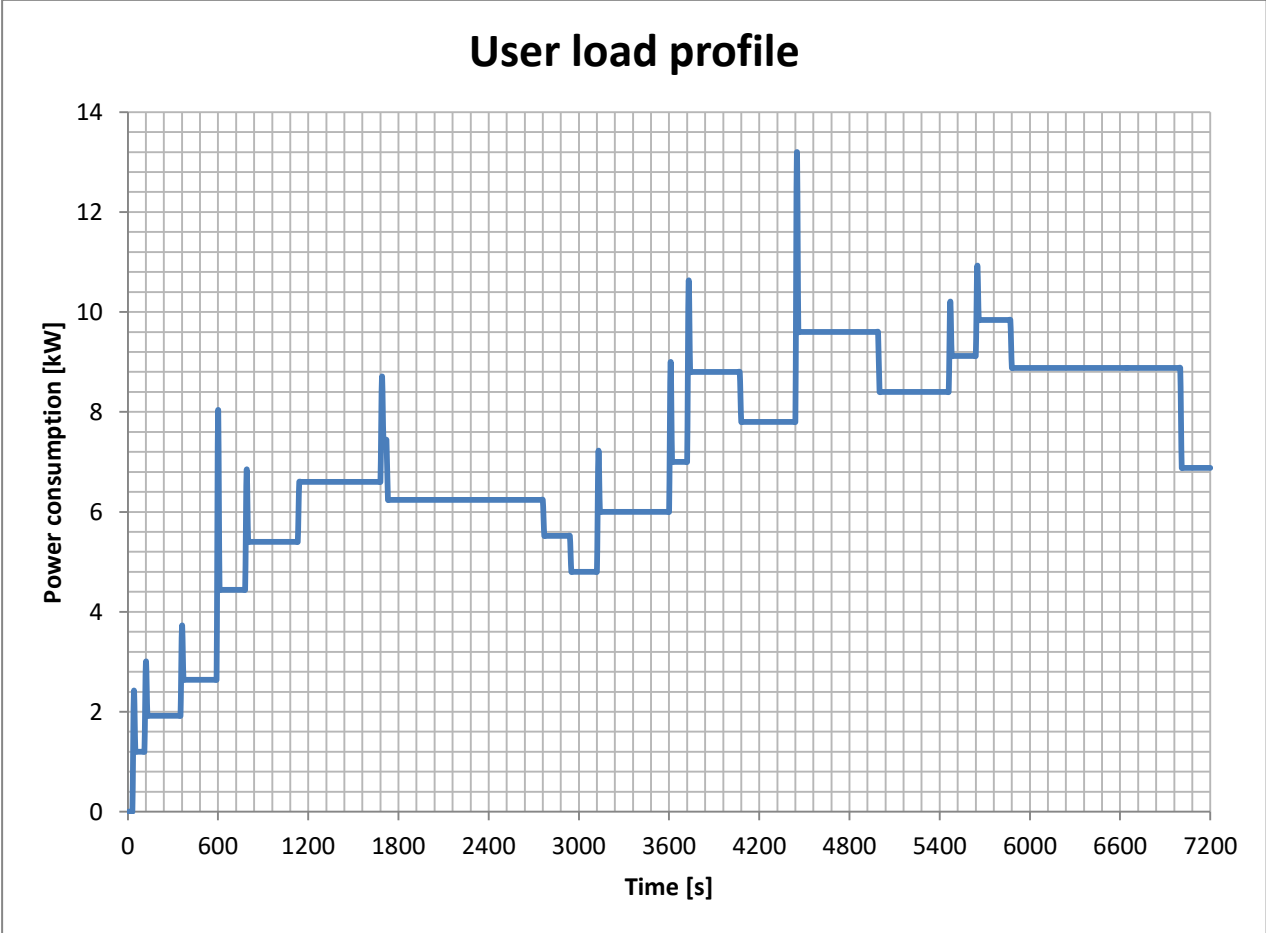


Figure 3.1: Electrical consumption profile

As we notice from the profile above, the variation in time of the request of power is quite oscillating depending on the tools connected, anyway, the higher fluctuations occur especially during the connection or disconnection of a tool. In fact, during this time step, the request of power is quite high, resulting in a peak that in some way needs to be satisfied. This point is quite important for what concerns the response of the device due to some restrictions that we will better explain later on.

3.1.1 Gen-set sizing

At this point, in order to proceed with the modelling of our generator set, we need to determine its size, but, since the purpose of our thesis is to study the response of our device to a certain load profile, we will not enter too much into detail on this aspect, giving us only an overall idea of the variation between different size solutions. Then, considering the cost of the entire system as a criteria, we choose the best solution for our type of application. Said that, we decide to make the analysis for three different sizes that are respectively 6, 8 and 10 kW. These three values were chosen looking at the user load profile that we are expecting to have. In fact, the lower size tends to maximize the labour of the gen-set, while the higher one tends to minimize the battery support. For what concern, instead, the size of 8 kW, we can consider it as a compromise between the two extreme solutions.

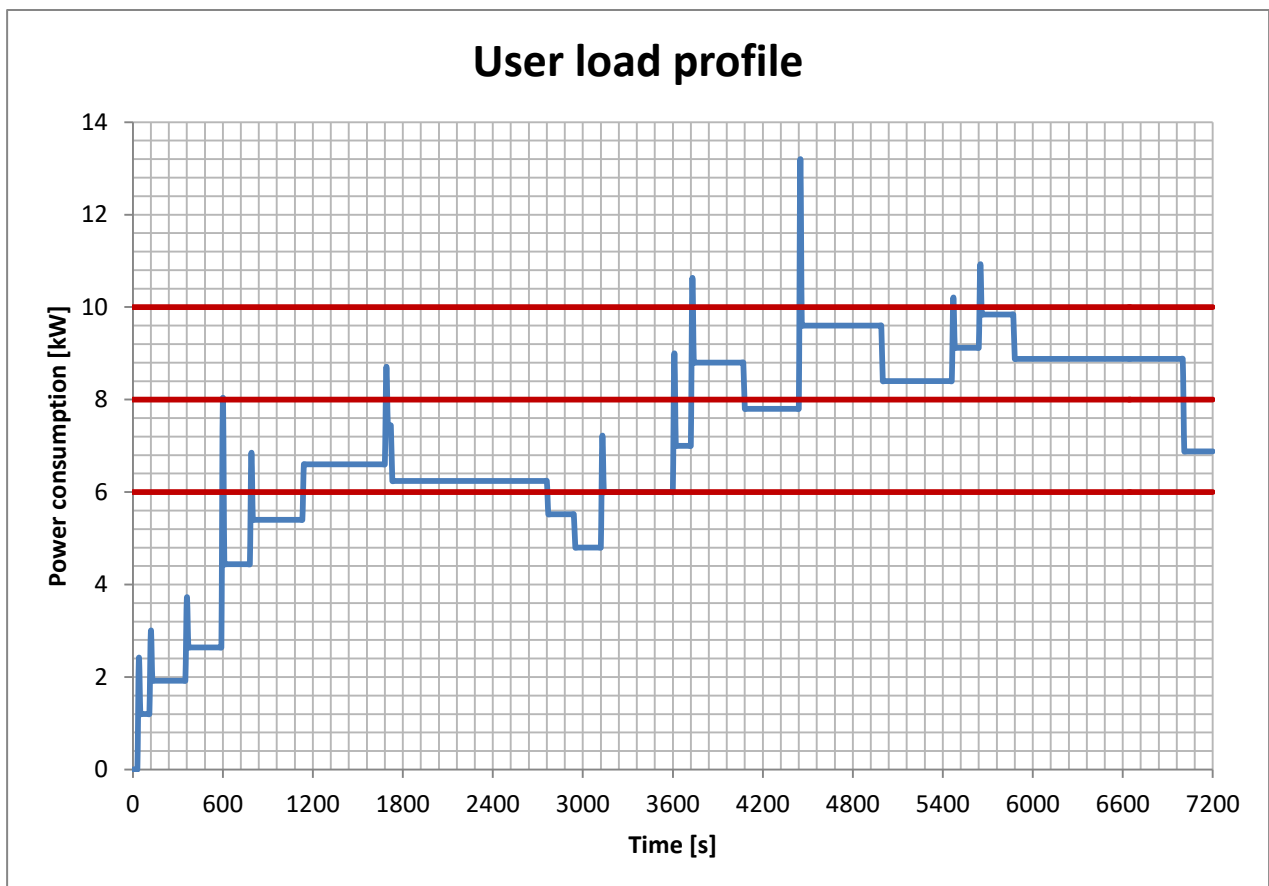


Figure 3.2: Comparison between the gen-set sizes chosen and the user load

Regarding the maximum size, it is chosen after making the consideration that the peaks have to be inevitable covered by a bank of batteries due to the limits of the gen-set during load variations. So, made this assumption, seems quite acceptable not considering the load peaks above 10kW since anyway they will be partial covered by the support battery. Otherwise, we risk to oversize the device reducing the efficiency of the entire system.

Finally, we need to point out that generally Diesel generators are sized considering the fact that they have to cover all the consumption plus the higher starting wattage, but in our case we operate differently considering that a support battery is necessary.

3.2 System configuration

In the current model, as described in the previous chapter, the fuel cell is supported by other subsystems, which have the role to maintain some of the key parameters under control. Regarding the fuel cell, we have considered a stack made by 56, 73 or 90 cells of area of 500 cm². Of course, the number depends on the size under analysis, since we suppose to use the same type of cells for all the three configurations. For what concern the net electric power produced by the stack, it is obtained considering the power consumed to move all the auxiliary components such as the blower and the pumps.

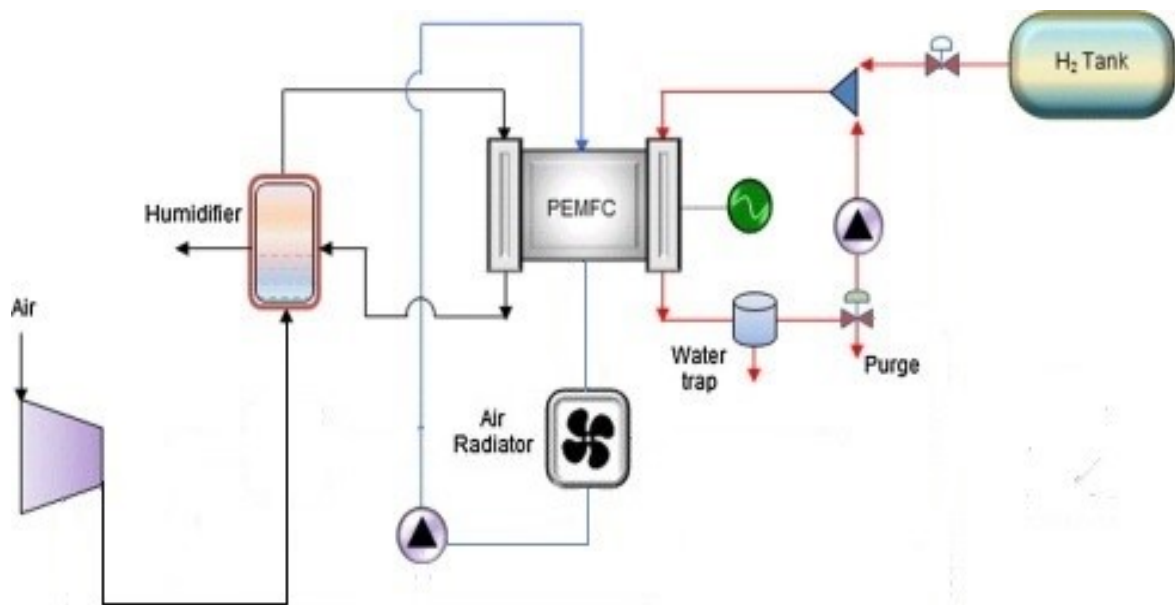


Figure 3.3: System configuration

The streams entering the stack are made principally by hydrogen and air in the anode and cathode side respectively. For what concerns the hydrogen, it is supposed to be get from a pressurized tank at 200 bar and ambient temperature. While the condition of temperature and pressure of the hydrogen entering the anode side of the stack is 44° C and 1.2 bar respectively. Regarding the anodic pressure, we have that its value is controlled and reduced, through a regulation valve, from the tank pressure before entering the stack. Concerning instead the anodic temperature, it has a value that is under the range of operability of a PEMFC that is around 60-80 °C, but could be considered acceptable since its value is not too far from this range, otherwise an anodic pre-heater should be added leading to a more complex BOP (balance of plant) of the

entire system. Anyways, this could be considered also as an option for further improvements when we recover the heat released by the stack. On the cathode side instead, the air is considered taken from the external environment at 1 bar and 25°C, but the cathodic inlet conditions are more variable due to the amount of water added in the humidification section. Both streams present in their composition a specific amount of water depending on the humidification and water crossover effect respectively. In order to optimize the utilization of the fuel, an anodic recirculation is considered, in fact, in this way, the fuel in excess, caused by technical difficulties in the supply inside the cells, is not wasted. To do so, an anodic blower is added, but in order to maintain a good working operability and durability of the machinery we need to recirculate only vapours. For this reason in the recirculation circuit there is also a water separator that has the purpose of separate the water condensed on the anode stream. In this way, only the vapour has to be considered recirculated. In fact, we suppose to recirculate only a saturated mixture in order to maintain the amount of water under control. In addition to that, we limit the maximum current exploitable in order to avoid the drying of the electrolyte and the addition of a humidification section, also on the anode side. In fact, at high currents above 270-280 A, we realise that the electro-osmotic drag effect becomes more relevant than the back diffusion effect, causing a quick dehydration of the electrolyte. To determine this maximum value, a Matlab code (see appendix A.2) is implemented. In this way, some interesting results to use for the implementation of the Aspen model are obtained, avoiding further complexity to the simulation in Aspen Plus.

For the calculations, a fixed relative humidity at the cathode side is assumed and it is equal to 0.95. For what concerns, instead, the relative humidity of the anode stream entering the stack, it is computed during the running of the code considering that at least its exiting stream has to have a $RH=0.80$. This is the relative humidity of the portion stream that is recirculated and its value is selected in order to ensure a good hydration of the membrane during any load configuration of the gen-set. In this way, during normal operation of the device the RH of the stream exiting the anode is always higher than this limit, letting us to not add an humidification section on the anode side due to the good amount of water exiting with the excess of fuel. Of course, due to the presence of the water separator, the RH of the stream exiting the anode has to be checked in order to separate the amount of water condensed when it is needed.

At this point, after pointing out these main assumptions, we need to explain how we obtain the relative humidity at the exit of the anode side. Regarding that, a water balance of the cell is done, so all the equations reported in the paragraph 2.5 are used in order to compute the net water crossover inside the electrolyte. But, since the steady-state conditions inside the membrane at the

beginning of the code are unknown, a for cycle is used in order to repeat all these calculations, updating the appropriate variable involved until the results stabilize. In this way, the amount of water present in the anodic inlet streams is updated, letting us to compute a more realistic water activity and consequently a more precise value of the water content inside the cell. After that, since the current at the beginning of the code is the variable we are interested in, we vary its value in order to verify current by current if the anodic condition considered at the exit is not overcome. At this point, the range of operation in which our device is supposed to work is determined as the range of current where this condition is satisfied.

At the end, the range of current density of the stack resulted by these calculation is 0-0.4 A/cm² (corresponding to 0-200 A), because in this condition, as we explained before, we have that the electro-osmotic drag effect is less relevant than the back diffusion one, permitting us to ensure a correct level of hydration of the cell in all the range of operability. This of course can vary with the size, so we need to point out that these results are obtained referring to the case in which the size of the gen-set is equal to 10 kW.

3.3 Fuel cell modelling

Before talking about the response of the system under operability we will describe how the model was created since this aspect is quite important due to the limits of the programs used. In fact, one of the drawbacks that results from the use of Aspen Plus is the impossibility to work in dynamic condition since the program simulate only steady-states. So, in order to still make a dynamic simulation, we suppose to work in semi steady-state condition, running the simulation for each variation of the working condition during the period of operation. Of course, this solution is not completely equal to what happens in reality, but it still remains a good approximation of the global response of the device. Another problem encountered during the realization of the model in Aspen Plus, was the lack of the component fuel cell. In fact, for whom knows the program, Aspen Plus contains a vast library of component models incorporated into the program that are ready to be used. In our case, to solve the problem, we considered the two electrodes separately, in fact the anode side has been replaced by a separator, while the cathode side has been replaced by a Gibbs reactor that simulates the reaction of formation of the molecule of water. Of course, the separator has the role to separate the amount of hydrogen that would be transferred by the electrolyte to the cathode side, so it carries out the role of the electrolyte.

Since the anode and the cathode are separated components, we have to correct the condition of the excess in the anode exhausts. To do so, we add to the system an heat exchanger HEAT-H2

that fixes the temperature of the exhaust stream at 70°C, simulating better what happens in reality. Of course, the heat used to heat up the stream is picked up from the energy released by the Gibbs reactor as we would happen in reality.

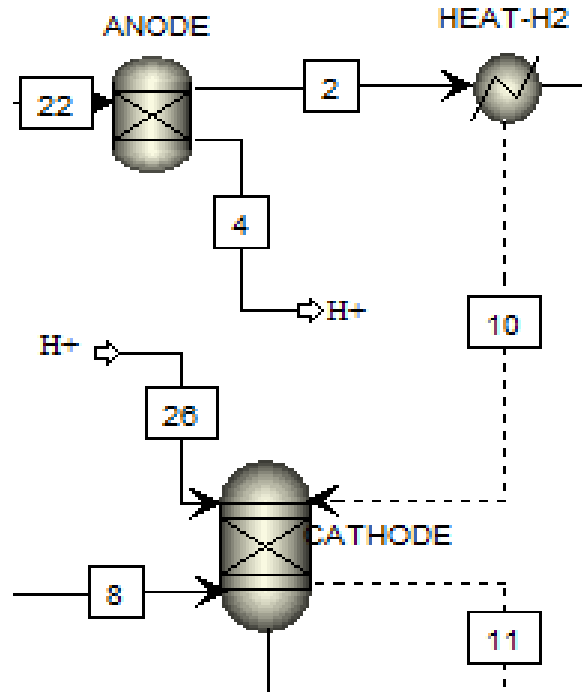


Figure 3.4: Aspen modelling of the FC

The lack of the component fuel cell in the Aspen library leaves us another point for which we need to find a solution, that is how to simulate the balance equation of heat in the FC. From the theory we know that the total energy entering the fuel cell is drained by the electrical power output, by the heat removed by the coolant and by the heat stored in the stack:

$$C_{th} \cdot \frac{dT}{dt} = - \frac{(\Delta h_{f,H_2O}^{\circ}(v))}{z_F \cdot F} \cdot I - V_C \cdot I - Q_{loss}$$

Of course, since we are working in steady-state condition the term related to the heat stored in the stack is not present and the equation results to be:

$$- \frac{(\Delta h_{f,H_2O}^{\circ}(v))}{z_F \cdot F} \cdot I - V_C \cdot I - Q_{loss} = 0$$

This is of course an approximation, but is quite acceptable after the start-up since we suppose to maintain the temperature of operation under control and at a fixed value equal to 70°C. During the start-up instead, other arrangements will be made, but since the PEMFC is very quick to heat-up the necessity to give big importance to this aspect is quite unnecessary, especially for the

stationary application considered. Anyway, we will address this aspect when we will talk about the load following on the next chapter.

Turning back on the terms of the previous equation we can say that only the term related with the heat of formation is calculated directly by Aspen, while, the other two terms, are obtained by calculator blocks and artifices. Anyway, the results obtained by the model are checked by the handmade calculations done previously for a specific working condition.

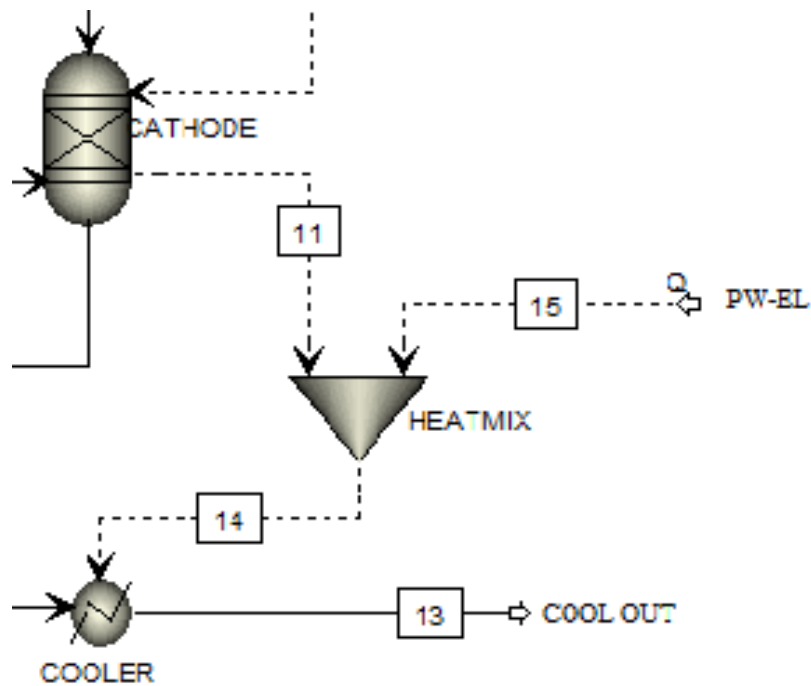


Figure 3.5: Aspen modelling of the heat equation

As we noticed from the former picture, the heat balance equation is addressed by the Aspen component HEATMIX that has the purpose to calculate the heat removed by the coolant. Of course, this component does only a difference between two power terms that are respectively the heat generated by the formation of the water (output of the Gibbs reactor), and the electrical power produced during the operation by the stack. To do so, a prior calculation of the electrical power output of the stack is necessary since it is needed as an input for the component HEATMIX. This is achieved through the use of calculator blocks that we will explain better on a next appropriate paragraph. Regarding the result of this difference, it is used to determine the coolant flow rate through a design specification where the variable is the mass flow rate and the target to achieve is the temperature of the coolant exiting the stack fixed to 60°C.

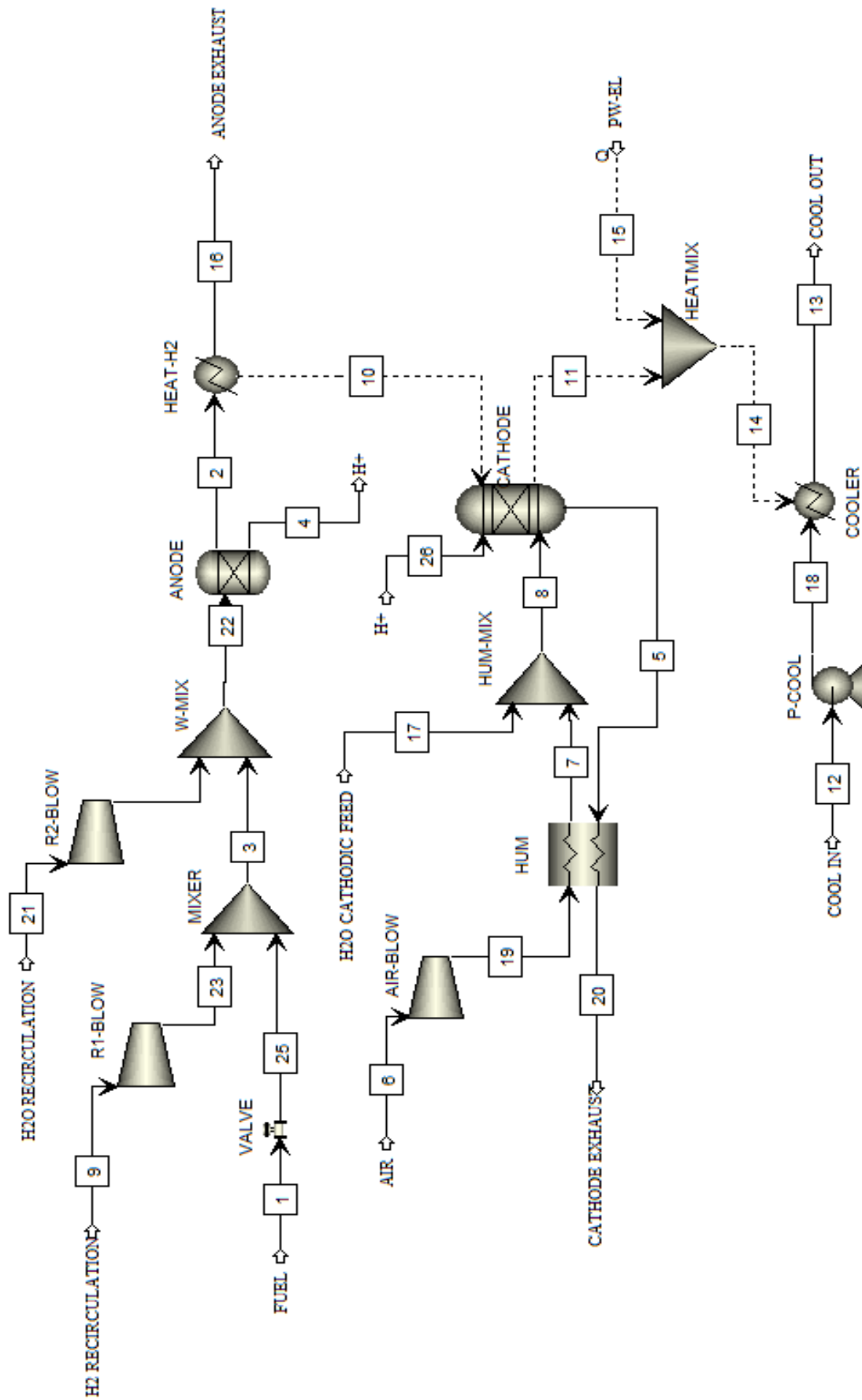


Figure 3.6: Aspen modelling of the BOP configuration

3.4 Humidification modelling

Regarding the humidification, as we said before, we have that the anode side is self-humidified through the water crossover effects, while the cathode side is internally humidified by the recovery of water produced by the stack. In order to do so, a humidifier based on membranes is considered. This solution is quite interesting since it let us to exploit an amount of the water exiting the cathode that cannot be used anyway, but, at the same time, it permits us to recover a partial heat from the cathode exhausts.

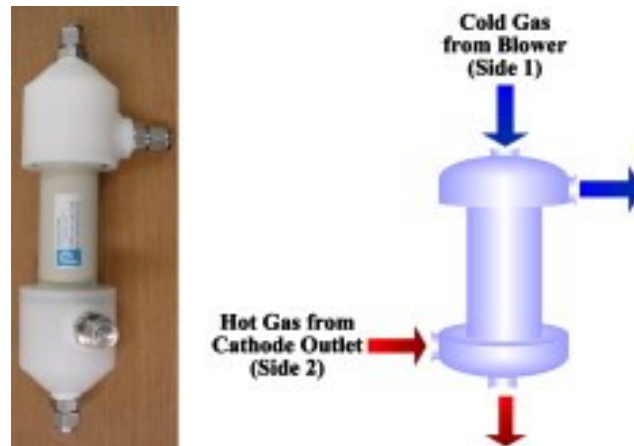


Figure 3.7: Membrane humidifier

In order to model these two humidification process, we start computing, through calculator blocks, the amount of water that has to be added to the anodic and cathodic stream respectively. Referring to the stream 21 (H₂O RECIRCULATION) for the humidification of the anodic stream, we have that this is obtained through recirculation from the stream exiting the anode. In fact, the stream 21 (water based flow) represents the amount of water contained in the recirculation stream and together with the stream 9 (hydrogen based flow) forms the recirculation stream that is mixed with the main anodic stream 25 entering the stack. Of course, the values of the stream 21 and 9 vary in the range of operation, depending on the working condition considered. This due to the fact that the RH, at the anode exit, varies in the range of current considered. In fact, looking at the profile in figure 3.8, we have that the relative humidity at the anode exit is pretty constant for low current densities, while decreases linearly at high values of it. For what concerns the point, after which the RH starts decreasing, it depends on the size. This aspect can be easily seen from the figure 3.9, where the effects of the size on the humidity of the anodic stream exiting the stack are shown. Looking at the plot, we can, also notice how higher is the power produced by stack, higher is the ease to incur into the dehydration of the anode side. This is an important aspect to take in consideration, since from it depends the necessity to have an external anodic humidification section.

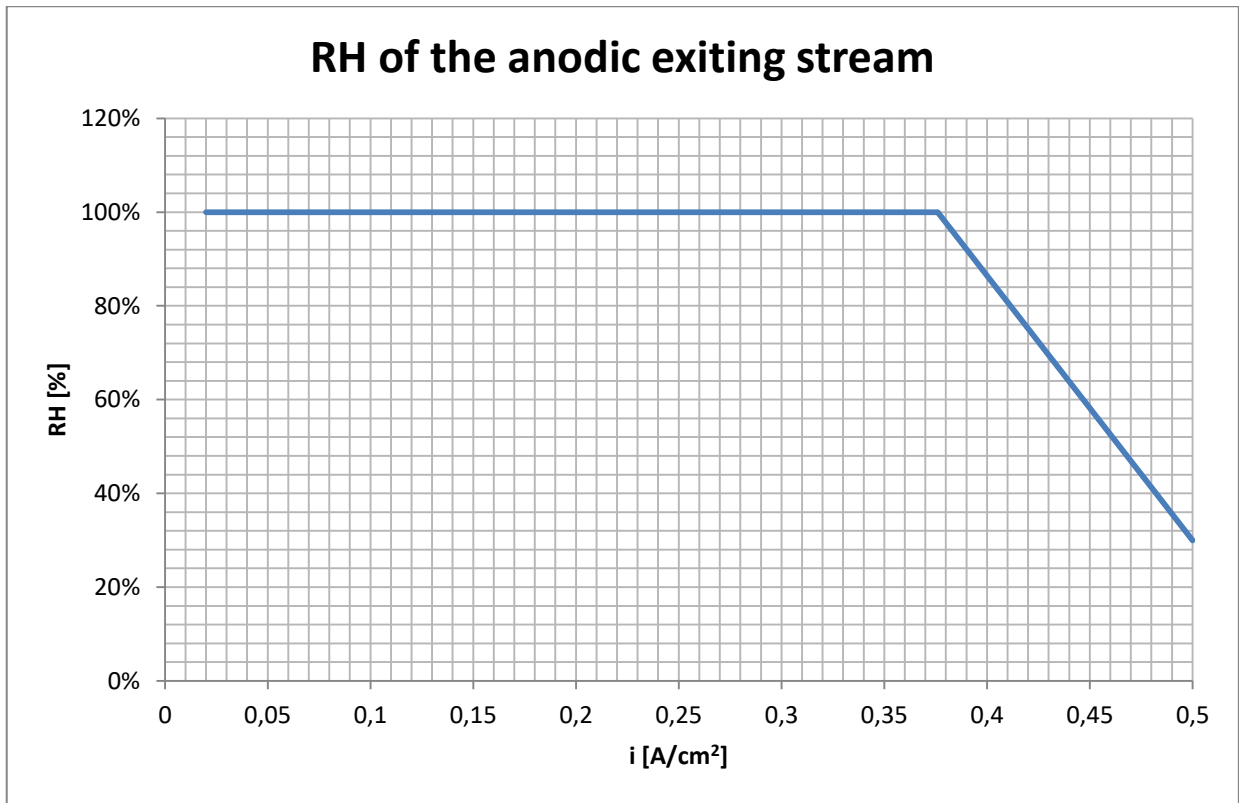


Figure 3.8: RH profile at the anode exit for the size of 10 kW at varying of current

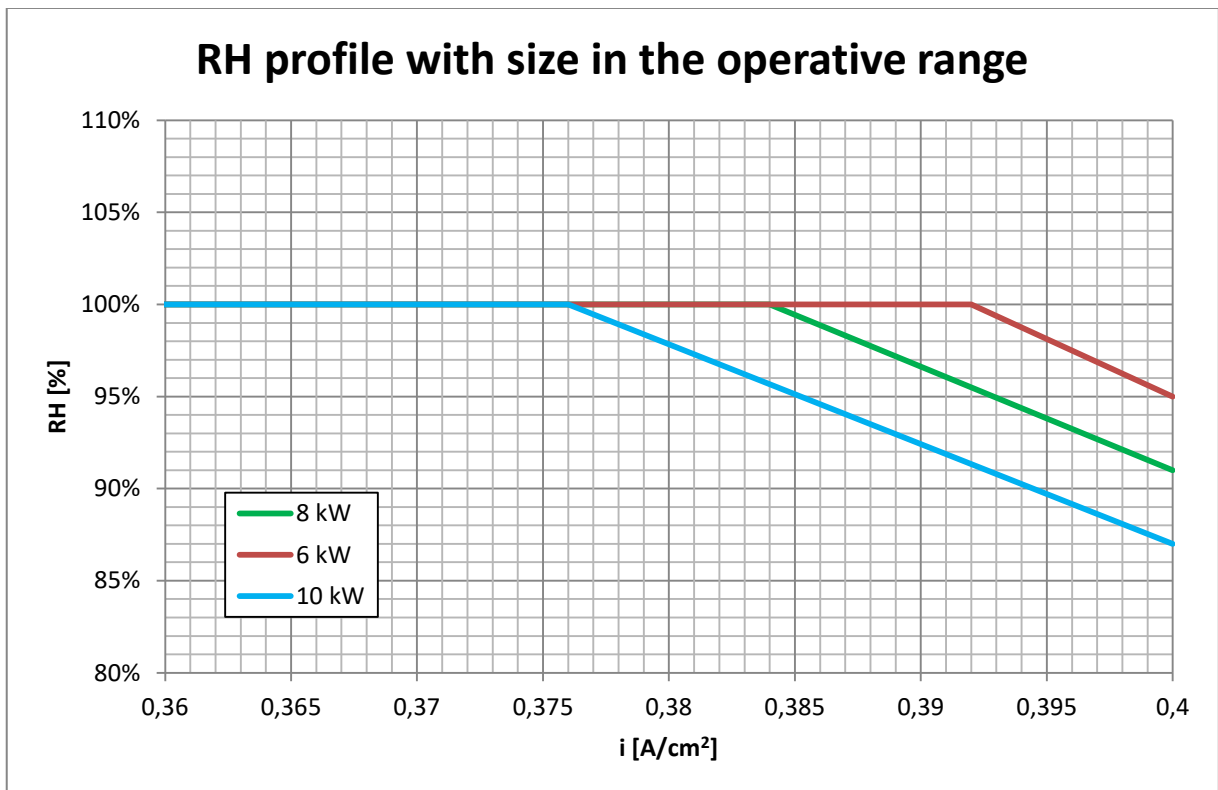


Figure 3.9: Variation of the RH profiles at the anode exit with size

Regarding, instead, the humidification of the cathode side, we have that the stream 17 (H₂O CATHODIC FEED) is the amount of water that let the stream 7 (main cathodic stream) to reach the relative humidity imposed equal to 0.95. In fact, the transportation of the water through the membrane of the humidifier cannot be considered otherwise due to the lack of this component in the Aspen library. Said that, we need to accomplish with the effect of heat-up of the membrane, that in our model is taken into account by the component HUM. So in the end, the membrane humidifier is represented by both the blocks HUM and HUM-MIX.

3.5 Calculator blocks

As we previously mentioned, during the modelling of the heat equation, all calculations that are outside the Aspen program are made through the use of a calculator block, tool presented among the “Flowsheeting Options” in the data browser of Aspen Plus. In fact, this tool is quite useful since it let us to insert code statements into the flowsheet computation using the Fortran language. This means that the conditions and properties of the streams could be used as input, but also modified during the simulation sequence depending on the necessity. Regarding the use of this tool on our study, we can underline six important calculator blocks.

3.5.1 C-ICURR

This is the calculator block that starts our simulation. In fact, imposing on it the value of current with which we want to simulate, we automatically modify the values of the molar flow rates entering the stack, but also the anodic recirculation molar flow rate. Of course, this calculator block is put at the beginning of the sequence of simulation in order to compute and update all the variables needed. From the code (see appendix **B.1**) is quite interesting to underline how we compute the values for the fuel utilization and air utilization. In fact, we suppose to vary their values between a defined range that goes from 0 to 50 A, while the remaining part has supposed to have a fixed value. This is due to the fact that, at low currents, the excess of air and fuel is quite important respect to the case at high currents. In fact, in this condition a high feeding of fuel is needed in order to maintain a sufficient concentration of H₂ in all the cells of the stack, while the excess of air is needed to prevent the poisoning of the platinum catalyst with foreign particles presented in the anodic reactant flow.

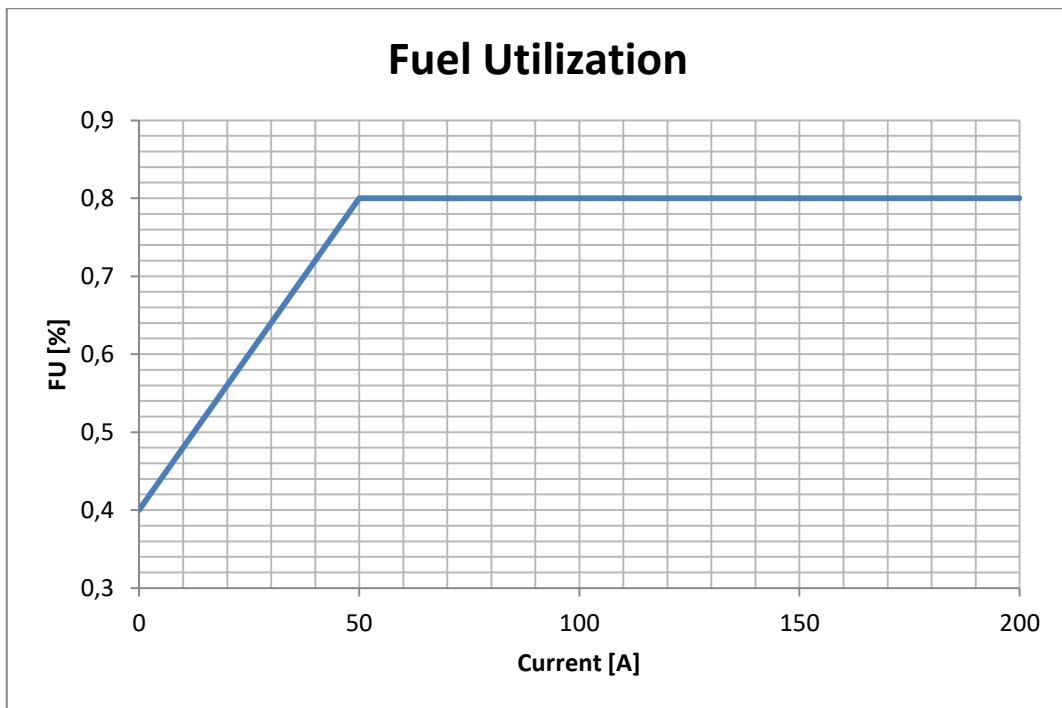


Figure 3.10: Fuel utilization profile at varying current

From the profile above we can see that the fuel utilization (FU) varies in the range that goes from 0.4 to 0.8. This according to other studies [6], [9] is the range of values we can usually incur during operation in standard PEMFC.

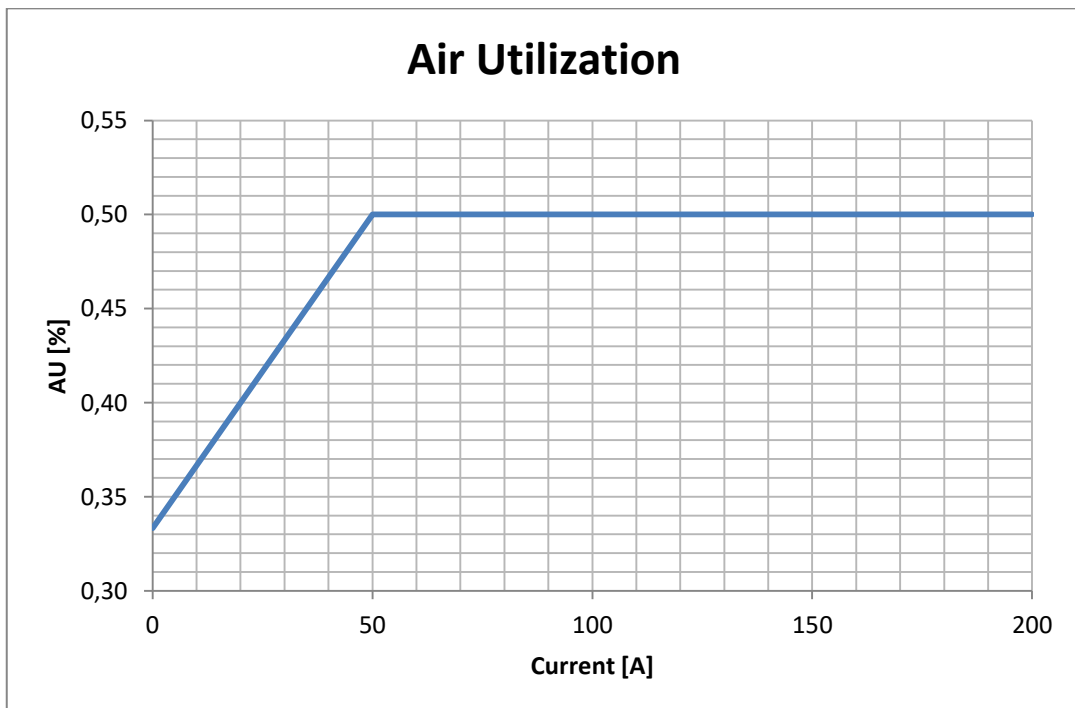


Figure 3.11: Air utilization profile at varying current

Regarding the air utilization (AU) profile instead, we can see that it varies in the range from 0.33 to 0.5. Also, in this case the values taken are in accordance with other studies [6] and for this

reason we will not enter too much into details. It is important to underline the fact that the values of utilization between anode and cathode are quite different from each other due to the different kinetics of the two electrodes of the cell.

For the creation of the profile, we suppose a linear increase of the utilization of the reactants with current until the condition of current equal to 50 A is reached. In fact, over this value, working conditions of the device are the nominal ones, so there is no more the necessity to consider further excess for the streams entering the stack. From this point forward, the excess of the reactants is the minimum necessary to maintain the good working operability inside the cell. The values of excess used from this point on are respectively 1.25 for the anodic stream and 2 for the cathodic stream.

3.5.2 C-WREC

For what concerns this calculator block (see appendix **B.2**), it has the role to compute the amount of water entering the stack together with the anodic stream thanks to recirculation. In fact, as we have explained on previous chapters, this stream is not supposed to be humidified from the outside, but only from the inside. This is due to the crossover effects, especially back diffusion, since at the currents of operation considered this phenomenon is the most relevant, letting the anode exhaust stream rich of water. In order to make these calculations, the profiles in figure 3.9 are considered. In this way, the anodic stream of the recirculation will be humidified according to the configuration of the system considered.

Table 3.2: Data of the relative humidity exiting the anode

Size [kW]	Current density i [A/cm ²]	Relative Humidity [%]
6	0.020	100
	0.392	100
	0.400	95
8	0.02	100
	0.384	100
	0.400	91
10	0.020	100
	0.376	100
	0.400	87

Of course, the RH of the recirculated stream cannot overcome the saturated condition due to the fact that the system has a separator for the water condensed on the anodic circuit as we have seen on the figure 3.3.

3.5.3 C-HUMC

This is the calculator block (see appendix B.3) that works with the parameters of the humidification section of the cathode side. In fact, as we explained before, a fixed relative humidity is imposed, so all the calculations required to obtain the amount of water needed are incorporated in this block. Of course, the input parameters such as the air temperature are taken from the Aspen results since this calculator block is put between the HUM and HUM-MIX block in the resolution sequence.

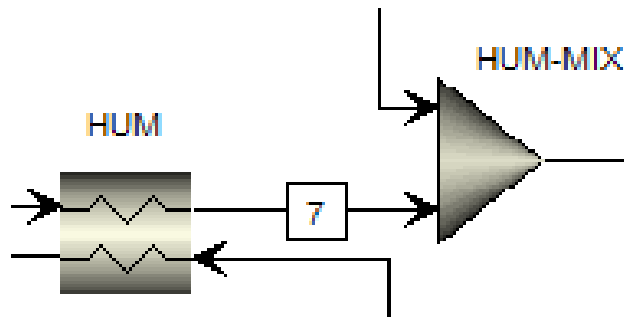


Figure 3.12: Aspen modelling of the cathode's humidifier

Regarding these blocks, we can say that are both “fictitious” components, but as we explained before they are needed for the simulation of the effects caused by the humidifier membrane. In fact, each of them are added to accomplish a specific role, that are respectively to control the amount of water transferred through the membrane to the air (HUM-MIX), and to increase the temperature of the air entering the stack caused by the humidifier (HUM). Of course, this is due to how the humidification occurs, since the amount of water gained is obtained from the cathode exhaust at higher temperature and at higher content of water.

3.5.4 C-FU

This is the calculator block (see appendix B.4) that computes the amount of hydrogen passing through the electrolyte. In fact, as we said before, we assume to consume only a specific quantity of hydrogen given by the Faraday's law, which depends on the load requested. Since the fuel utilization varies with the load condition, the amount of hydrogen entering the stack varies consequently, so, in order to ensure that the right amount is entering the Gibbs reactor, we decide to use this calculator block. In fact, we have that the split fraction of the hydrogen in the separator component (ANODE) is not a variable that we can modify in progress automatically

due to the impossibility of working in dynamic mode with Aspen Plus. So this calculator block is needed to avoid this difficulty during the implementation. This, of course, creates a discrepancy in terms of molar flow rate between the streams 4 and 26, even if they should be identically the same. So, lastly, we have assumed that the split fraction remains constant and equal to 0.4 (this of course is referred only to the hydrogen) in all range of operation in order to be conservative. This of course creates a slight increase in the value of the heat taken from the reaction by the block (HEAT-H2), since the flow rate is higher than the real one, but, since the term is quite negligible compared to the heat released by the reaction, we can consider acceptable this inaccuracy looking at the global results.

3.5.5 C-PEMFC

Regarding this calculator block (see appendix **B.5**), it has the purpose to evaluate the voltage of the cell starting from the current imposed at the beginning of the simulation. In order to do that we start from the polarization curve computing all its components separately. The equations used are the ones described before on paragraph 2.3. For what concerns instead the inputs, they are obtained from assumptions and external data. One important aspect that has to be underlined is the impossibility of varying the temperature of the stack in the code since it was fixed at 70°C during the definition of the CATHODE block. This is surely due to the limit of Aspen Plus since, as we said before, it can only work on stationary conditions. Anyway, these assumptions can be considered understandable in operative conditions where we are supposed to maintain under control the temperature, while it is a less negligible aspect during the start-up and shut down. For this reason these two operation modes have to be further analysed later on.

3.5.6 C-COOL

The last calculator block (see appendix **B.6**), but not less important, is the one that computes the amount of water needed for the cooling circuit. Of course, it is obtained starting from the energy balance equation, as we explain before, since in order to compute the amount of water requested, we need to know the amount of heat to remove from the device. For what concerns the inlet and outlet temperature conditions, we can say that they were selected considering the fact that we want to avoid to generate a thermal gradient inside the cell as we have seen in [10].

In addition to that, also a design specification is considered during the process since not only the amount of water is unknown, but also the temperature of the water exiting the PEMFC stack. Supposing to fix the coolant temperature exiting the stack at 60°C, we have that only the coolant flow rate has to be iteratively changed in order to obtain this value. Regarding the value of

temperature assumed, we choose the value of 60 °C in order to maintain a pinch point of 10°C between the stack temperature and the cooling circuit.

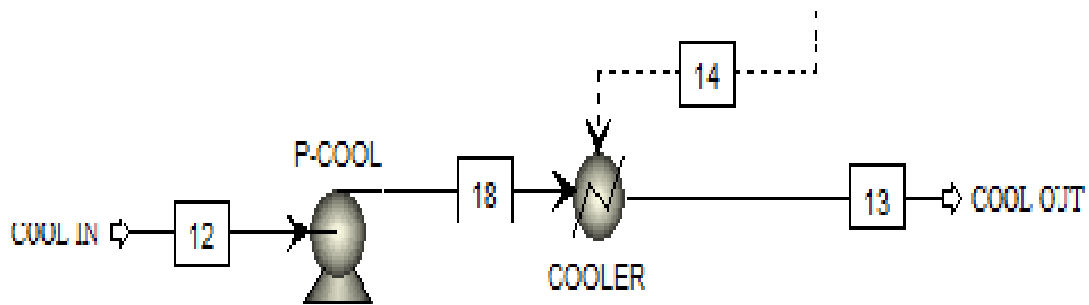


Figure 3.13: Aspen modelling of the cooling circuit

3.6 Simulation sequence

Now, after the description of all the calculator blocks needed for the resolution, we need to explain where they are put in the simulation sequence. But, in order to do so, we need before to explain how Aspen Plus solves the process flowsheet. Regarding this point, we can say that Aspen Plus follows a sequential modular approach where each unit operation block is solved in a certain sequence. This means that, in order to have the effect desired, each calculator block has to be put in a specific position, otherwise its effects cannot be taken into account during the resolution. Said that, the execution sequence of our balance of plant (BOP) configuration is reported below:

1. C-ICURR
2. C-WREC
3. R2-BLOW
4. AIR BLOW
5. VALVE
6. R1-BLOW
7. MIXER
8. W-MIX
9. C-HUMC
10. HUM-MIX
11. ANODE
12. C-FU
13. HEAT-H2
14. CATHODE

15. C-PEMFC
16. C-COOL
17. HUM
18. HEATMIX
19. P-COOL
20. COOLER

As we can notice, the calculator block C-ICURR is at the beginning of the sequence. This is due to the fact that the block C-ICURR has the role to modify the random values put during the creation of the model according to the working operation condition under consideration. In fact, depending on the power that we need to produce, the amount of reactants change, and for this reason this block cannot be put elsewhere in the simulation sequence. An analogue argumentation can be done for the calculator block C-WREC since has to follow the block C-ICURR due to the calculation involved, but at the same time has to precede the block W-MIX in order to be considered in the results. Regarding the following blocks, they are automatically put in sequence by the program. In fact, the executive program contains procedures for the optimal ordering of the calculations to promote convergence. It also identifies loops while interacting with the unit operations library, physical properties databank and the other subroutines. Similar to the block C-WREC, the calculator block C-HUMC has to precede the block HUM-MIX in order to be taken in consideration. After that, the following calculator block in the simulation sequence is the C-FU that, as we can easily understand, has to precede the block CATHODE. This of course is done in order to obtain reasonable results as we have explain also for the others calculator blocks. For what concerns instead the calculator block C-PEMFC, it has to precede the block HEAT-MIX since to solve the heat equation this value is needed. Regarding the last block C-COOL it has to follow the block HEAT-MIX, but, at the same time, has to precede the block P-COOL. This is due to the fact that this calculator block needs to know the amount of heat that has to be removed owing to the calculations involved. In fact, as we explained before, this calculator block has the role to compute the amount of water needed in the cooling circuit represented by the stream 12. So, seems quite understandable the fact that this calculator block has to precede the block of the pump. Also, because we need to modify the random values put at the inlet stream 12, during the creation of the model, in order to obtain a meaningful result for the pump. Furthermore, we need to point out the fact that this calculator block is needed only to have an early value of the coolant flow rate since, as we know, it will be further optimized during the design specification imposed afterwards. In fact, the calculation done in it can be considered a good approximation of the result needed to run the simulation without giving rise to errors.

3.7 Stack Temperature

Regarding the stack temperature, as we said before, it is supposed to be constant during the operation thanks to the temperature control system. But, of course, this is not occurring during the start-up and shutdown of the device, so further considerations have to be made. Anyway, considering we are working with a PEM fuel cell that has a very quick start-up, the fact, that the temperature is not equal to 70°C during this period, can be considered in some way less important respect to other types of fuel cell.

3.7.1 Temperature during the start-up

In order to analyse the temperature during the start-up, we need to make some assumptions, so that we can fix some of the variable involved. Starting with the ambient conditions we suppose a temperature and pressure equal respectively to 25°C and 1 bar. We consider also the cooling circuit off during this period in order to avoid extension of the period of start-up. In fact, we need to reach, as fast as possible, the temperature of operation of 70°C, so a high current during this period is assumed. At this point, since we are considering a transient analysis of the stack where the term due to the heat removal is not considered, the equation used results equal to:

$$C_{th} \cdot \frac{dT}{dt} = - \frac{(\Delta h_{f,H_2O}(v))}{z_F \cdot F} \cdot I - V_C \cdot I$$

Where the heat capacity of the stack is computed in the following way:

$$C_{FC} = c_{p,FC} \cdot M_{FC}$$

Table 3.3: FC stack data

Data	Value
$c_{p,FC}$ [J/(kg·K)]	1000
P/W [kW/kg]	0.227
M_{FC} [kg]	46.55

At this point, in order to solve the heat equation above, the forward Euler method is adopted.

$$\frac{y_{n+1} - y_n}{\Delta t} = f(y_n, t_n)$$

This numerical method was chosen due to its simplicity and good appliance in the resolution of the heat equation that in our case becomes equal to:

$$C_{th} \cdot \frac{T_{c,n+1} - T_{c,n}}{\Delta t} = \phi(t_n, T_{c,n})$$

Since the amount of calculations involved, a Matlab implementation (see appendix A.3) is considered. In fact, in the code not only the changes in terms of polarization curve are taken into account, but also the variation of the enthalpy and entropy of the reaction with the temperature of the stack. In this way, a more precise evaluation of the time needed for the start-up is obtained.

To consider the effect of the starting current, a study with two different values of current is made, and, as we can see from the plot below, the value chosen are respectively 150 A and 200 A. This is done to underline the fact that higher is the current less is the time to warm up. In fact, this is the reason why higher currents are considered preferable respect to lower currents. Now, looking at the plot we can see that at a current of 200 A we have that the time to warm-up the device is equal to 150 s, while at 150 A the start-up requires 70 s more. This of course is done for a specific size of the gen-set (in this case 10 kW), since a variation of the size brings to different results as we will see later.

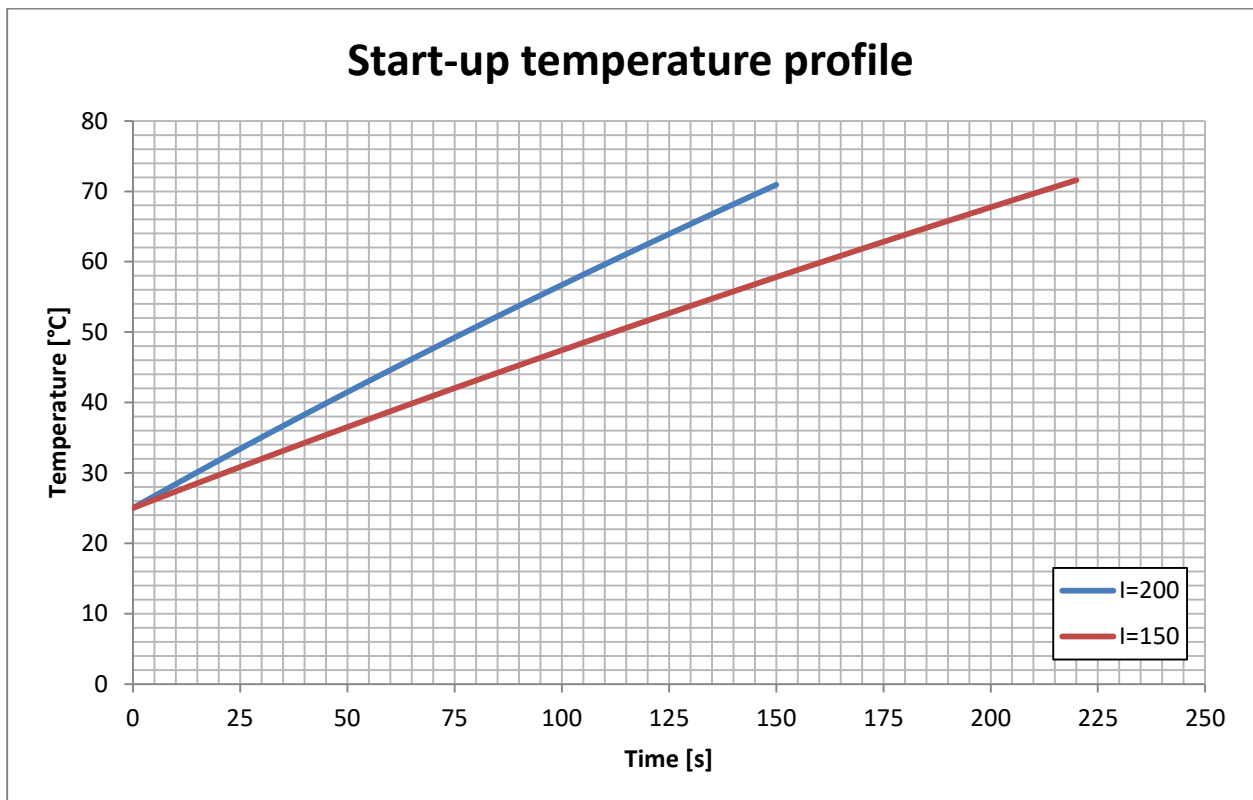


Figure 3.14: Temperature profile during start-up at varying of the starting current

Said that, depending on the application, the selection of the optimal current could be a cardinal point to take in consideration. In our case, we prioritize the minimization of the period of start-up and for this reason a current of 200 A is chosen. This is especially due to the fact that the

electricity during this period is provided by a battery which, for this reason, becomes a quite essential component for the support of the gen-set. In addition to that, it is useful not only during the start-up, but also during changes in the load following, as we will see later on the next chapter. Regarding the calculations that lead us to these results, we suppose to consider a time step of 10 s with a current ramp rate of 20 A/s [9], so after 10 s the current circulating in the stack will be equal to 200 A that is the maximum current achievable in our configuration.

At this point to complete the study of the start-up, we need also to take in consideration the effects of the size on the period of warm up. In fact, this is a quite important aspect that has to be analysed, since from it depends a possible increase of the period in which the support battery has to cover the user's consumptions.

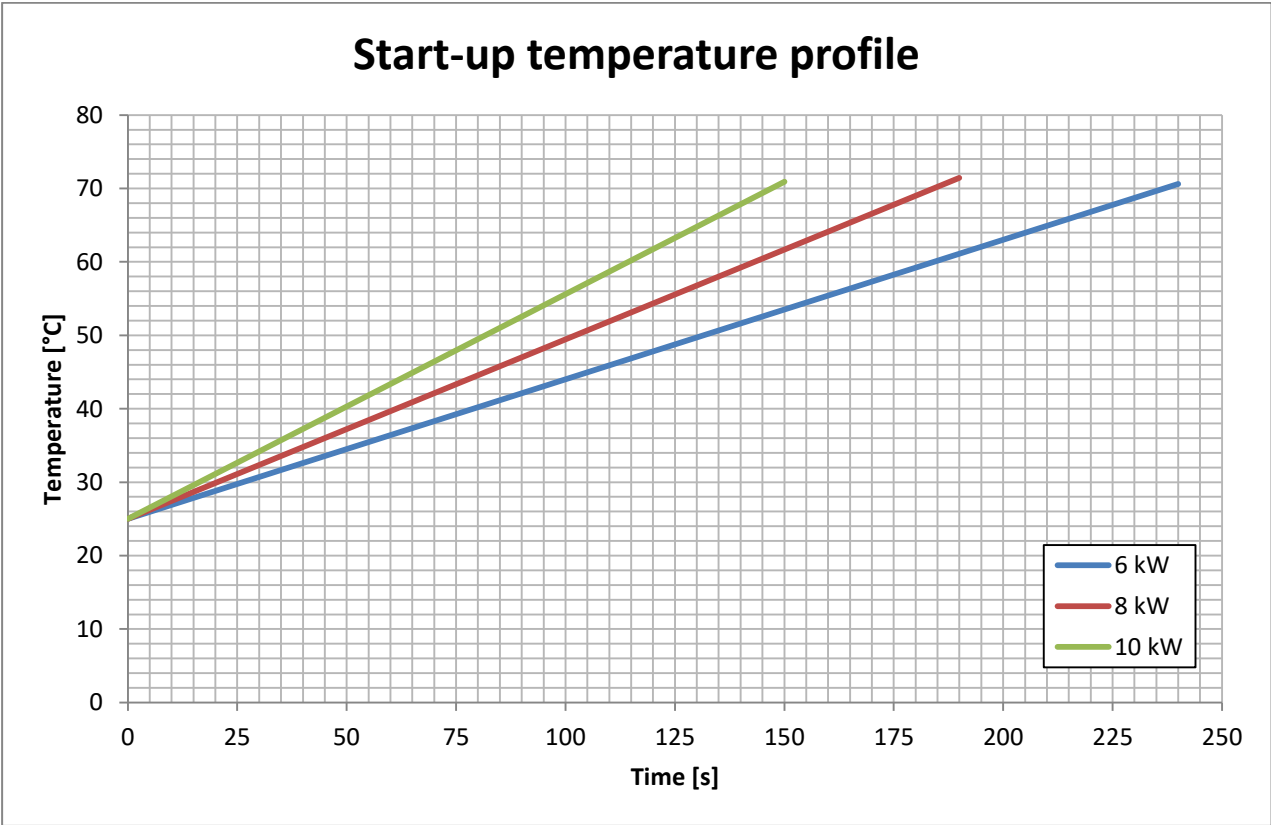


Figure 3.15: Temperature profile during start-up at varying of the size

As we can see from the profile above, we have that higher is the size less is the time to warm-up the stack. This aspect, in some extent, can be considered understandable, supposing the fact that higher is the number of cells, greater is the heat released by the stack.

Chapter 4

LOAD FOLLOWING AND FINAL CONFIGURATION

4.1 Load following

Considering we need to be independent from the electrical grid, due to the role of the device in the working environment considered, the load following seems to be the only modulation strategy applicable. In fact, this is the only modulation strategy that has the aim to minimize the electricity taken from other sources. In order to do so, a complex electronic regulation of the system is needed in a way that a certain level of precision is maintained. But, of course, the user load cannot be always followed due to the limitations of the devices considered. In our case, the first big limitation is given by the fuel cell. In fact, in order to maintain a certain level of good operability, the device has to stay between specific limits given by the constructor that cannot be overcome. Regarding these limitations, we have that the electrical ramp rate cannot exceed a specific value that in our case is fixed to 30 W/s [9]. This means that all the peaks generating by the difference between the starting and running electrical consumption should be covered by a supporting component that, in our case, is the battery. So, seems necessary a properly size of the battery in order to avoid possible failures in the supply of power to the user. But, before doing this stuff, we need to know how much the device could cover the average consumption of a usually day of work. To do so, we need to recreate the response of the device for each request of load of the user, associating it with a specific known working operation condition of the gen-set. At this point seems quite necessary the need to have a mapping of all the operation conditions of the device in the range of 0-200 A (see appendix C.1). In fact, in this way, we are able to associate to the power produced not only the current of operation needed, but also the consumption of the auxiliary components of the BOP such as pumps and blowers.

Turning back to the estimation of the response of the device, we write a Matlab code (see appendix A.4) where the limitation on the ramp rate is taken into account together with some assumption for the consideration of the start-up. In fact, after detecting that the gen-set is off, we assume that for the time needed to heat up, the device will not produce usable power since the

condition of operation of the PEMFC are not optimal. During this period, we suppose that the power produced is used only to move the auxiliary components. This can be easily seen from the plot resulted by the code where, although the request of power increases, we have that the power produced is still zero until the optimum condition of the device is reached. This means that, during this period, the power provided to the user is supplied by the battery. It is also important pointing out the fact that the response of the device is simulated only for 2 hours, although a normal working operation takes place in a total of 8 hours. This is done due to the lack of a real user profile, in fact, the sample time of the curve considered for the study was reduced to give us only an idea of the problems related to it. Anyway, a higher sample time would not give us more useful information respect to the case under consideration, so the simplification is quite acceptable considering how the profile was obtained.

In addition to that, since the response of the device varies, depending on the size considered, we need to make this evaluation for each size previously taken into account. The plots showing the behaviour of the response are reported down below.

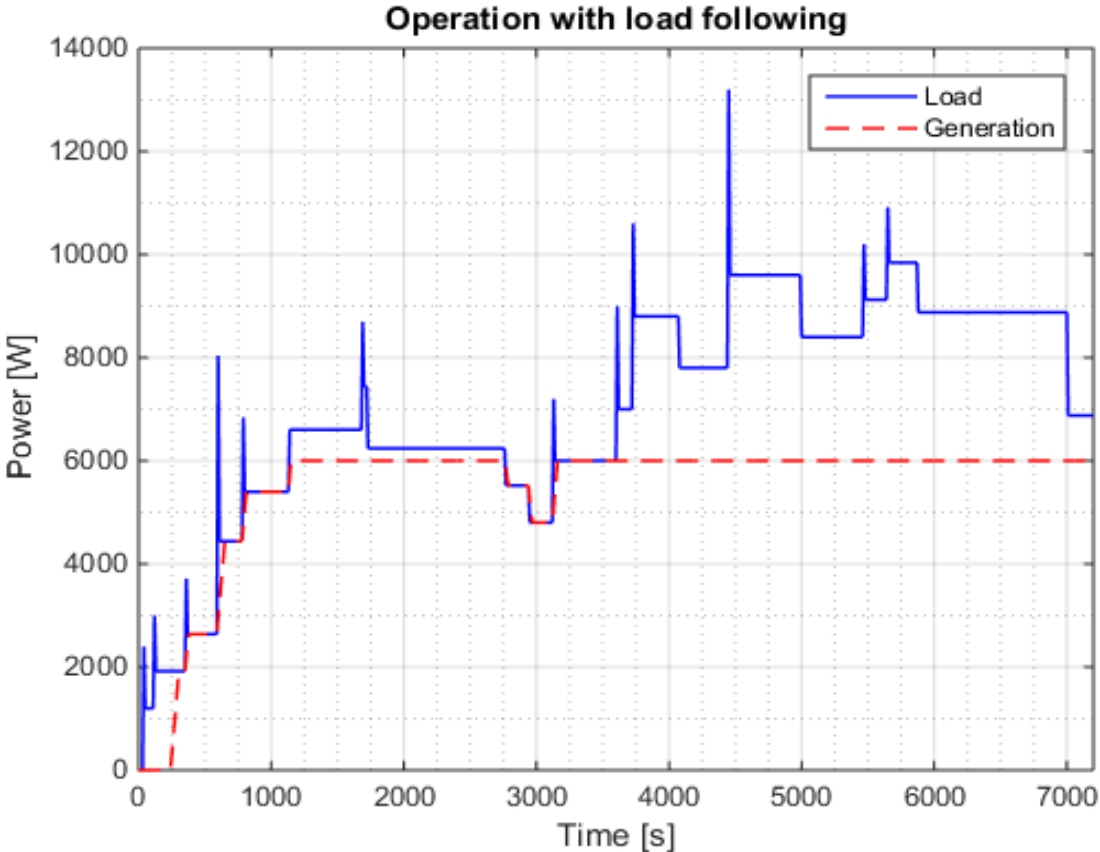


Figure 4.1: Load following profile of a 6 kW gen-set

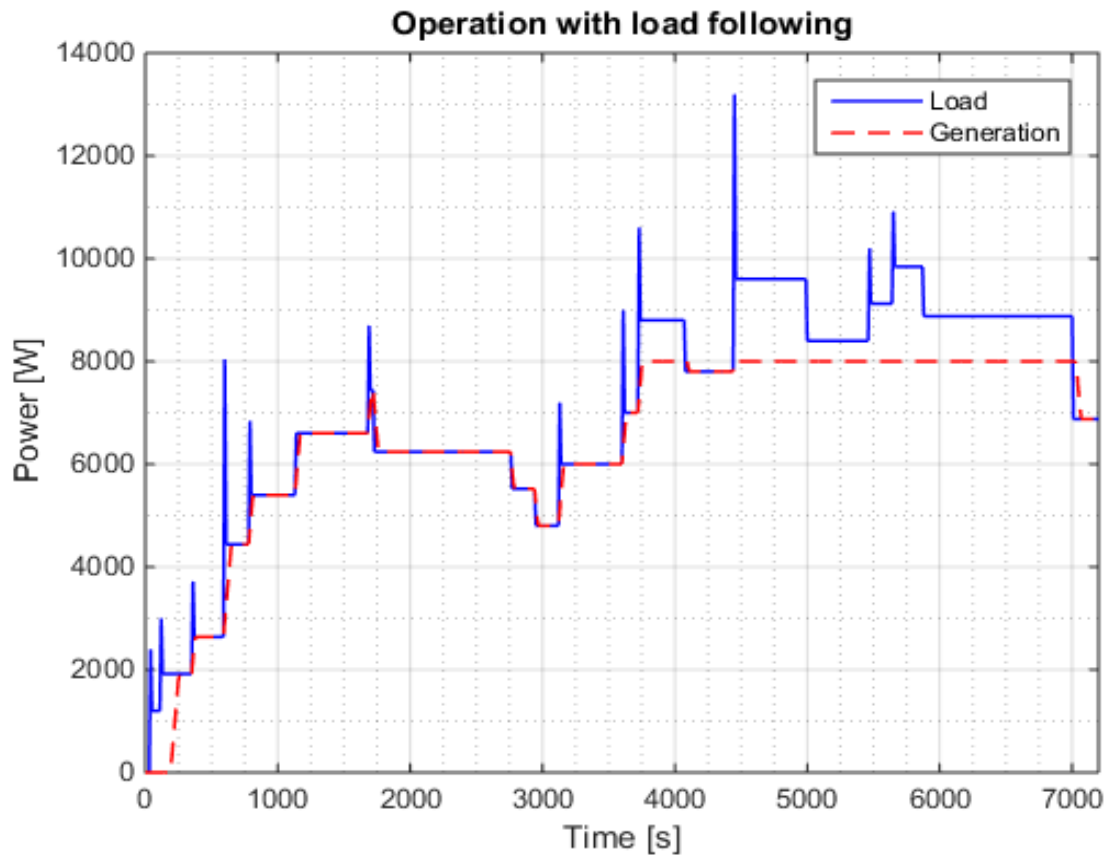


Figure 4.2: Load following profile of a 8 kW gen-set

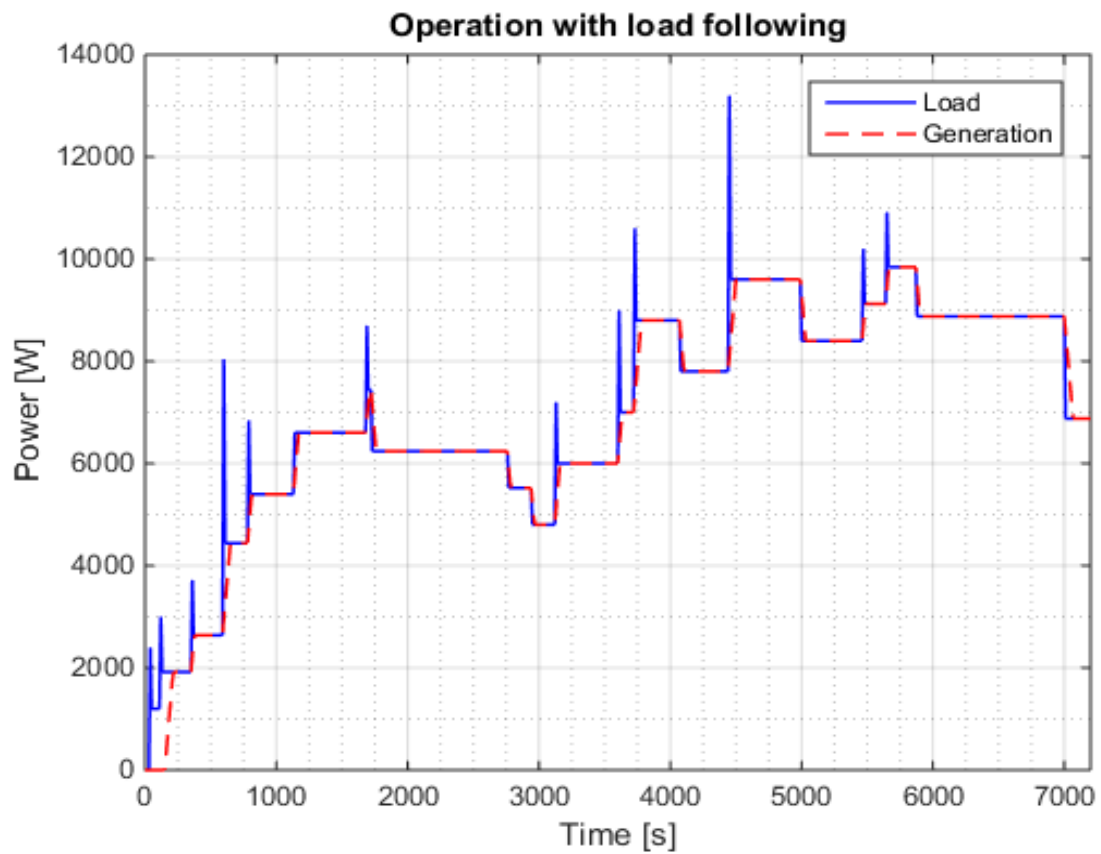


Figure 4.3: Load following profile of a 10 kW gen-set

Looking at the plots, we can easily confirm how the response of the device is not sufficient to cover all the user consumptions. In fact, we have that at least the peaks have to be covered by the supporting battery. But of course, depending on the size considered, the portion of the load covered by the battery increases, as we can especially see in the case of 6 kW.

Table 4.1: Load following results summary

Size [kW]	Gen-set covering factor [%]	Battery covering factor [%]
6	78.15	21.85
8	93.04	6.96
10	98.97	1.03

Now, in order to complete the analysis of the response given by the device, we decide to plot also other parameter's profile that are respectively the one of the current and system efficiency. Starting with the current profile, we can see that the gen-set never reaches the maximum current available. This is due to the fact that the machinery is a little oversize respect to the power selected which represents the net power achievable by the device. In fact, this is necessary in order to be able to cover all the auxiliary consumptions that are needed. Of course, our study does not consider all the possible consumptions that we have during normal operation, so an higher safety range is considered, generating this effect on the results.

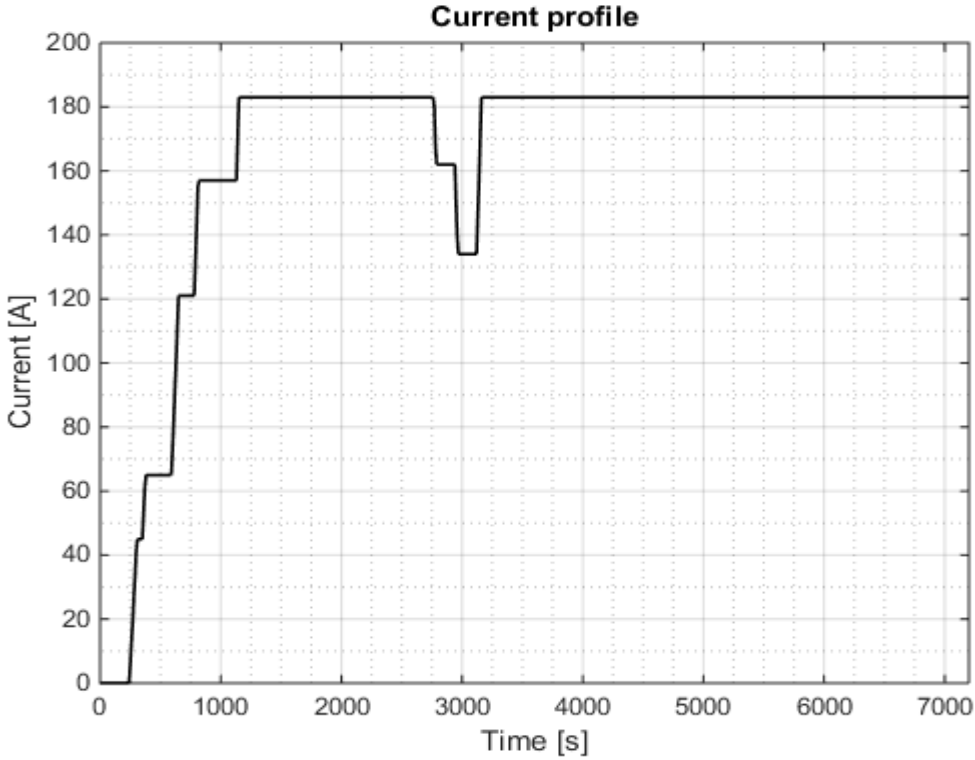


Figure 4.4: Current profile of a 6 kW gen-set

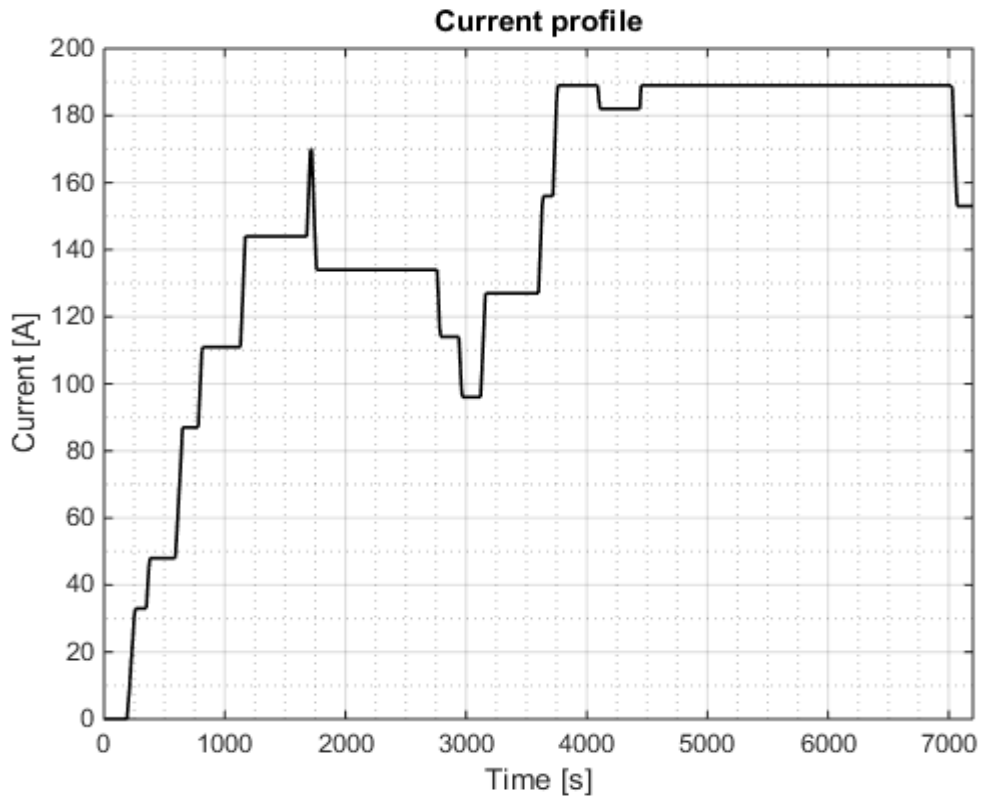


Figure 4.5: Current profile of a 8 kW gen-set

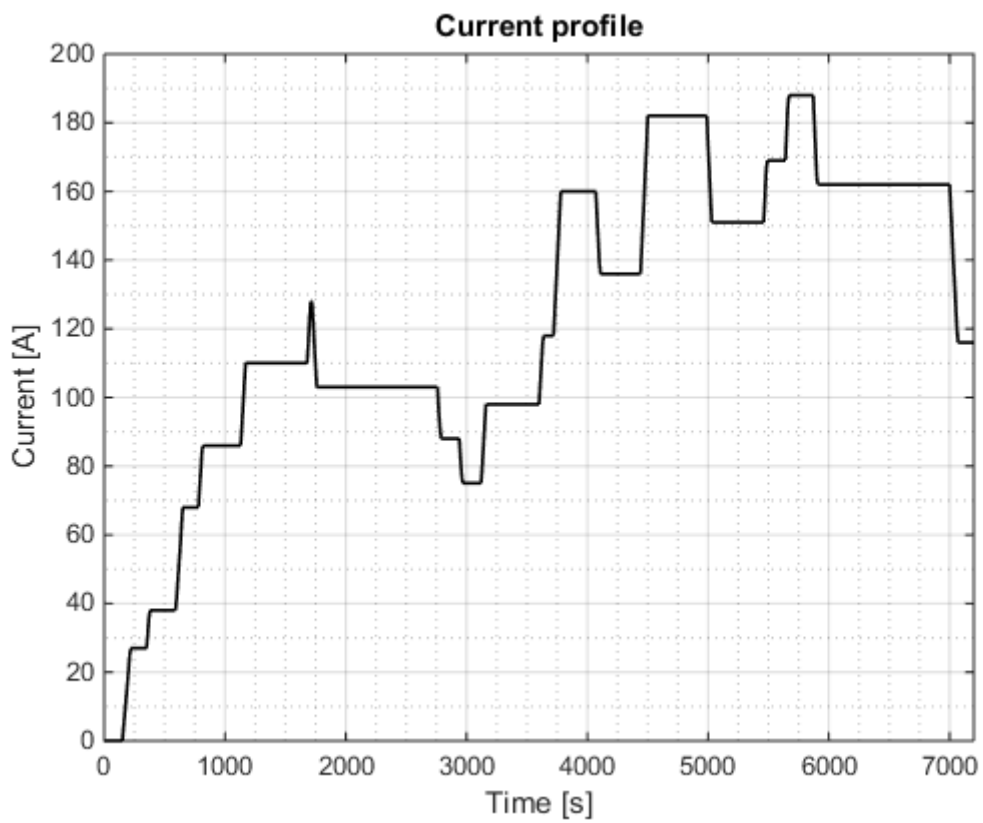


Figure 4.6: Current profile of a 10 kW gen-set

Regarding, instead, the profile of the efficiency of the gen-set, we can say that, depending on the size selected, the average efficiency, at which the device is operating, is different. This, of course, is easily understandable considering the fact that higher is the size of the gen-set, higher is the gap between the working condition and the nominal one. In fact, referring to the case of study, we have that the curve, in general, is not constant during the operation, so higher is the size, lower is the probability that the machinery operates at a constant load equal to the nominal condition. Obviously, the opposite occurs for lower sizes.

Table 4.2: Average efficiency at varying of the size

Size [kW]	Average efficiency [%]
6	48.23
8	50.78
10	52.62

Said that, the plots related to these results are represented down below:

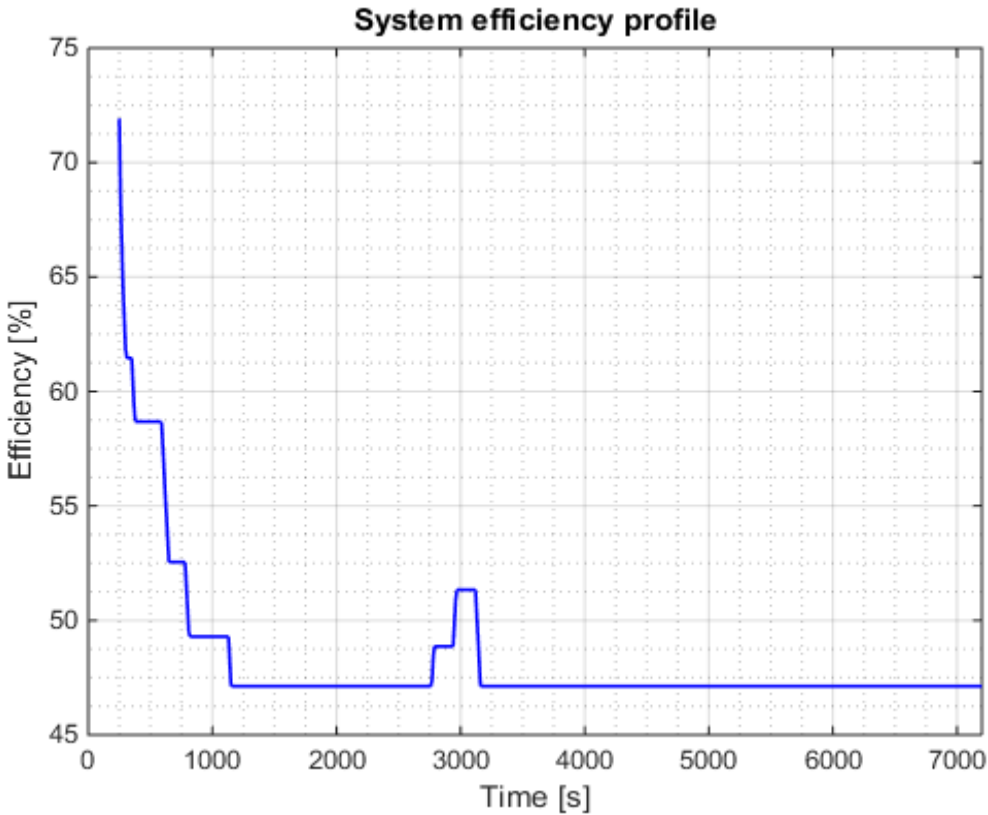


Figure 4.7: Stack efficiency profile of a 6 kW gen-set

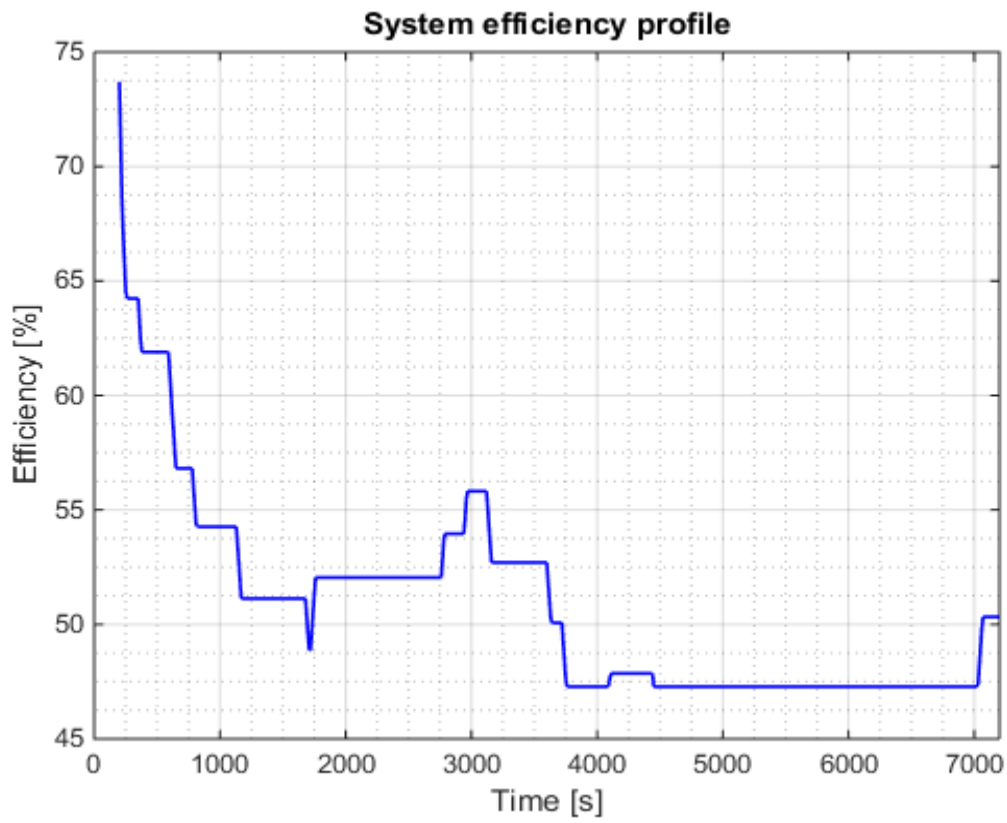


Figure 4.8: Stack efficiency profile of a 8 kW gen-set

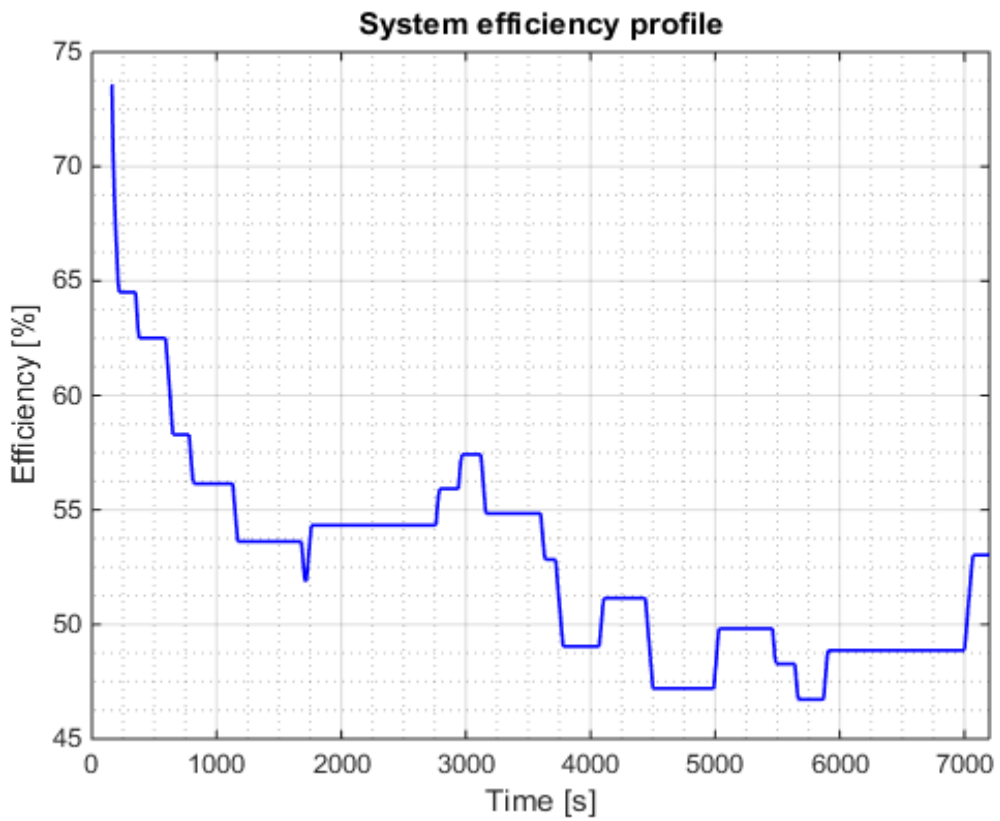


Figure 4.9: Stack efficiency profile of a 10 kW gen-set

4.2 Gen-set size analysis

At this point, in order to proceed with the modelling of the gen-set and its components, we need to evaluate which is the best size for our device. In order to do so an economic analysis is necessary. But, before entering into the calculations we need to determine which are the main components that we have to take into account. Considering the results obtained by the load following, we can easily understand that the battery is one of these key components, since it varies a lot with the size of the gen-set. So at the end, we should expect that the best solution will be mainly a trade-off between the cost of the fuel cell and the battery, since they are the main components affected by this analysis. For this reason, we need to make some considerations on the sizing of the battery in order to able, lately, to evaluate its cost.

4.2.1 Battery bank sizing

In order to size appropriately the component, we need to start computing the average power that is requested by the battery. This is done in order to have an idea of the capacity (Ah) that the battery has to have, which is needed for the next steps of the evaluation. To do so, a Matlab code (see appendix A.5) is written where the energy that is not covered by the gen-set is obtained through a difference between the area of the load and response profile respectively. In order to do the integral of both curves the trapezoid rule is considered:

$$A = (b - a) \cdot \frac{f(a) + f(b)}{2}$$

Where the difference between b and a represents the length of the interval of integration that is supposed to be equal to the discretization time of 10 s. At the end, from the sum of the results in each interval, the total energy requested, represented by the total area, is obtained.

For the calculation of the battery capacity, we refer to the *Trojan* battery company guidelines [11] since we suppose to support our device with a lead-acid battery. The equation used for the calculation is the following:

$$Ah = \frac{\left(\frac{E_{ot}}{\eta_{inv}}\right)}{BV}$$

As we can notice, both the efficiency of the inverter and the battery bank voltage are considered. In addition to this, it is important to point out that for this calculation is required to have the energy consumption in Wh, so a preventive conversion is required.

At this point, from this value we need to consider some adjustment factors that will serve to calculate the adjusted and final battery capacity required to run the system appropriately.

$$Ah_{adj} = \frac{Ah \cdot TC \cdot DA \cdot DM}{DOD}$$

Table 4.3: Adjusted capacity factors

Data	Value
Temperature correction factor (TC)	1.00
Days of autonomy (DA)	1.00
Design margin (DM)	1.10
Depth of discharge (DOD)	0.20

From the value of days of autonomy (DA) in the table above, we can see that the battery is supposed to be sized for one day of work. This is due to the fact that the battery has to be recharged during the operation, supposing to have the device not working all day at maximum power. Regarding, instead, the depth of discharge (DOD), we select a safety value of 0.2, in order to take under consideration the uncertainty of the peaks that could occur during operation. In fact, we want absolutely to avoid to incur the situation in which the battery bank is over discharged. At this point, the battery bank capacity computed can be now used to determine the amount of batteries needed for our configuration.

But, before doing this, we need to point out the fact that, depending on the size, the results are different for obvious reasons, so, in order to give a better idea of the difference between each configuration, a resume of the values obtained is reported down below:

Table 4.4: Results of the battery bank capacity at varying of the size

Size [kW]	Battery energy coverage [Wh/day]	Battery bank capacity [Ah]
6	12284	1466.2
8	3911.1	466.82
10	578.22	69.02

At this point, to complete the analysis of the battery configuration, we need to compute the amount of batteries needed to obtain that precise battery bank capacity. In order to do that, some considerations has to be done. First of all, we need to decide the voltage output of our system and the characteristics that the single battery cell has to have. Referring to data of solar system, the values used for the evaluation are reported in the following table:

Table 4.5: Data for the calculation of the battery configuration

Data	Value
Inverter efficiency	0.96
Battery bank voltage [V]	48
Battery cell voltage [V]	12
Battery cell capacity [Ah]	100

As we can see from the table, a battery cell capacity of 100 Ah is selected. Now, in order to configure our battery bank, some notions about the possibilities of connection among batteries have to be given.

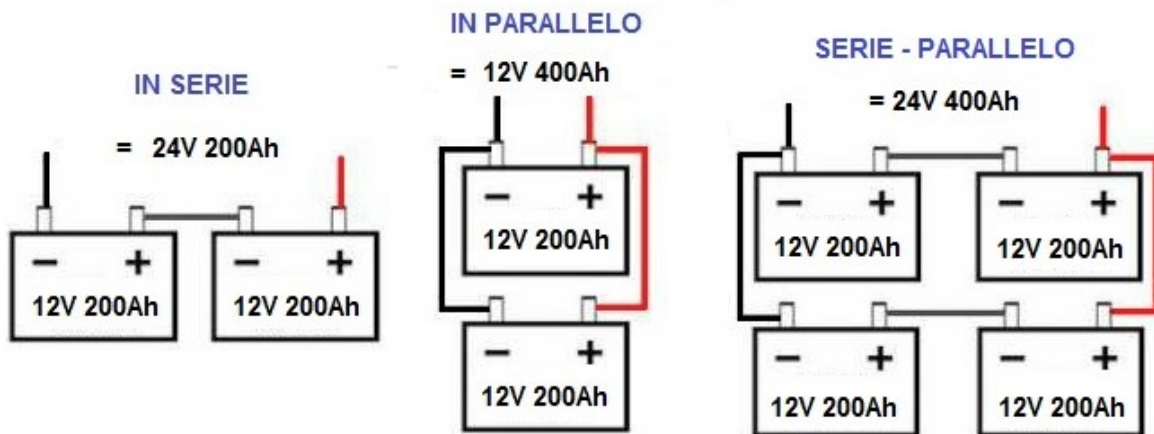


Figure 4.10: Possibilities of connection among batteries

Looking at the figure, we understand that in our case at least four batteries in series have to be connected. For what concern, instead, the number of batteries in parallel, they depends on the battery capacity (Ah) requested. In any case, the better solution remains the one that reduced more the number of batteries in parallel due to charging problems over time, but this is not always possible, especially in the cases in which higher battery capacities are needed. Said that the final battery configuration for all the size considered results to be:

Table 4.6: Battery configuration at varying of the size

Size [kW]	N° of batteries in parallel	N° of batteries
6	15	60
8	5	20
10	1	4

4.3 Gen-set cost analysis

At this point, after determining the size of the battery configuration, we can proceed with the cost analysis of each solution. This, as explained before, is a decisive factor for the final decision of the best size for the application and, at the same time, for the availability in the market of the machinery. Said that, for the cost of the gen-set we refer to the DOE (U.S Department of energy) [12], where the 2015 status of the fuel cell, used as back-up power system, is reported. Considering this source, the following data are obtained:

Table 4.7: Gen-set economic data

Data	Value
Lifetime [years]	10
Fuel cell system cost [€/kW]	4930
Annual maintenance cost [€/kW]	25

For what concern, instead, the cost of the battery, we refer to a technical report of the NREL (National Renewable Energy Laboratory) [13]. From this report the following data are obtained:

Table 4.8: Battery economic data

Data	Value
Battery cost [€/kWh]	206
Battery cell voltage [V]	12

Now, considering the results obtained in the previous paragraph, we have that the cost of the fuel cell system and battery are respectively the following ones:

Table 4.9: Resume of the main initial costs

Size [kW]	Fuel system cost [€]	Battery bank cost [€]	Investment cost [€]
6	29580	14506	44086
8	39440	4618	44058
10	49300	692	49992

As we can see from these results, the initial investment cost is not so much different among the various size solutions. This is due to the fact that the savings gained by the reduction of the size are substituted by an increase of the battery bank's cost.

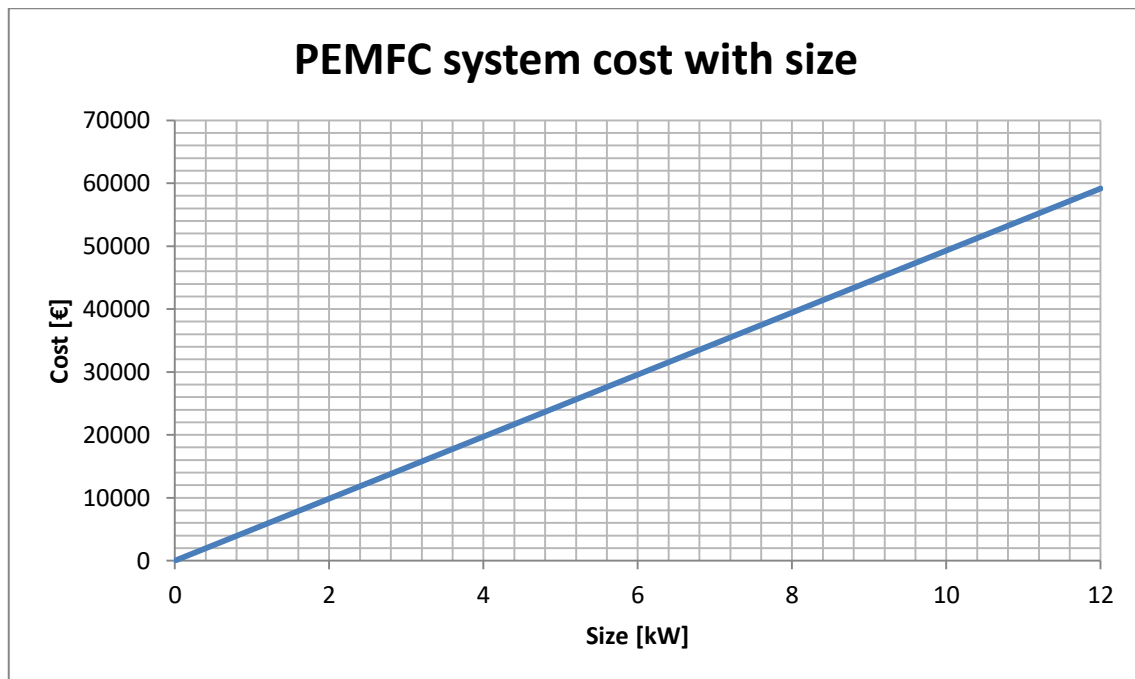


Figure 4.11: Cost trend of the PEMFC system with size

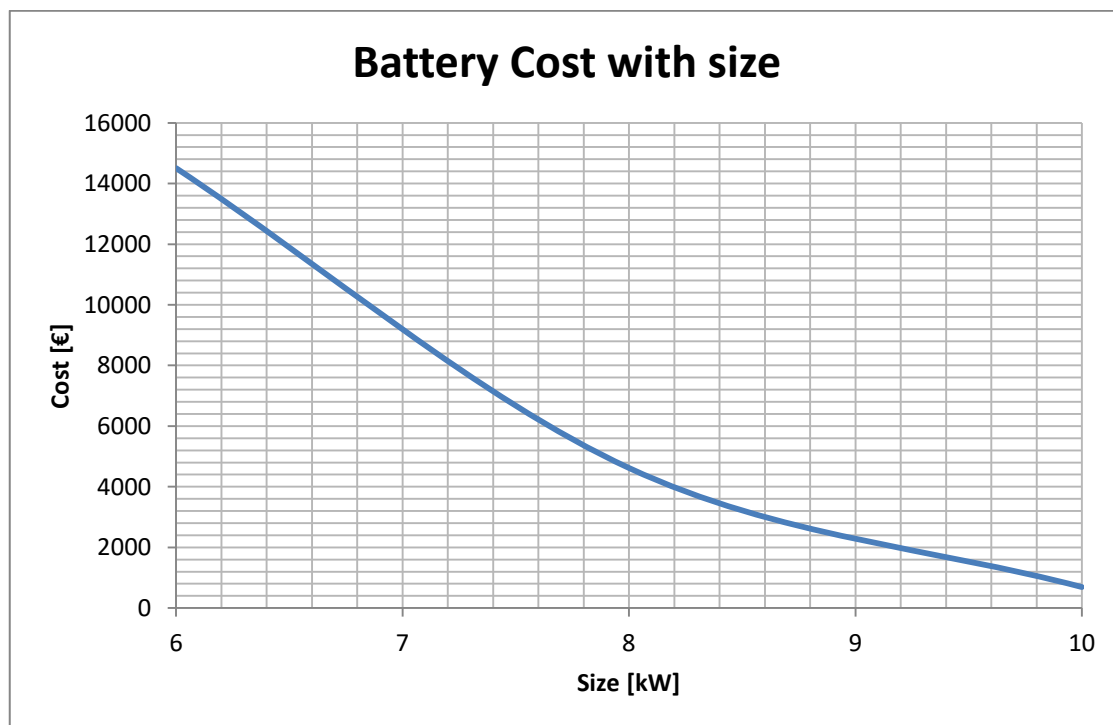


Figure 4.12: Cost trend of the battery bank with size

At this point, in order to have a better overview of which solution is better, we need to consider also the operative costs. In fact, reducing the size, we have also savings on the hydrogen consumed by the device. This is a quite relevant aspect when the period of operation becomes widespread. But, before proceeding with this part of the analysis, it is important to define a period for the comparison. Considering the area of analysis, we decide to refer the consumptions

to a period of one year, since this is the standard time of reference for the evaluation of a new technology from an energetic and economic point of view.

Table 4.10: Hydrogen operative cost and consumption

Size [kW]	H ₂ consumption [kg/year]	H ₂ annual cost [€/year]
6	835.23	3340.92
8	968.51	3874.04
10	985.17	3940.68

For the evaluation of the cost of hydrogen, we refer to a particular record of the DOE [14], in which the H₂ is produced by a solid oxide electrolyzer. Looking at the document, we have that the cost of production of 1 kg of H₂ is around 4 €, but we need to point out that this cost does not take into account the cost of delivery and transport. In that case the cost results to be much higher and around 7 € [15].

At this point, in order to proceed with the final calculations, we need to refer the cost, seen in table 4.9, on a year basis for the reasons discussed above. But, in order to do so, we need, first, to evaluate the lifetime of the battery chosen. Considering that, in our case, an AGM lead acid battery used for solar applications was selected, we have that the curve of the life cycle at varying of the depth of discharge is the following one:

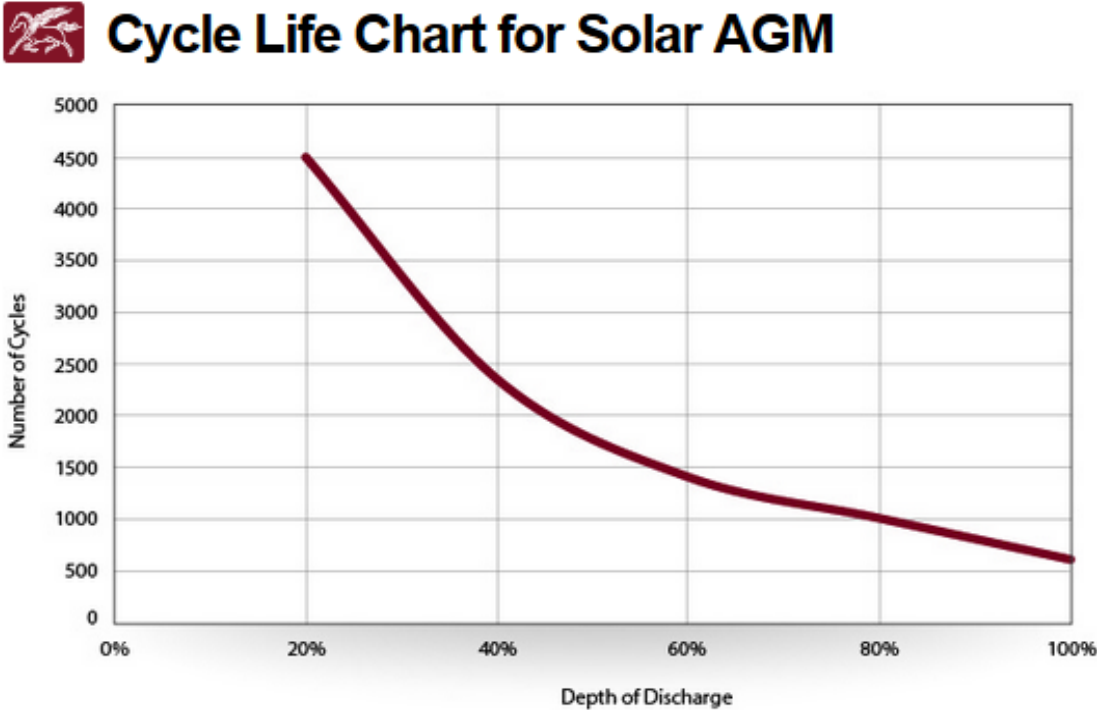


Figure 4.13: Life cycle profile at varying of the DOD [16]

Looking at the plot, we can see that for the DOD used for the sizing of the battery bank we have a life of around 4500 cycles. Then from this value, considering that the days of work in a year are around 302, we have that at least the battery bank would have a lifetime of 15 years.

At the end, considering both the investment and operative costs on a year basis, we are able to make the comparison between each solution, obtaining the following results:

Table 4.11: Economic results at varying of the size

Size [kW]	Investment cost [€/year]	Operative cost [€/year]	Total cost [€/year]
6	3925.1	3490.9	7416.0
8	4251.9	4074.0	8325.9
10	4976.1	4190.7	9166.8

From the results, we can see that the size of 6 kW emerges to be the most convenient from an economic point of view. This is especially due to the savings on the operative costs, as we can see from the table. Said that, from this point on, we will only consider this size for the next evaluations and for the final configuration of the gen-set.

4.4 Main components sizing

Before proceeding with the representation of the final scheme of the device, we need, first, to give an idea of the main characteristics of the other important components that are respectively the storage tank and the auxiliary components such as pumps and blowers.

4.4.1 Storage tank sizing

Starting with the storage tank, we can say that it is a main component from which depends the reliability of the entire system. In fact, if the size is not appropriately dimensioned, we can incur the risk to leave uncovered the user, but also the oversize has to be avoided due to the increasing cost of the tank with the volume. Said that, two alternative solutions are considered for the sizing of the hydrogen storage.

The first solution considers a daily storage tank size in which the bottle has to be changed every day. This solution, of course, reduces the cost of the storage, but at the same time increases the operative cost during time. The second solution, instead, considers a weekly storage tank. In this case, we have a higher cost of the tank, but with a reduced cost of the vessel substitutions. Of course, the best solution depends on the type of application that the gen-set considered has to face, since from it depends the period of working operation of the device. Anyway, for the type

of application we focused more on, there is no preference since the construction site could work for a wide variety of periods, so seems quite interesting to consider this aspect during the study.

At this point considering the chosen size for the generation set, we can easily compute (see appendix A.6) the amount of hydrogen and the size of the storage tank required for both the configurations.

Table 4.12: Configuration tank results

Data	Daily solution	Weekly solution
M_{H_2} [kg]	3.04	18.23
V_{H_2} [liter]	203	1218
C_{tank} [€]	710	4263

Of course, these results are obtained considering the condition in which the hydrogen is stored, that is respectively 200 bar and 25°C. In fact, these conditions are quite important for the calculation of the hydrogen’s density inside the tank. Said that, it is important to point out how the cost of the tank is varied between the two solutions. This is due to the fact that the cost of the storage tank is determined through the amount of hydrogen contained on it, so, for obvious reason, the weekly solution has to have a cost approximately 6 times higher than the daily one. Anyway, the best solution has to be obtained considering the period of time we think the device has to operate. This aspect can be easily seen in the following plot:

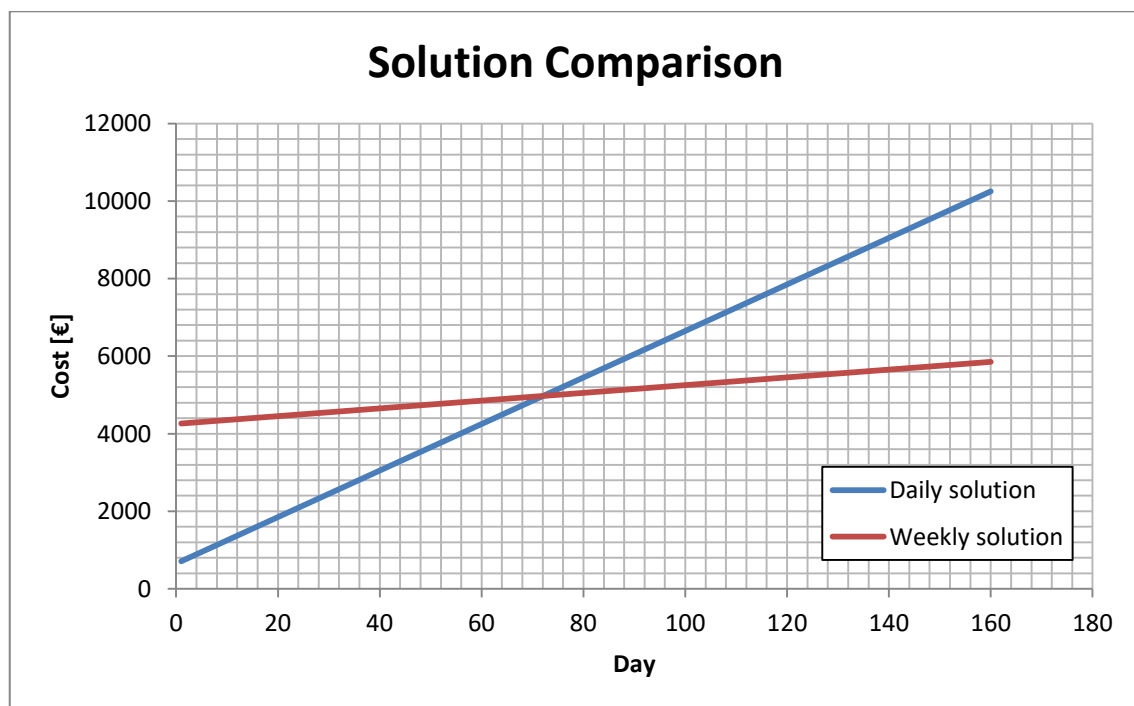


Figure 4.14: Cost trend of both solution during time

In order to obtain this plot some considerations are made. But, before entering into detail on this aspect, we need to give some information about the type of hydrogen vessel chosen. We suppose to consider a steel storage vessel similar to the one used for the methane [17]. This is important to point out, since this choice is reflected in terms of cost in the plot. In fact, this is a quite standard solution for consolidated high pressure vessel where the structural stress component is less critical. In addition to that, we choose to operate with 200 bar due to the regulation regarding the transport of hydrogen compressed, but also due to the fact that our application has no limit of space in contrast to the automotive application where higher pressure are quite necessary.

At this point, turning back on the figure 4.14, we can see that the cost due to the substitution over time is not negligible. As a consequence, the period of operation is a key point on the evaluation of the best solution. So, in order to achieve a quite good comparison between the two alternative options, we refer to the *Rivoira S.p.a* [18] for the estimation of the cost of substitution which is not different between the two solutions due to the small dimensions of the storage tanks considered. Said that, another important thing to point out is the fact that we suppose to consider a construction site operating 8 hours a day and 6 days a week, so, approximately, the period represented in the plot is around 6 months. This is important since this kind of machinery can operate also in other working environments where a reduced period of operation is requested. At this point, a resume of all the data used for the calculations are reported in table below:

Table 4.13: Data for the calculation of the storage size

Data	Value
H ₂ density [kg/m ³]	15
Hour of operation [h/day]	8
Days of operation [day/week]	6
Storage unit cost [€/liter]	3.5
Cost of substitution [€]	60

4.4.2 Blower sizing

Regarding this type of component, we have used it to move the recirculated stream and the air entering the stack, since thanks to it the fluid is able to reach the stack at the required pressure condition, covering all the losses that the fluid incur during the process. Said that, we can easily understand that, in order to size it, we need to estimate these pressure losses. Now, considering the fact that this device has to be “compact”, we have supposed to neglect the distributed pressure losses in the pipelines in order to simplify the analysis. In fact, from a raw calculation

we have seen that this type of losses is less relevant respect to the concentrated pressure losses that we have inside some components such as the stack and the membrane humidifier.

Table 4.14: Stack pressure drops [6]

Data	Value
Anodic pressure drop [bar]	0.15
Cathodic pressure drop [bar]	0.20

Looking at the table, we can see that the pressure drops inside the flow channels are quite high. This is due to the fact that the flow channels inside the stack have a very small section, so the pressure losses results to be quite relevant. In addition to that, we need to consider that these values are referred to the stack working at maximum power, since this is the nominal condition at which the device is supposed to operate.

Regarding the membrane humidifier, we refer to the Perma Pure [19]. From its catalogue, we choose the FC-400 series, since it is the best designed humidifier for the range of power size considered.

Table 4.15: Perma Pure FC-400 data

Data	Value
P_{\max} [bar]	1.72
G_{\min} [m ³ /h]	12
G_{\max} [m ³ /h]	60
ΔP [bar]	0.05

At this point, in order to proceed with the sizing, we need to define the conditions at which the blower have to operate. To do so, not only the static pressure is needed, but also the nominal flow rate and the density at which the fluid is at that particular condition.

For what concerns the recirculation blower, we have that it works with a mixture of hydrogen and water vapour. But, considering that only a part of the anodic flow exiting the stack has to be recirculated, we have that this component operates with a reduced mass flow rate given by the control system of the humidification at the condition of 70°C and 1 bar. The further reduction in terms of pressure is caused by the water separator put between the stack and the recirculation circuit. Said that, the operative parameters, needed for the sizing of the recirculation blower, are the following:

Table 4.16: Recirculation blower sizing parameters

Data	Value
Nominal flow rate [m ³ /h]	1.53
Static pressure [bar]	0.2
Density of the fluid [kg/m ³]	0.086
Efficiency	0.7

Regarding, instead, the air circulation blower, we have that it works with air taken from the environment at the condition of 1 bar and 25°C. In this case, considering the pressure drops caused by the membrane humidifier, we have that a higher static pressure has to be considered.

Table 4.17: Air circulation blower sizing parameters

Data	Value
Nominal flow rate [m ³ /h]	24.65
Static pressure [bar]	0.25
Density of the fluid [kg/m ³]	1.16
Efficiency	0.7

From the table, it is important to point out that the nominal condition resulted in the air circuit are in accordance with the operative condition of the membrane humidifier chosen, strengthening the hypothesis made.

4.4.3 Pump sizing

Similarly to the cases described above, in order to size the pump, we need to know the head and the nominal flow rate. To do so, we need first to consider the pressure drop that we have in the cooling circuit. But, as we have seen for the blower, the pressure drop results to be, in general, caused by the circulation of the coolant in the cooling channels inside the stack. In fact, the value obtained from it is quite relevant respect to the distributed pressure losses. So, also in this case we will consider only the concentrated pressure losses that we suppose to split in this way:

Table 4.18: Cooling circuit pressure drops

Data	Value
Stack pressure drop [bar]	0.15
Cooler system pressure drop [bar]	0.05

For what concerns the first term, it refers to the pressure drop generated inside the stack, while the second term refers to the pressure drops generated by the other components such as the air cooler and the expansion tank.

Said that, the operative parameters for the sizing of the cooling pump are:

Table 4.19: Pump sizing parameters

Data	Value
Nominal flow rate [m ³ /h]	0.60
Static head [m]	2.10
Efficiency	0.9

4.5 Scheme and final configuration

At this point, to complete the study a scheme of the final configuration is reported in the figure 4.15. As we can see from the picture, a lot of sensors are considered. These are quite important for the control regulation of the device at varying of load, since temperature, pressure and level of humidity of the various streams are a key aspects to maintain under control. In fact, all of them individually can impact on the fuel cell performance leading to a less desired operative condition. For this reason, we consider to put temperature and pressure sensors on the streams entering the stack, in a way that the blowers and regulator valves could be regulated accordingly to reach the desired conditions.

In addition to that, it is important to point out the presence of a nitrogen bottle connected to both the reactant pipelines. This is a safety system used in case there is a clog of reactants inside the stack. It is also used for the venting of the device at the end of the working operation, since the nitrogen is a neutral component that does not react inside the stack.

For what concerns the cooling circuit, a lot of considerations are made. Starting with the regulation of the coolant flow rate, we have that it is controlled by the temperature sensors put downstream the pump. This is due to the fact that the amount of heat dissipated by the air cooler depends on the flow rate imposed by the pump. So regulating the pump, we have a better regulation of the amount of heat dissipated and, therefore, of the coolant temperature entering the stack. It is important, also, to point out the addition of the three-way valve and expansion tank. These are components quite important during the start-up, since during this period there is an higher variation of temperature of the coolant. Regarding the expansion tank, it has the role to

counter the fluctuations of pressure we have in the circuit due to the dilation of the fluid caused by the increase of temperature. For what concerns, instead, the three-way valve, it is used to let the coolant by-pass the air cooler during the start-up since we need to reach the optimal temperature of operation of the stack as quick as possible.

Lastly, from the scheme we can notice also the electronic components such as battery, converter and inverter. Regarding the supporting battery, there is nothing to add, except for the fact that is coupled with the DC-DC converter, since this one is used to convert a source of direct current from one voltage level to another. For what concerns the inverter, instead, it is used to change the direct current (DC) produced to alternating current (AC) in order to be able to generate the power tools connected to the gen-set.

As a conclusion, in order to give an overall idea of all the study, a resume of the principal characteristics of the main components is reported in the table down below.

Table 4.20: Resume table of the final configuration

FC Data		FC Data	
T_c [°C]	70	Size [kW]	6
P_c [bar]	1.2	$T_{\text{start-up}}$ [s]	240
n_c	56		
Battery Data		Tank Data	
Capacity [Ah]	1466.2	P_{tank} [bar]	200
N_{cell}	60	V_{tank} [lt]	1218
DOD	0.2		
Recirculation blower Data		Air circulation blower Data	
Nominal flow rate [m ³ /h]	1.53	Nominal flow rate [m ³ /h]	24.65
SP [bar]	0.2	SP [bar]	0.25
Fluid density [kg/m ³]	0.086	Fluid density [kg/m ³]	1.16
Efficiency	0.7	Efficiency	0.7
Pump Data		Pump Data	
Nominal flow rate [m ³ /h]	0.60	Static head [m]	2.1
Efficiency	0.9		

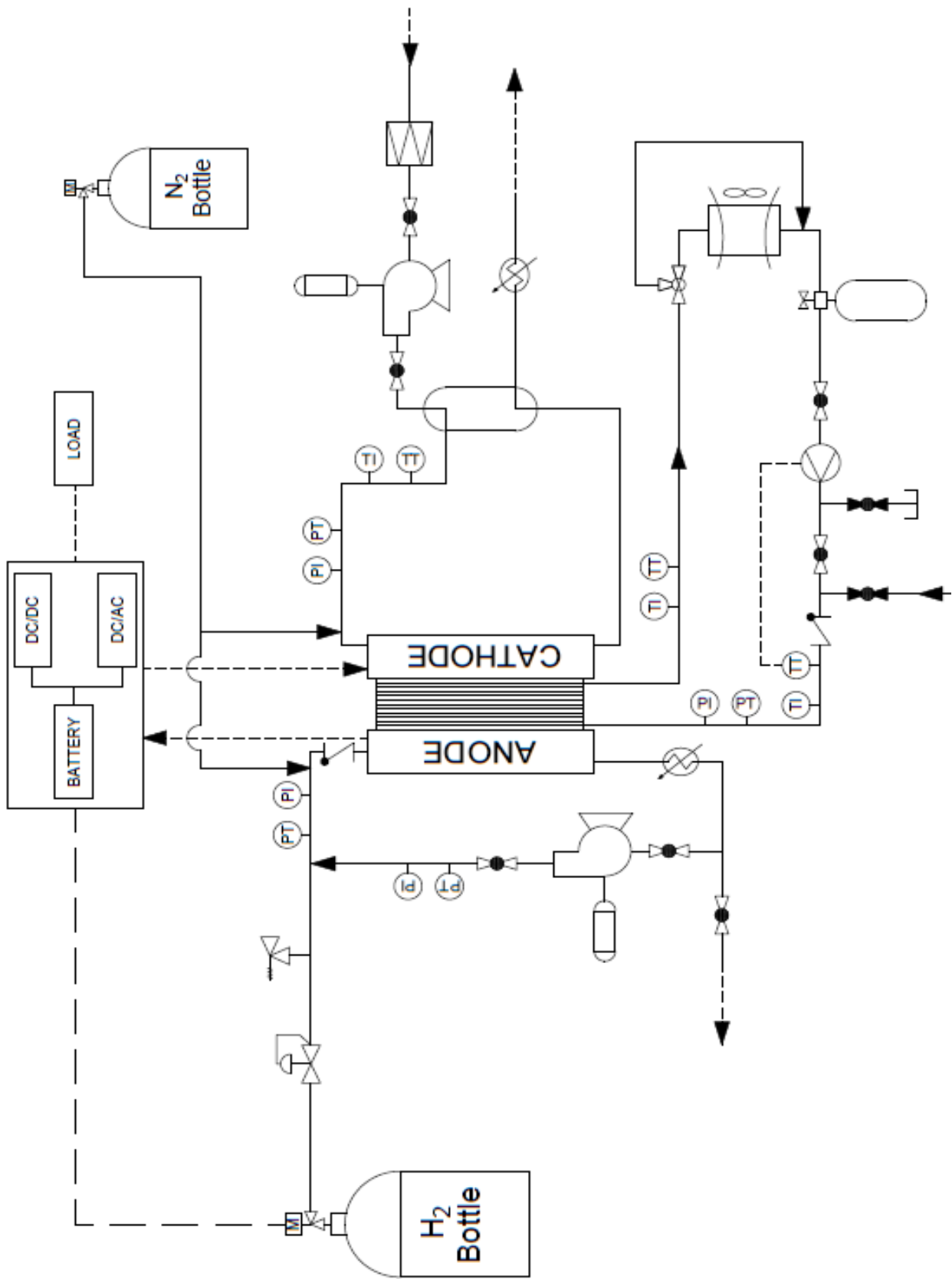


Figure 4.15: Scheme of the final configuration of the gen-set

Chapter 5

CONCLUDING REMARKS

5.1 Conclusions and consideration

As a resume of the study carried out until this point, we have that the solution of the PEM fuel cell as a generation set is resulted to be a quite interesting alternative to the traditional Diesel generator. This is due to some notable aspects that has to be considered making this comparison. First of all, the process through which the electrical energy is produced is environmental friendly letting us to reduce the utilization of fossil fuels. In addition to that, the lack of a combustion process decreases the sum of moving parts, reducing the amount of maintenance these devices need. On the contrary, we have seen that this type of devices has a big cost of supporting components such as battery and storages. In fact, from the study results that there is a trade-off between the cost of the supporting battery and the cost of the fuel cell itself. In any case it is hard to make a comparison between the two alternative solutions. But, what we can say for sure is that the operative cost due to the substitution of the hydrogen storage bottle is not negligible over time. Said that, another interesting point of comparison is the efficiency of the BOP system. As we have seen by the simulation made in Aspen Plus, the efficiency of the entire system is around 0.45-0.50 for the maximum power range, while for a Diesel generator of the same power size is around 0.4-0.45 [20]. This is a quite interesting aspect to not overlook, especially for lower size of power generator. Considering, instead, higher sizes of gen-set around 300-1500 kW, we have that Diesel generators are the best solution not only due to its increased efficiency (equal to 0.50-0.55), but especially due to the difficulty of providing such a huge amount of hydrogen, if we consider to operate with a PEMFC gen-set. This is an important aspect and a big constraint to consider when we are thinking to operate with hydrogen.

Finally, another important aspect to take into consideration is that Diesel generator is a well-consolidated technology, while the PEMFC gen-set for obvious reasons is a less tested solution (few commercial companies are available on the market, such as *Hydrogenics* and *Plug Power*). This is a key aspect when we consider applications for which a high reliability is required, such

as back-up supply power generators. In the case studied, this is not a big constraint, but anyway, the device has to maintain a good reliability under operability among years. Another big difference, as anticipated before, it is the importance of the battery in both solutions. In fact, as we have seen in the PEMFC gen-set, the battery is a quite important component used, not only at the start-up, but also during operation due to limits on ramp rates of the PEMFC.

At the end, looking at all these aspects we can say that both solutions have pros and cons. Anyway, the determining factor remains always the cost of the entire system. This is an aspect that is not completely covered by the study due to the goal of the thesis, but, of course, it is not a negligible aspect when we are talking about new technologies. So, in order to have a better idea of the feasibility of this solution into the market, a specific economic analysis of the case of study should be done, especially making an economic comparison with the current technology.

REFERENCE

- [1] AKSA Power Generation, [Online]. Available: <http://www.jatpower.com/blog/parts-of-a-diesel-generator/>.
- [2] PERIN Generators, [Online]. Available: <http://www.gruppielettrogeni.it/index.html>.
- [3] I.S.O. International Organization for Standardization, *8528-1*, 2005.
- [4] Diesel Service and Supply, [Online]. Available: http://www.dieselserviceandsupply.com/Power_Consumption_Chart.aspx.
- [5] INEVA Centre National de Recherche Technologique, Belfort-Montbéliard-Nancy.
- [6] A. Rabbani, *Dynamic performance of a PEM fuel cell system*, 2013.
- [7] P. T. M. P. J. P. J.-P. S. Albert Lehmani, «Ion Transport in Nafion 117 membrane,» *Journal of Electroanalytical Chemistry*, 1996.
- [8] ABB. [Online]. Available: <https://library.e.abb.com/public/3baadd9082d84787a3e32e921614ea44/1SDC007106G0901.pdf>.
- [9] M. G. A. L. M. S. R. Napoli, «Techno-economic analysis of PEMFC and SOFC micro-CHP fuel cellsystems for the residential sector,» *Science direct*, 2014.
- [10] R. T. A. Fly, «A comparison of evaporative and liquid cooling,» *Elsevier*, 2016.
- [11] Trojan, [Online]. Available: http://www.trojanbattery.com/pdf/TRJN0168_BattSizeGuideFL.pdf.
- [12] Department of Energy, [Online]. Available: <https://www.energy.gov/eere/fuelcells/doe-technical-targets-fuel-cell-backup-power-systems>.
- [13] National Renewable Energy Laboratory, «Economic Analysis Case Studies of Battery Energy Storage with SAM,» 2015.

- [14] Department of Energy, «Hydrogen Production Cost from Solid Oxide Electrolysis,» 2016.
- [15] Department of Energy, «Hydrogen Delivery Cost Projections – 2015,» 2016.
- [16] Trojan, [Online]. Available: <http://www.trojanbattery.com/solar-agm/>.
- [17] A. Bassi, 2003. [Online]. Available: http://www.aimnet.it/allpdf/pdf_pubbli/2/bassi.pdf.
- [18] Rivoira spa, [Online]. Available: <http://www.rivoiragroup.it/it-it>.
- [19] Perma Pure, [Online]. Available: <http://www.permapure.com/products/gas-humidification/fc-series-humidifiers/>.
- [20] SHAKTI Sustainable Energy Foundation, [Online]. Available: <http://shaktifoundation.in/wp-content/uploads/2014/02/Shakti-Diesel-Generators-FINAL1.pdf>.

APPENDIX

A.1 Matlab code for the simulation of the cell characteristics

```
clear all
close all
clc

% Initial data
Ppmfc=1.2; %[bar]
A=500; %[cm^2]
F=96485; %[s*A/mol]
OCV=1.18; %[V]
nc=1; % number of cells
i_int=0.002; %[A/cm^2]
tm=0.0183; %[cm] Nafion thickness
R=8.314; %[J/mol/k]
beta=0.5;
wc=8.5; % water content
sigma30=0.005139*wc-0.00326;
LHV=121000; %[kJ/kg]

Imin=0; %[A]
Imax=350; %[A]
ii=(linspace(Imin, Imax, (Imax-Imin)))/A;

Tpmfc=70+273.15; %[K]
% Transfer coefficients
tc_an=beta*4;
tc_cath=(1-beta)*1;
% Exchange current density
i0_an=0.1;
i0_cath=0.2*10^-3;

for j=1:(Imax-Imin)

    I=Imin+j;
    i=I/A; %[A/cm^2]
    % Activation Overvoltage
    k1=(i+i_int)/(2*i0_an);
    k2=(i+i_int)/(2*i0_cath);
    eta_act(j)=R*Tpmfc/(tc_an*F)*log(k1+sqrt(k1^2+1))+...
        R*Tpmfc/(tc_cath*F)*log(k2+sqrt(k2^2+1)); %[V]

    % Ohmic Overvoltage
    sigma=exp(1268*(1/303-1/Tpmfc))*sigma30;
    ASR=tm/sigma; %[Ohm*cm^2]
    eta_ohm(j)=ASR*(i+i_int); %[V]

    % Diffusion Overvoltage
    i_max=1.5; %[A/cm^2]
    il_an=1*i_max;
    il_cath=0.5*i_max;
    eta_diff(j)=abs(R*Tpmfc/(2*F)*log(1-(i+i_int)/il_an))+...
        abs(R*Tpmfc/(4*F)*log(1-(i+i_int)/il_cath)); %[V]

    % Polarization Curve
    V(j)=OCV-eta_act(j)-eta_ohm(j)-eta_diff(j); % [V]
    % Electric power of the stack
    P(j)=V(j)*I*nc/1000; % [kW]
```

```

% Calculation of the air and fuel utilization
if I<=50
    FU=1/(-1/40*I+2.5);
    AIRU=1/(-1/50*I+3);
else
    FU=0.8;
    AIRU=0.5;
end

% Efficiency of the stack
G(j)=I/(2*F)*nc*2/1000; %[kg/s]
eta(j)=P(j)/(G(j)*LHV)*100;

end

figure(1)
hold on; grid on; box on; grid minor;
plot(ii,V,'b','linewidth',1.2);
title('Polarization curve');
xlabel('Current density [A/cm^{2}]');
ylabel('Cell voltage [V]');

figure(2)
hold on; grid on; box on; grid minor;
plot(ii,P,'b','linewidth',1.2);
title('Cell power');
xlabel('Current density [A/cm^{2}]');
ylabel('Electric power [kW]');

figure(3)
hold on; grid on; box on; grid minor;
plot(ii,eta,'b','linewidth',1.2);
title('Cell efficiency');
xlabel('Current density [A/cm^{2}]');
ylabel('Efficiency [%]');

```

A.2 Matlab code for the check of the level of hydration inside the cell

```
clear all
close all
clc

% Input variable
I=250; %[A]

% Input data
A=500; %[cm^2]
F=96485; %[s*A/mol]
nc=90; % number of cell
PM_air=28.92; %[g/mol]
PM_H2=2; %[g/mol]
i=I/A; %[A/cm^2] current density
Tc=70; %[°C]
nd_sat=2.5;

% Nafion input data
rhon=1.98; %[g/cm^3]
tm=0.0183; %[cm]
Mm=1100; %[g/mol]

% Calculation of the air and fuel utilization
if I<=50
    FU=1/(-1/40*I+2.5);
    AIRU=1/(-1/50*I+3);
else
    FU=0.8;
    AIRU=0.5;
end

% Inlet anode stream calculations
G_H2i=I/(2*F)/FU*nc; %[mol/s]
M_H2i=G_H2i*PM_H2/1000; %[kg/s]
% Inlet cathode stream calculations
G_airi=I/(4*F)*1/0.21/AIRU*nc; %[mol/s]
M_air=G_airi*PM_air/1000; %[kg/s]

% Outlet anode stream calculations
G_H2o=I/(2*F)*(1/FU-1)*nc; %[mol/s]
M_H2o=G_H2o*PM_H2/1000; %[kg/s]
% Outlet cathode stream calculations
G_O2o=G_airi*0.21-I/(4*F)*nc; %[mol/s]
G_N2o=G_airi*0.79; %[mol/s]
G_airo=G_O2o+G_N2o; %[mol/s]

% Temperature of water streams entering the stack
Tan=43; %[°C]
Tcath=60; %[°C]

% Pressure of the streams entering the stack
Pan=1.2; %[bar]
Pcath=1.2; %[bar]

% Initialization humidification variable
RHan_out=0;
RHcath=0.95;
xw_c=RHcath*Psat(Tcath)/Pcath;
xw_a=RHan_out*Psat(Tc)/Pan;
```

```

G_H2Oci=(xw_c*M_air)*1000/18; %[mol/s]
G_H2Oai=(xw_a*M_H2o)*1000/18; %[mol/s]
G_H2Oco=G_H2Oci+I/(2*F)*nc; %[mol/s]
G_H2Oao=G_H2Oai;

Gnet=0;

% Counter variable
count=1000;

for ii=1:count

    % Cathodic relative humidity
    RHcath=0.95;

    % Calculation of the inlet water molar flow rate
    xw_c=RHcath*Psat(Tcath)/Pcath;
    xw_a=RHan_out*Psat(Tc)/Pan;
    G_H2Oci=(xw_c*M_air)*1000/18; %[mol/s]
    G_H2Oai=(xw_a*M_H2o)*1000/18; %[mol/s]

    % Calculation of the inlet anode molar flow rate
    Gtot_ai=G_H2i+G_H2Oai; %[mol/s]
    % Calculation of the outlet anode molar flow rate
    Gtot_ao=G_H2o+G_H2Oao; %[mol/s]

    % Calculation of the inlet cathode molar flow rate
    Gtot_ci=G_airi+G_H2Oci; %[mol/s]
    % Calculation of the outlet cathode molar flow rate
    Gtot_co=G_airo+G_H2Oco; %[mol/s]

    % Dehydration control check
    if G_H2Oao<0
        G_H2Oao=0; %[mol/s]
    end

    % Calculation of the vapour partial pressure
    y_H2Oai=G_H2Oai/Gtot_ai;
    y_H2Oao=G_H2Oao/Gtot_ao;
    y_H2Oci=G_H2Oci/Gtot_ci;
    y_H2Oco=G_H2Oco/Gtot_co;

    Pw_ai=Pan*y_H2Oai;
    Pw_ao=Pan*y_H2Oao;
    Pw_ci=Pcath*y_H2Oci;
    Pw_co=Pcath*y_H2Oco;

    % Calculation of the water activity
    aw_ai=Pw_ai/Psat(Tan);
    aw_ao=Pw_ao/Psat(Tc);
    aw_ci=Pw_ci/Psat(Tcath);
    aw_co=Pw_co/Psat(Tc);

    aw_an=aw_ai*0.2+aw_ao*0.8;
    aw_cath=aw_ci*0.2+aw_co*0.8;

    % Calculation of the anode water content
    if aw_an>=1 && aw_an<=1
        lambda_an=0.043+17.18*aw_an-39.85*aw_an^2+36.0*aw_an^3;
    else
        lambda_an=14+1.4*(aw_an-1);
    end
end

```

```

end

% Calculation of the cathode water content
if aw_cath>0 && aw_cath<1
    lambda_cath=0.043+17.18*aw_cath-39.85*aw_cath^2+36.0*aw_cath^3;
else
    lambda_cath=14+1.4*(aw_cath-1);
end

% Water content of the membrane
lambda=(lambda_an+lambda_cath)/2;

% Calculation of the electro-osmotic drag molar flow rate
nd=lambda*nd_sat/22;
Gel_drag=2*nd*I/(2*F); %[mol/s]

% Calculation of the back-diffusion molar flow rate
DL=10^-6*(2.563-0.33*lambda+0.0264*lambda^2-0.000671*lambda^3);
Dw=DL*exp(2416*(1/303-1/(273+Tc)));
Gdiff=rhom/Mm*Dw*(lambda_cath-lambda_an)/tm*A; %[mol/s]

% Update of the net water crossover
Gnet=Gel_drag-Gdiff; %[mol/s]

% Calculation of the outlet water molar flow rate
G_H2Oco=G_H2Oci+I/(2*F)*nc+Gnet; %[mol/s]
G_H2Oao=G_H2Oai-Gnet; %[mol/s]

% Control of the level of hydration in the cell at the exit
xw_ao=(G_H2Oao*18/1000)/(M_H2o+G_H2Oao*18/1000);
RHan_out=xw_ao*Pan/Psat(Tc);

% Elimination of the water condensed
if RHan_out>1
    RHan_out=1;
end

% Check of the exiting water RH
RHan_out

% Calculation of the amount of water exiting the separator
xw_ao=RHan_out*Psat(Tc)/Pan;
Mtot_ao=(G_H2o*2/1000)/(1-xw_ao); %[kg/s]
M_H2Oao=xw_ao*Mtot_ao; %[kg/s]

end

```

A.3 Matlab code for the simulation of the start-up

```
clear all
close all
clc

% Initial data
Pc=1.2; %[bar]
I=200; %[A]
A=500; %[cm^2]
i=I/A; %[A/cm^2]
F=96485; %[s*A/mol]
nc=90; % number of cells
i_int=0.002; %[A/cm^2]
tm=0.0183; %[cm] Nafion thickness
R=8.314; %[J/mol/k]
beta=0.5;
wc=8.5; % water content
sigma30=0.005139*wc-0.00326;
M_FC=46.546; %[kg]
cp_FC=1000; %[J/kg*K]
Cc=cp_FC*M_FC; %[J/kg]

% Enthalpy and entropy coefficients
a_H2=27.1;
b_H2=0.0093;
c_H2=-0.0000138;
d_H2=7.65e-9;

a_O2=28.1;
b_O2=0;
c_O2=0.0000175;
d_O2=-1.07e-8;

a_H2O=32.2;
b_H2O=0.0019;
c_H2O=0.0000106;
d_H2O=-3.6e-9;

% Initial temperature
Tc=25+273.15; %[K]

% Time step
dt=10; %[s]

err=1;
count=0;

while err==1

    % Number of time steps
    count=count+1;

    % Calculation of the enthalpy of the components
    h_H2=a_H2*Tc+0.5*b_H2*Tc^2+1/3*c_H2*Tc^3+1/4*d_H2*Tc^4; %[kJ/kmol]
    h_O2=a_O2*Tc+0.5*b_O2*Tc^2+1/3*c_O2*Tc^3+1/4*d_O2*Tc^4; %[kJ/kmol]
    h_H2O=a_H2O*Tc+0.5*b_H2O*Tc^2+1/3*c_H2O*Tc^3+1/4*d_H2O*Tc^4; %[kJ/kmol]

    % Calculation of the entropy of the components
    s_H2=a_H2*log(Tc)+b_H2*Tc+0.5*c_H2*Tc^2+1/3*d_H2*Tc^3+...
        -R*log(Pc*10^5); %[kJ/kmol*K]
```

```

s_O2=a_O2*log(Tc)+b_O2*Tc+0.5*c_O2*Tc^2+1/3*d_O2*Tc^3+...
-R*log(Pc*10^5); %[kJ/kmol*K]
s_H2O=a_H2O*log(Tc)+b_H2O*Tc+0.5*c_H2O*Tc^2+1/3*d_H2O*Tc^3+...
-R*log(Pc*10^5); %[kJ/kmol*K]

% Enthalpy and entropy of formation of water vapour
hf_H2O=-242000; %[kJ/kmol]
sf_H2O=-44.4; %[kJ/kmol*K]

ht_H2O=hf_H2O+h_H2O;
st_H2O=sf_H2O+s_H2O;

% Calculation of the Gibbs free energy
dh=ht_H2O-h_H2-0.5*h_O2;
ds=st_H2O-s_H2-0.5*s_O2;
dG=dh-Tc*ds;

% Calculation of the open circuit voltage
OCV=-dG/(2*F);

% Amount of heat produced by the stack
Q=dh*I/(2*F)*nc;

%-----Calculation of the cell voltage-----

% Transfer coefficients
tc_an=beta*4;
tc_cath=(1-beta)*1;
% Exchange current density
i0_an=0.1; %[A/cm^2]
i0_cath=0.6*F*exp(-tc_cath*F*OCV/(R*Tc)); %[A/cm^2]

% Calculation of the activation overvoltage
k1=(i+i_int)/(2*i0_an);
k2=(i+i_int)/(2*i0_cath);
eta_act=R*Tc/(tc_an*F)*log(k1+sqrt(k1^2+1))+...
R*Tc/(tc_cath*F)*log(k2+sqrt(k2^2+1)); %[V]

% Area specific resistance
sigma=exp(1268*(1/303-1/Tc))*sigma30;
ASR=tm/sigma; %[Ohm*cm^2]

% Calculation of the ohmic overvoltage
eta_ohm=ASR*(i+i_int); %[V]

% Limiting current density
i_max=1.5; %[A/cm^2]
il_an=1*i_max;
il_cath=0.5*i_max;

% Calculation of the diffusion overvoltage
eta_diff=abs(R*Tc/(2*F)*log(1-(i+i_int)/il_an))+...
abs(R*Tc/(4*F)*log(1-(i+i_int)/il_cath)); %[V]

% Polarization Curve
V=OCV-eta_act-eta_ohm-eta_diff; %[V]

% Dissipated heat
Qc=(-dh/(2*F)-V)*I*nc;

% Electric power of the stack

```

```

P=V*I*nc/1000; % [kW]

% Update of the temperature of the stack
Tc=Tc+Qc/Cc*dt;
T_FC(count)=Tc;

if Tc>=70+273.15
    % Fuel cell ready to work
    err=0;
end

end

% Time to start-up
t_start=count*dt;
tt=0:dt:t_start;

figure(1)
hold on; grid on; box on; grid minor;
plot(tt,[25,T_FC-273.15],'b','linewidth',1.25);
ylabel('Temperature [°C]');
ylim([0 80]);
xlabel('Time [s]');
title('FC Temperature');

```

A.4 Matlab code for the simulation of the load following

```
clear all
close all
clc

% Initial data
i=xlsread('WorkingLoad.xlsx','Map','B4:B204'); %[A/cm^2]
Pfc=xlsread('WorkingLoad.xlsx','Map','C4:C204'); %[W]
Ppump=xlsread('WorkingLoad.xlsx','Map','F4:F204'); %[W]
Pcomp=xlsread('WorkingLoad.xlsx','Map','D4:D204'); %[W]
Prec=xlsread('WorkingLoad.xlsx','Map','E4:E204'); %[W]
Qcool=xlsread('WorkingLoad.xlsx','Map','G4:G204'); %[W]
Pload=xlsread('WorkingLoad.xlsx','Load','E3:E723'); %[W]
time=xlsread('WorkingLoad.xlsx','Load','B3:B723'); %[s]

% Calculation of the net power of the Gen-set
Pconsump=Ppump+Pcomp+Prec;
Pnet=Pfc-Pconsump;

% Calculation of the current
A=500; %[cm^2]
I=i*A; %[A]

% Maximum ramp rate
Ramp_max=30; %[W/s]
t_step=10; %[s]

% Time to start-up
T_start=150; %[s]
% Condition to shut down
T_shut=3600; %[s]
shut=T_shut/t_step;

% Initialization
Pfol=zeros(length(Pload),1);
count=0;

for t=2:length(Pload)

    % Check of start-up
    if Pfol(t-1)==0

        % Counter of the time steps of not production
        count=count+1;

        % Checking if the device is off
        if (t-1)==1
            % The device is off
            work=0;
        elseif count>shut
            % The device is off
            work=0;
        else
            % The device is not producing but is on
            work=1;
        end

        if work==0
            % Determine the time step of running
            ind=(t-1)+T_start/t_step;
```

```

        Pfol(ind)=1;
        % Update of the working flag
        work=1;
        % Update of the counter
        count=0;
    end

else
    %-----The device is running-----

    % Reset of the initial condition for the specify time step
    Pfol(ind)=0;
    % Ramp rate calculation
    m=(Pload(t)-Pfol(t-1))/t_step;

    if m>=0
        % Increasing of load
        if m<=Ramp_max
            % Load can be followed
            Pfol(t)=Pload(t);
        else
            % Load can not be followed
            Pfol(t)=Pfol(t-1)+t_step*Ramp_max;
        end
    else
        % Decreasing of load
        if abs(m)<=Ramp_max
            % Load can be followed
            Pfol(t)=Pload(t);
        else
            % Load can not be followed
            Pfol(t)=Pfol(t-1)-t_step*Ramp_max;
        end
    end
end

end

% Check for the shut down
if count>shut
    % Shut down after 1h of not working
    Pfol(t)=0;
end

end

% Check of the results
P=[(0:t_step:7200)',Pload,Pfol];

figure(1)
hold on; grid on; box on; grid minor;
plot(time,Pload,'b','linewidth',1.1);
plot(time,Pfol,'r--','linewidth',1.1);
xlabel('Time [s]');
ylabel('Power [W]');
legend('Load','Generation');
title('Operation with load following');
xlim([0 7200]);

% Other data
nc=90;
F=96485;
LHV=120; %[MJ/kg]

```

```

PM_H2=2; %[g/mol]

% Initialization
Ifol=zeros(length(Pload),1);
Qfol=zeros(length(Pload),1);
eff=zeros(length(Pload),1);
Pconsumpfol=zeros(length(Pload),1);
Pcheck=zeros(length(Pload),1);

for kk=1:length(Pfol)

    % Find the corresponding value of current
    Pdif=abs(Pfol(kk)-Pnet);
    val=min(abs(Pdif));
    ind=find(val==Pdif);
    Ifol(kk)=I(ind);
    Qfol(kk)=Qcool(ind);
    Pconsumpfol(kk)=Pconsump(ind);
    MH2=Ifol(kk)/(2*F)*nc*PM_H2/1000; %[kg/s]

    % Check
    Pcheck(kk)=Pnet(ind);

    % Calculation of the system efficiency
    eff(kk)=(Pfc(ind)-Pconsump(ind))/(MH2*LHV*10^6);

end

% Verification control matrix
C=[Pcheck,Pfol];

% Saving of the results obtained
xlswrite('WorkingLoad.xlsx',[Ifol,Pfol,Qfol,eff],'Load','G3:J723');

figure(2)
hold on; grid on; box on; grid minor;
plot(time,Ifol,'k','linewidth',1.2);
xlabel('Time [s]');
ylabel('Current [A]');
title('Current profile');
ylim([0 200]);
xlim([0 7200]);

figure(3)
hold on; grid on; box on; grid minor;
plot(time,Qfol,'r','linewidth',1.2);
xlabel('Time [s]');
ylabel('Heat [W]');
title('Discharging heat profile');
xlim([0 7200]);

figure(4)
hold on; grid on; box on; grid minor;
plot(time,eff*100,'b','linewidth',1.2);
xlabel('Time [s]');
ylabel('Efficiency [%]');
title('System efficiency profile');
xlim([0 7200]);

```

A.5 Matlab code for the sizing of the battery bank

```
clear all
close all
clc

% Initial data
Pload=xlsread('WorkingLoad.xlsx','Load','E3:E723'); %[W]
Pfol=xlsread('WorkingLoad.xlsx','Load','H3:H723'); %[W]
time=xlsread('WorkingLoad.xlsx','Load','B3:B723'); %[s]
t_step=10; %[s]
h_work=8; % hours of working (hyp.)
n_inv=0.96; % inverter efficiency
BV=48; %[V] bank voltage
batV=12; %[V] battery cell voltage
nb=1; % number of cell in parallel

%-----Sizing of the battery-----

for i=1:length(time)-1

    % Calculation of the energy requested in each time step
    Eload(i)=(time(i+1)-time(i))*(Pload(i+1)+Pload(i))/2; %[J]
    Efol(i)=(time(i+1)-time(i))*(Pfol(i+1)+Pfol(i))/2; %[J]

end

% Check matrix
C=[Eload' Efol'];

% Calculation of the total energy required to the battery
Eload_tot=sum(Eload); %[J]
Efol_tot=sum(Efol); %[J]
Ebattery=Eload_tot-Efol_tot; %[J]

Ph=Ebattery/7200; %[Wh]
Ptot=Ph*h_work; %[Wh/day]

% Covering factors
CF_g=Efol_tot/Eload_tot*100;
CF_b=Ebattery/Eload_tot*100;

% Calculation of the battery bank capacity
A=(Ptot/n_inv)/BV; %[Ah]

% Calculation of the adjusted battery bank capacity
TC=1; % temperature correction factor
DA=1; % days of autonomy
DM=1.10; % design margin
DOD=0.2; % depth of discharge
Aa=A*TC*DM*DA/DOD; %[Ah]

% Calculation of the Ah cell battery capacity
r=BV/batV; % number of row
Abat=ceil(Aa/nb); %[Ah] cell battery capacity
nb_tot=r*nb; % total number of batteries
```

A.6 Matlab code for the sizing of the hydrogen storage tank

```
clear all
close all
clc

% Initial data
I=xlsread('WorkingLoad6kW.xlsx','Load','G3:G723'); %[A]
P=xlsread('WorkingLoad6kW.xlsx','Load','H3:H723'); %[W]
F=96485;
t_step=10; %[s]
nc=56;
h_work=8; % hours of working (hyp.)
d_work=6; % days of work in a week (hyp.)
daywork2018=302; % days of work in a year (hyp.)
rho=15; %[kg/m3] hydrogen density at 25°C and 200 bar
LHV_H2=121000; %[kJ/kg]
Uc=3.5; %[€/liter] % storage unit cost per liter
Us=60; %[€] % substitution cost

%-----Sizing of the hydrogen tank-----

% Calculation of the total hydrogen consumption in 1 day
G=(I./(2*F))*nc; %[mol/s]
Gh=mean(G); %[mol/s]
Gtot=Gh*h_work*3600; %[mol/day]
Mcons=Gtot*2/1000; %[kg/day]

% Calculation of the hydrogen consumed at the size of 10kW
Pfc=6; %[kW]
eta_max=0.47; % efficiency of the cell at maximum power
Etot=Pfc*h_work*3600; %[kJ/day]
Mtot=Etot/(eta_max*LHV_H2); %[kg/day]
Gtot=Mtot*1000/2; %[mol/day]

% Dimensioning of the hydrogen storage based on the size of 6kW
Vfol_tot=Mtot/rho; %[m^3/day]
V_tank=ceil(Vfol_tot/0.001); %[liter]

% Calculation of the cost of the storage
Cost=Uc*V_tank; %[€]

% Weekly sizing solution
Mtot_w=Mtot*d_work; %[kg/day]
Vtank_w=V_tank*d_work; %[liter]
Cost_w=Uc*Vtank_w; %[€]

% Calculation of the hydrogen consumption in 1 year
My_tot=Mcons*daywork2018; %[kg/year]
```

B.1 Fortran code of the calculator block C-ICURR

I=200

NC=90

F=96485

YO2=0.21

M1=-0.025

Q1=2.5

IF (I .LE. 50) THEN

H2U=M1*I+Q1

ELSE

H2U=1.25

END IF

M2=-0.02

Q2=3

IF (I .LE. 50) THEN

AIRU=M2*I+Q2

ELSE

AIRU=2

END IF

NH2=I/(2*F)/1000*NC

NAIR=I/(4*F*YO2)/1000*AIRU*NC

NREC=I/(2*F)/1000*(H2U-1)*NC

write(nterm,1)NH2

1 format('Fuel molar flow (kmol/s)',G12.5)

write(nterm,2)NAIR

2 format('Air molar flow (kmol/s)',G12.5)

write(nterm,3)NREC

3 format('Anodic recirculation flow (kmol/s)',G12.5)

write(nterm,4)I

4 format('Stack current (A)',G12.5)

B.2 Fortran code of the calculator block C-WREC

```
PSAT=0.61121*DEXP((18.678-TH2/234.5)*(TH2/(257.14+TH2)))
```

```
PSAT=PSAT/100
```

```
ACELL=500
```

```
IDEN=I/ACELL
```

```
M=-5
```

```
Q=2.55
```

```
IF (IDEN .LE. 0.31) THEN
```

```
  RH=1
```

```
ELSE
```

```
  RH=M*IDEN+Q
```

```
END IF
```

```
PH2=1.2
```

```
XW=RH*PSAT/PH2
```

```
MH2O=XW*MH2
```

```
write(nterm,1)PSAT
```

```
1 format('Vapour pressure (bar)',G12.5)
```

```
write(nterm,2)XW
```

```
2 format('Water fraction',G12.5)
```

```
write(nterm,3)MH2O
```

```
3 format('Humidifying water mass flow (kg/s)',G12.5)
```

```
write(nterm,4)RH
```

```
4 format('Anodic relative humidity ',G12.5)
```

B.3 Fortran code of the calculator block C-HUMC

```
PSAT=0.61121*DEXP((18.678-TAIR/234.5)*(TAIR/(257.14+TAIR)))
```

```
PSAT=PSAT/100
```

```
RH=0.95
```

```
PAIR=1.2
```

```
XW=RH*PSAT/PAIR
```

```
MH2O=XW*MAIR
```

```
write(nterm,1)PSAT
```

```
1 format('Vapour pressure (bar)',G12.5)
```

```
write(nterm,2)XW
```

```
2 format('Water fraction',G12.5)
```

```
write(nterm,3)MH2O
```

```
3 format('Humidifying water mass flow (kg/s)',G12.5)
```

```
write(nterm,4)TAIR
```

```
4 format('Inlet air temperature (°C)',G12.5)
```

B.4 Fortran code of the calculator block C-FU

```
IF (I. LE. 50) THEN
```

```
  FU=1/(-I/40+2.5)
```

```
ELSE
```

```
  FU=0.8
```

```
END IF
```

```
H2FC=GAN*FU
```

```
write(nterm,1) H2FC
```

```
1 format('Consumed anodic flow rate (kmol/s)',G12.5)
```

```
write(nterm,2) FU
```

```
2 format('Fuel utilization',G12.5)
```

B.5 Fortran code of the calculator block C-PEMFC

R=8.314

F=96485

IINT=0.002

ACELL=500

IDENS=I/ACELL

OCV=1.18

AAN=2

ACAT=0.5

I0AN=0.1

I0CAT=0.0002

ARGAN=(IDENS+IINT)/(2*I0AN)

ARGCAT=(IDENS+IINT)/(2*I0CAT)

VACAN=R*(TC+273.15)/(AAN*F)*(DLOG(ARGAN+DSQRT(ARGAN**2+1)))

VACCAT=R*(TC+273.15)/(ACAT*F)*(DLOG(ARGCAT+DSQRT(ARGCAT**2+1)))

VACT=VACAN+VACCAT

WC=8.5

SIG30=0.005139*WC-0.00326

K=303

TM=0.0183

SIG=DEXP(1268*(1/K-1/(TC+273.))) * SIG30

ASR=TM/SIG

VOHM=ASR*(IDENS+IINT)

IMAX=1.5

ILAN=1*IMAX

ILCAT=0.5*IMAX

VDFAN=DABS(R*(TC+273.15)/(2*F)*DLOG(1-(IDENS+IINT)/ILAN))

VDFCAT=DABS(R*(TC+273.15)/(4*F)*DLOG(1-(IDENS+IINT)/ILCAT))

VDIFF=VDFAN+VDFCAT

VC=OCV-VACT-VOHM-VDIFF

PFC=VC*I

write(nterm,1)VC

1 format('Fuel cell voltage (V)',G12.5)

write(nterm,2)PFC

2 format('Fuel cell power (W)',G12.5)

write(nterm,3)VACT

3 format('Activation Overvoltage (V)',G12.5)

write(nterm,4)VDIFF

4 format('Diffusion Overvoltage (V)',G12.5)

write(nterm,5)VOHM

5 format('Ohmic Overvoltage (V)',G12.5)

B.6 Fortran code of the calculator block C-COOL

F=96485

TH2OI=50

TH2OO=60

CP=4185

QTHERM=-QCATH-VC*I*NC

GH2O=QTHERM/(CP*(TH2OO-TH2OI))

write(nterm,1)QTHERM

1 format('FC Waste heat (W)',G12.5)

write(nterm,2)GH2O

2 format('Estimated Coolant mass flow (kg/s)',G12.5)

C.1 Mapping of the Gen-set conditions at varying of load

i (A/cm²)	P_{FC} (W)	P_{comp} (W)	P_{rec} (W)	P_{pump} (W)	Q_{cool} (W)	P_{aux} (W)
0	0	0	0	0	0	0
0,002	56,068	1,36	0,34	0,014	13,5	1,71
0,004	109,38	2,70	0,66	0,030	29,8	3,39
0,006	161,08	4,03	0,97	0,048	47,7	5,05
0,008	211,66	5,33	1,28	0,067	66,7	6,68
0,01	261,35	6,62	1,57	0,088	86,5	8,28
0,012	310,31	7,89	1,85	0,109	107,2	9,85
0,014	358,64	9,14	2,11	0,130	128,4	11,39
0,016	406,42	10,37	2,37	0,152	150,2	12,90
0,018	453,71	11,59	2,62	0,175	172,5	14,38
0,02	500,55	12,78	2,85	0,198	195,2	15,83
0,022	546,98	13,96	3,07	0,222	218,3	17,26
0,024	593,03	15,12	3,28	0,245	241,8	18,65
0,026	638,71	16,26	3,48	0,270	265,7	20,02
0,028	684,07	17,39	3,67	0,294	289,9	21,35
0,03	729,1	18,49	3,85	0,319	314,4	22,66
0,032	773,83	19,63	4,01	0,344	339,2	23,98
0,034	818,27	20,70	4,17	0,370	364,3	25,23
0,036	862,43	21,75	4,31	0,396	389,7	26,46
0,038	906,33	22,79	4,44	0,422	415,3	27,65
0,04	949,97	23,80	4,56	0,448	441,2	28,81
0,042	993,36	24,80	4,67	0,474	467,3	29,94
0,044	1036,5	25,78	4,76	0,501	493,7	31,04
0,046	1079,4	26,74	4,85	0,528	520,3	32,12
0,048	1122,1	27,68	4,92	0,555	547,1	33,16
0,05	1164,6	28,61	4,99	0,583	574,1	34,18
0,052	1206,8	29,51	5,04	0,611	601,3	35,16
0,054	1248,9	30,40	5,08	0,638	628,7	36,12
0,056	1290,7	31,27	5,11	0,666	656,4	37,04
0,058	1332,4	32,12	5,12	0,695	684,2	37,94
0,06	1373,8	32,96	5,13	0,723	712,2	38,81
0,062	1415,1	33,77	5,12	0,752	740,4	39,65

0,064	1456,1	34,57	5,11	0,781	768,7	40,45
0,066	1497	35,34	5,08	0,810	797,3	41,23
0,068	1537,7	36,10	5,04	0,839	826,0	41,98
0,07	1578,2	36,85	4,99	0,868	854,9	42,70
0,072	1618,6	37,57	4,92	0,898	883,9	43,39
0,074	1658,7	38,27	4,85	0,927	913,1	44,05
0,076	1698,7	38,96	4,76	0,957	942,5	44,68
0,078	1738,5	39,63	4,67	0,987	972,0	45,28
0,08	1778,2	40,28	4,56	1,017	1001,6	45,86
0,082	1817,7	40,91	4,44	1,047	1031,4	46,40
0,084	1857	41,52	4,31	1,078	1061,4	46,91
0,086	1896,2	42,12	4,17	1,108	1091,5	47,39
0,088	1935,2	42,70	4,01	1,139	1121,7	47,85
0,09	1974,1	43,25	3,85	1,170	1152,1	48,27
0,092	2012,8	43,79	3,67	1,201	1182,5	48,67
0,094	2051,3	44,32	3,48	1,232	1213,2	49,03
0,096	2089,7	44,82	3,28	1,263	1243,9	49,37
0,098	2128	45,30	3,07	1,294	1274,8	49,67
0,1	2166,1	45,77	2,85	1,326	1305,7	49,95
0,102	2204	46,69	2,91	1,358	1337,2	50,95
0,104	2241,8	47,60	2,96	1,390	1368,9	51,96
0,106	2279,5	48,52	3,02	1,422	1400,6	52,96
0,108	2317	49,43	3,08	1,455	1432,5	53,97
0,11	2354,4	50,35	3,13	1,487	1464,6	54,97
0,112	2391,6	51,26	3,19	1,520	1496,8	55,98
0,114	2428,7	52,18	3,25	1,553	1529,1	56,98
0,116	2465,7	53,10	3,31	1,586	1561,6	57,99
0,118	2502,5	54,01	3,36	1,619	1594,2	58,99
0,12	2539,2	54,93	3,42	1,652	1627,0	60,00
0,122	2575,8	55,84	3,48	1,686	1659,9	61,00
0,124	2612,2	56,76	3,53	1,719	1692,9	62,01
0,126	2648,5	57,67	3,59	1,753	1726,0	63,02
0,128	2684,6	58,59	3,65	1,787	1759,3	64,02
0,13	2720,6	59,50	3,70	1,821	1792,7	65,03

0,132	2756,5	60,42	3,76	1,855	1826,3	66,03
0,134	2792,3	61,33	3,82	1,889	1859,9	67,04
0,136	2827,9	62,25	3,88	1,923	1893,8	68,05
0,138	2863,4	63,16	3,93	1,958	1927,7	69,06
0,14	2898,8	64,08	3,99	1,992	1961,7	70,06
0,142	2934,1	65,00	4,05	2,027	1995,9	71,07
0,144	2969,2	65,91	4,10	2,062	2030,2	72,08
0,146	3004,2	66,83	4,16	2,097	2064,7	73,08
0,148	3039,1	67,74	4,22	2,132	2099,2	74,09
0,15	3073,8	68,66	4,27	2,167	2133,9	75,10
0,152	3108,4	69,57	4,33	2,202	2168,7	76,11
0,154	3143	70,49	4,39	2,238	2203,7	77,11
0,156	3177,3	71,40	4,45	2,273	2238,7	78,12
0,158	3211,6	72,32	4,50	2,309	2273,9	79,13
0,16	3245,7	73,23	4,56	2,345	2309,2	80,14
0,162	3279,8	74,15	4,62	2,381	2344,6	81,15
0,164	3313,7	75,07	4,67	2,417	2380,1	82,16
0,166	3347,5	75,98	4,73	2,453	2415,8	83,16
0,168	3381,1	76,90	4,79	2,490	2451,5	84,17
0,17	3414,7	77,81	4,84	2,526	2487,4	85,18
0,172	3448,1	78,73	4,90	2,563	2523,4	86,19
0,174	3481,4	79,64	4,96	2,599	2559,5	87,20
0,176	3514,6	80,56	5,02	2,636	2595,8	88,21
0,178	3547,7	81,47	5,07	2,673	2632,1	89,22
0,18	3580,7	82,39	5,13	2,710	2668,6	90,23
0,182	3613,6	83,30	5,19	2,747	2705,2	91,24
0,184	3646,3	84,22	5,24	2,784	2741,9	92,25
0,186	3678,9	85,14	5,30	2,822	2778,7	93,26
0,188	3711,4	86,05	5,36	2,859	2815,6	94,27
0,19	3743,8	86,97	5,41	2,897	2852,6	95,28
0,192	3776,1	87,88	5,47	2,935	2889,8	96,29
0,194	3808,3	88,80	5,53	2,973	2927,0	97,30
0,196	3840,4	89,71	5,59	3,010	2964,4	98,31
0,198	3872,3	90,63	5,64	3,049	3001,9	99,32

0,2	3904,2	91,54	5,70	3,087	3039,5	100,33
0,202	3935,9	92,46	5,76	3,125	3077,2	101,34
0,204	3967,5	93,37	5,81	3,163	3115,0	102,35
0,206	3999	94,29	5,87	3,202	3152,9	103,36
0,208	4030,5	95,21	5,93	3,241	3190,9	104,37
0,21	4061,7	96,12	5,98	3,279	3229,1	105,38
0,212	4092,9	97,04	6,04	3,318	3267,3	106,40
0,214	4124	97,95	6,10	3,357	3305,7	107,41
0,216	4155	98,87	6,16	3,396	3344,1	108,42
0,218	4185,8	99,78	6,21	3,435	3382,7	109,43
0,22	4216,6	100,70	6,27	3,475	3421,4	110,44
0,222	4247,3	101,61	6,33	3,514	3460,2	111,45
0,224	4277,8	102,53	6,38	3,554	3499,1	112,47
0,226	4308,2	103,44	6,44	3,593	3538,1	113,48
0,228	4338,6	104,36	6,50	3,633	3577,2	114,49
0,23	4368,8	105,27	6,55	3,673	3616,4	115,50
0,232	4398,9	106,19	6,61	3,713	3655,7	116,51
0,234	4428,9	107,11	6,67	3,753	3695,1	117,53
0,236	4458,8	108,02	6,73	3,793	3734,7	118,54
0,238	4488,6	108,94	6,78	3,833	3774,3	119,55
0,24	4518,3	109,85	6,84	3,873	3814,0	120,57
0,242	4547,9	110,77	6,90	3,914	3853,9	121,58
0,244	4577,4	111,68	6,95	3,954	3893,8	122,59
0,246	4606,8	112,60	7,01	3,995	3933,9	123,60
0,248	4636,1	113,51	7,07	4,036	3974,0	124,62
0,25	4665,3	114,43	7,12	4,077	4014,3	125,63
0,252	4694,3	115,34	7,18	4,118	4054,6	126,64
0,254	4723,3	116,26	7,24	4,159	4095,1	127,66
0,256	4752,2	117,18	7,30	4,200	4135,7	128,67
0,258	4781	118,09	7,35	4,241	4176,3	129,68
0,26	4809,6	119,01	7,41	4,283	4217,1	130,70
0,262	4838,2	119,92	7,47	4,324	4258,0	131,71
0,264	4866,7	120,84	7,52	4,366	4298,9	132,73
0,266	4895	121,75	7,58	4,408	4340,0	133,74

0,268	4923,3	122,67	7,64	4,449	4381,2	134,76
0,27	4951,4	123,58	7,69	4,491	4422,5	135,77
0,272	4979,5	124,50	7,75	4,533	4463,8	136,78
0,274	5007,5	125,41	7,81	4,575	4505,3	137,80
0,276	5035,3	126,33	7,87	4,618	4546,9	138,81
0,278	5063,1	127,25	7,92	4,660	4588,6	139,83
0,28	5090,7	128,16	7,98	4,702	4630,4	140,84
0,282	5118,3	129,08	8,04	4,745	4672,2	141,86
0,284	5145,8	129,99	8,09	4,788	4714,2	142,87
0,286	5173,1	130,91	8,15	4,830	4756,3	143,89
0,288	5200,4	131,82	8,21	4,873	4798,5	144,90
0,29	5227,5	132,74	8,26	4,916	4840,7	145,92
0,292	5254,6	133,65	8,32	4,959	4883,1	146,93
0,294	5281,6	134,57	8,38	5,002	4925,6	147,95
0,296	5308,4	135,48	8,44	5,046	4968,2	148,97
0,298	5335,2	136,40	8,49	5,089	5010,8	149,98
0,3	5361,8	137,32	8,55	5,132	5053,6	151,00
0,302	5388,4	138,23	8,61	5,176	5096,5	152,01
0,304	5414,9	139,15	8,66	5,219	5139,4	153,03
0,306	5441,3	140,06	8,72	5,263	5182,5	154,05
0,308	5467,5	140,98	8,78	5,307	5225,7	155,06
0,31	5493,7	141,89	8,83	5,351	5268,9	156,08
0,312	5519,8	142,81	8,89	5,395	5312,3	157,09
0,314	5545,8	143,72	8,95	5,439	5355,8	158,11
0,316	5571,6	144,64	9,01	5,483	5399,3	159,13
0,318	5597,4	145,55	9,06	5,528	5443,0	160,14
0,32	5623,1	146,47	9,12	5,572	5486,7	161,16
0,322	5648,7	147,38	9,18	5,617	5530,5	162,18
0,324	5674,2	148,30	9,23	5,661	5574,5	163,20
0,326	5699,6	149,22	9,29	5,706	5618,5	164,21
0,328	5724,9	150,13	9,35	5,751	5662,7	165,23
0,33	5750,1	151,05	9,40	5,796	5706,9	166,25
0,332	5775,2	151,96	9,46	5,841	5751,2	167,26
0,334	5800,2	152,88	9,52	5,886	5795,6	168,28

0,336	5825,1	153,79	9,58	5,931	5840,2	169,30
0,338	5850	154,71	9,63	5,976	5884,8	170,32
0,34	5874,7	155,62	9,69	6,022	5929,5	171,34
0,342	5899,3	156,54	9,75	6,067	5974,3	172,35
0,344	5923,8	157,45	9,80	6,113	6019,2	173,37
0,346	5948,3	158,37	9,86	6,159	6064,2	174,39
0,348	5972,6	159,29	9,92	6,204	6109,3	175,41
0,35	5996,9	160,20	9,97	6,250	6154,5	176,43
0,352	6021	161,12	10,03	6,296	6199,8	177,44
0,354	6045,1	162,03	10,09	6,342	6245,2	178,46
0,356	6069	162,95	10,15	6,389	6290,7	179,48
0,358	6092,9	163,86	10,20	6,435	6336,2	180,50
0,36	6116,6	164,78	10,26	6,481	6381,9	181,52
0,362	6140,3	165,69	10,32	6,528	6427,7	182,54
0,364	6163,9	166,61	10,37	6,574	6473,5	183,56
0,366	6187,4	167,52	10,43	6,621	6519,5	184,58
0,368	6210,8	168,44	10,49	6,668	6565,5	185,60
0,37	6234,1	169,36	10,54	6,715	6611,7	186,61
0,372	6257,3	170,27	10,60	6,762	6657,9	187,63
0,374	6280,4	171,19	10,66	6,809	6704,3	188,65
0,376	6303,4	172,10	10,72	6,856	6750,7	189,67
0,378	6326,3	173,02	10,77	6,903	6797,2	190,69
0,38	6349,1	173,93	10,83	6,950	6843,8	191,71
0,382	6371,8	174,85	10,89	6,998	6890,5	192,73
0,384	6394,4	175,76	10,94	7,045	6937,4	193,75
0,386	6417	176,68	11,00	7,093	6984,3	194,77
0,388	6439,4	177,59	11,06	7,141	7031,3	195,79
0,39	6461,8	178,51	11,11	7,189	7078,3	196,81
0,392	6484	179,43	11,17	7,237	7125,5	197,83
0,394	6506,2	180,34	11,22	7,285	7172,8	198,85
0,396	6528,2	181,26	11,28	7,333	7220,2	199,87
0,398	6550,2	182,17	11,33	7,381	7267,6	200,88
0,4	6572,1	183,09	11,38	7,429	7315,2	201,90

RINGRAZIAMENTI

Dedico questo lavoro a tutti coloro che mi sono stati vicino in questi anni di studio.

Ringrazio i miei genitori per avermi permesso di essere qua a raggiungere questo importante traguardo, sebbene le difficoltà incontrate. Specialmente a te mamma che mi hai seguito costantemente nei miei studi, sopportandomi e supportandomi nei momenti di bisogno.

Ringrazio i mie amici e colleghi Arnaud e Fabio che mi hanno spronato in tutta la carriera universitaria al Politecnico ed in particolar modo in questo ultimo periodo di tesi.

Infine, per ultimo ringrazio tutti coloro che negli ultimi anni si sono interessati ed hanno costantemente seguito i miei passi fino al raggiungimento di tale obiettivo. Anche voi siete stati la mia forza.

Hector Francisco Elias Gutierrez